Role of enteroendocrine cells in intestinal homeostasis and ageing.

Inaugural-Dissertation
zur
Erlangung des Doktorgrades
der Mathematisch-Naturwissenschaftlichen Fakultät
der Universität zu Köln

vorgelegt von

Sina Azami
aus Teheran, Iran

Köln, 2022

Gutachter: **Prof. Dr. Linda Partridge**

                    Prof. Dr. Mirka Uhlirova

Tag der mündlichen Prüfung: 08. Dezember 2022

Table of contents

Acknowledgements

First of all, I would like to thank Prof. Dr. Linda Partridge for giving me the opportunity of joining her lab and doing my PhD. Thank you for your trust in me, and for the freedom that you gave me to develop my skills as an independent scientist. I would also like to thank my mentor and friend, Dr. Jerome Korzelius for being such a supportive person through and through, we had quite a journey together in the past four years and I learned a lot from you! I want to thank Dr. Sebastian Grönke for his helpful insights and his suggestions for my projects. I am also incredibly grateful to the members of my thesis advisory committee Prof. Dr. Mirka Uhlirova and Prof. Dr. Heinrich Jasper for their helpful inputs for my projects.

I would like to thank all members of our amazing department, I was so lucky to know you and work with you for the past four years! A big thank to Dr. Thomas Leech for being an amazing friend, always ready for discussion and help. I would also like to thank Javi for the lively discussions and also for showing me how to do many of the fly experiments including setting up lifespan crosses! Another very big thank to all other members of the LP lab, to Carolina, Lisonia, Jonathan, Annika, Pingze, Bruna, Maarof, Helena, Dennis, Sophie, Nathalie, Dr. Yu-Xuan Lu and Dr. Jiongming Lu for being incredible friends. I would also like to thank Rene, Sandra, Jenny, Andre, Jacky and all other amazing technicians of our lab. Moreover, I would like to thank Dr. Christine Lesch, Oliver Hendrich and Dr. Virginia Kroef for helping me with all aspects of lab life and making such a big lab run smoothly. Another thank you must go to Dr. Joris Deelen and his lab for their helpful inputs for my work. I would also like to thank Dr. Daniela Morick for her support and constant willingness to help. I would also like to thank Kiarash, a brilliant master student that I was fortunate enough to know and supervise.

I used the services and expertise of FACS and Imaging facility and Bioinformatics facility of the MPI-AGE, so I like to wholeheartedly thank Dr. Christian Kukat, Dr. Jorge Boucas, Ayesha, Marcel, Kat and Lena.

And finally to my family,,, Samira, thank you for being so patience and supportive, you are an amazing wife and my best friend, I know that I couldn't thank you enough, so I will stop here! I

wouldn't have been here if it wasn't because of support of my mom, my dad and my brother Sepehr, thanks a lot for all the love.

Abbreviations

AKH	Adipokinetic Hormone
AMPK	Amp-Activated Protein Kinase
A-P axis	Anterior-Posterior Axis
AS-C	Achaete-Acute Complex
ase	Asense
BHLH	Basic Helix-Loop-Helix
BMP	Bone Morphogenetic Protein
CBC	Crypt Base Columnar
CC	Corpora Cardiaca
CCHa 1	CC Hamide 1
CCHa1-r	CC Hamide 1 Receptor
CCHa2	CC Hamide 2
CCR	Copper Cell Region
CRC	Colorectal Cancer
DE	Differentially Expressed
Dh31	Diuretic Hormone-31
Dl	Delta
EB	Enteroblast
EC	Enterocyte
Ecc15	Erwinia Carotovora
EE	Enteroendocrine
EEP	Enteroendocrine Progenitor

Esg	Escargot
F/O	FlipOut
FKH	Fork Head
Gfi1	Growth Factor Independent Protein 1
GFP	Green Fluorescent Protein
GI	Gastrointestinal Tract
GIP	Glucose-Dependent Insulinotropic Polypeptide
GLP1	Glucagon-Like Peptide-1
GO	Gene Ontology
GRN	Gene Regulatory Network
Hes1	Enhancer of Split 1
HMG	High-Mobility Group
IGF	Insulin-Like Growth Factor
IIS	Insulin/Igf-1 Signaling
IPC	Insulin Producing Cell
ISC	Intestinal Stem Cell
Klu	Klumpfuss
LB	Luria-Bertani
LRC	Label Retaining Cell
MARCM	Mosaic Analysis with a Repressible Cell Marker
mTOR	Mechanistic Target Of Rapamycin
Ngn3	Neurogenin 3
NPF	Neuropeptide F

NPY	Neuropeptide Y
Pc	Polycomb
PCP	Planar Cell Polarity
PGRP-SC	Class SC of Peptidoglycan Recognition Protein
pH3	Phospho-Histone H3
Phyl	Phyllopod
Pros	Prospero
RNA pol II	RNA Polymerase Ii
Sc	Scute
scRNA-seq	Single Cell RNA Sequencing
SD	Standard Deviation
Snpf	Short Neuropeptide F
Su(H)	Suppressor Of Hairless
Svr	Silver
SYA	Sugar-Yeast-Agar
TF	Transcription Factor
TK	Tachykinin
UMAP	Uniform Manifold Approximation and Projection
Upd	Unpaired
WT1	Wilms Tumor 1

Summary

The Intestine is a large and dynamic organ with a defined population of stem cells (ISCs) that are capable of giving rise to different differentiated cell types. The enteroendocrine cells (EEs) in the gut are responsible for producing different hormones which affect physiological and cellular processes locally and systemically throughout the body. In the intestine of the fruit fly (*Drosophila melanogaster*), EEs cumulatively produce 12 different prohormones that give rise to more than 20 hormone peptides. Despite their physiological importance, not much is known about the role that EEs and their products play in intestinal homeostasis during ageing in *Drosophila*.

In the first part of my thesis, I investigated the mechanism by which the transcription factor Klumpfuss (Klu) determines the choice between enterocyte (EC) versus EE differentiation in the *Drosophila* intestine. We demonstrated that Klu acts in a cell-autonomous manner to restrict enteroblast (EB) cell fate to EC differentiation. Inhibition of *klu* expression by RNA interference resulted in excess EE differentiation. Ectopic expression of *klu* in ISCs reduces their proliferative capacity and blocked differentiation. Lastly, we showed that Klu acts down stream of Notch signaling in determining EC cell fate decision.

In the second part of my thesis I employed a combination of bulk and single cell RNA sequencing (scRNA-seq) to investigate the changes in EE cells during ageing in both males and females. We observed significant changes in transcript-level for different EE hormones in our bulk RNA sequencing dataset. We examined the functional consequence of knocking down these hormones on ISC-proliferation and discovered that several EE-derived hormones play a role in promoting ISC-proliferation after infection. Moreover, we observed upregulation of pathways that are related to cell cycle and differentiation in old EEs, signifying changes in EE differentiation in the aged intestine. Analyzing our scRNA-seq dataset using Seurat algorithm and supervised clustering confirmed several of the changes from our bulk RNA-seq experiment, while expanding our knowledge on EE subtype change with age. We identified 4 major EE clusters in all conditions: NPF, AstA, AstC and EE progenitor cells, and observed increases in EE progenitor and AstA cell types in old female samples. Moreover, we observed a decrease of cells in the NPF cluster in old versus young female samples. This change was confirmed by Gal4 reporter line analysis for this hormone. Interestingly, the reduction of NPF-producing EEs in old flies happened in both male and female samples, but in different anatomical regions of the intestine. Finally, we showed that transcript of the transcription factor Escargot, which was thought to be restricted solely to the ISC and EB, is unexpectedly present in almost all EE clusters.

With this study I have increased our understanding of ISC differentiation and cell fate determination in *Drosophila* intestine, and documented the changes that EE cells sustain during the ageing process. These results will be of crucial importance to better understand the role of EE cells in gut health and disease in an increasingly ageing population.

1. Introduction

Homeostatic balance between organs is necessary for the survival of living organisms. Multicellular organisms have several compartments (in animals several organ systems) that require tight communication to keep the organism in the homeostatic state. One of these systems is the gastrointestinal tract (GI) which in metazoans is responsible for doing three main tasks: Digestion and absorption of nutrients, protection against various types of environmental insults, and finally communicating metabolic and nutritional status by sending and receiving signals to other organ systems to ensure homeostasis.

Digestion of food happens in two forms: mechanical and chemical. The mechanical digestion starts with chewing and/or swallowing of food and continues by peristalsis and passing of food through the gut by movements of muscles surrounding the tube and finally ends with defecation. Tight regulation of start, progress and end of muscle movements is key for normal passage of food and also in situations where the intestine content needs to be emptied including vomiting and diarrhea. In mammals, peristalsis is under control of the enteric nervous system and independent of central nervous system. The autonomous gastrointestinal neural networks that are in the heart of this system are comprised of enteric neurons and enteric glial cells (Zhao et al. 2021).

The high metabolic activity of the gut results in a high turnover of cells. Indeed the entire intestinal lining is renewed in a matter of days in most mammals. A dedicated population of intestinal stem cells (ISCs) has been identified in both flies and mammals (Barker et al. 2007; Micchelli and Perrimon 2006; Ohlstein and Spradling 2006) that are crucial for replenishing lost cells and upon receiving appropriate signals start to divide and differentiate to give rise to the various cell types of the intestine. These cells can be divided into two major classes: absorptive cell lineages that are responsible for absorption of nutrients, and secretory lineages that produce different enzymes and hormones responsible for digestion of the food and short and long range communications.

Due to the high turnover of cells, the intestine is prone to develop cancerous lesions over the lifetime. Colorectal cancer (CRC) is one of the top 3 most lethal cancers and its

incidence increases dramatically with age. In addition, intestinal function is compromised with age, leading to more severe consequences of GI-infections in elderly people. Lastly, the gut plays a key role in the sensing of hunger and satiety, and the endocrine cells of the gut play a major role in the control of food intake. Therefore, a better understanding of the cellular composition, function and regulation of hormones in the intestine is key for understanding its biology, and overcoming complications that arise through malfunctioning of this system in cancer or during ageing.

1.1. Intestine in mammals: anatomy, physiology and cellular composition

The mammalian GI is a tubular structure that anatomically consists of four major parts (Figure 1). It starts with esophagus which is the only section of the digestive tract that has skeletal (voluntary) muscle in its upper section. The esophagus is followed by the stomach, which through signaling from the endocrine system, including enteroendocrine cells (EEs), produces gastric acid (hydrochloric acid) through activity of the H^+/K^+ ATPase pump. Entrance and exit of intestinal contents to/from stomach is controlled by two sphincters called lower esophageal sphincter and pyloric sphincter, respectively. After initial digestion with gastric acid, intestinal contents enter the small intestine, which has three main parts: duodenum, jejunum, and ileum. The small intestine is responsible for further digestion of food (mostly in duodenum and jejunum) and also absorption of nutrients and water (mostly in ileum). The last part of the digestive tract in mammals is the large intestine. Anatomically, the large intestine can be divided into four sections: cecum, colon, rectum and anal canal. Partly digested food enters the cecum and passes through the rest of large intestine, and in this process the remaining water and also electrolytes and nutrients get absorbed and finally the remnants called stool exit the body.
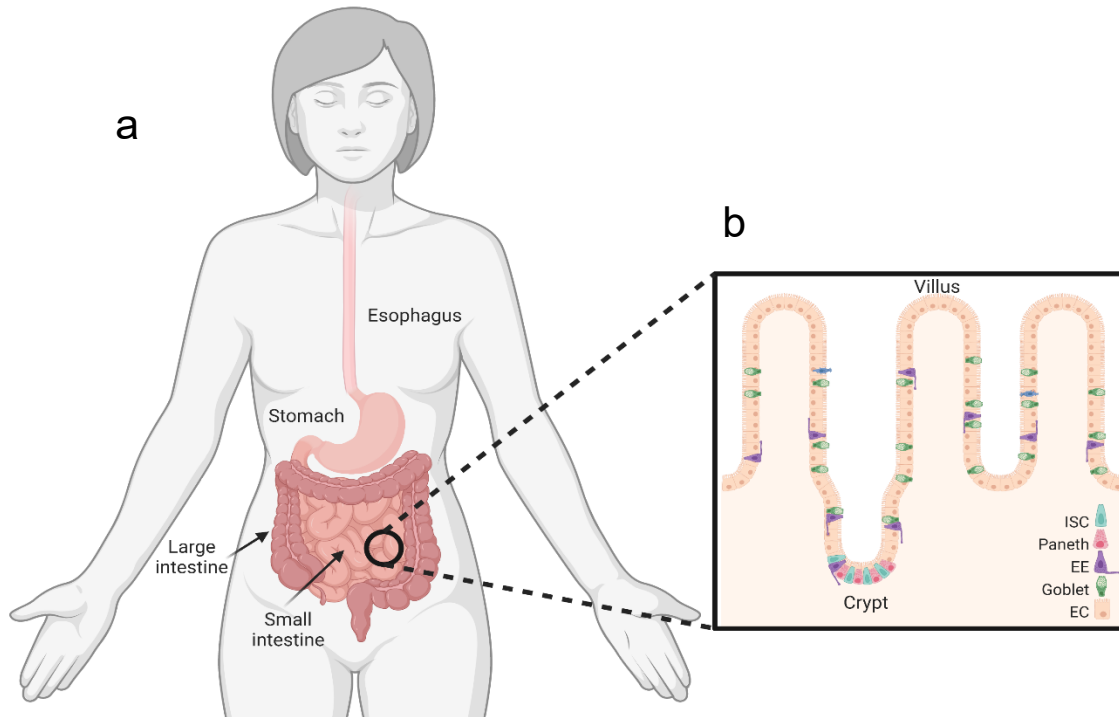
Figure 1: Schematic representation of human digestive system.
Regions of the gut and its anatomic composition are shown. a: Digestive tract of mammals is comprised of 4 different sections: Esophagus, Stomach, small intestine and large intestine. b: Crypt-villus composition.

The mammalian intestinal epithelium is made of specialized units called crypt and villus. Each unit consists of a protrusion of the intestinal wall (villus, plural villi) and invaginations (crypt) that surround it (Figure 1b). Structurally, a villus consists of a single layer of post-mitotic epithelial tissue. Beneath this layer are numerous capillaries and lymph vessels that receive absorbed nutrients that are transferred to the liver and subsequently the rest of the body. The size of villi decreases through the length of the intestine with the largest ones being present in the duodenum and smaller ones in ileum, with the colon completely lacking the villus structure. The position of villus, as a protrusion in the lumen, has it exposed to different mechanical and chemical activities of the intestine. Crypts, on the other hand, reside at the bottom of invaginations of the intestine and hence are protected from abovementioned hazards. Unlike cells in the villi, crypt cells are actively and continuously dividing. ISCs that reside at the bottom of the crypt are the source of this activity by producing daughter cells that will eventually mature and during this maturation process get pushed out of crypt structure towards the top of the villus. This mechanism provides the intestine with a steadily regenerating reservoir of mature cells at the top of

the villi where the environmental and mechanical strain causes each cell to remain functional for a short period of time before being shed into the lumen.

The mammalian intestinal epithelial lining is comprised of six different mature cell types that can be divided into secretory (enteroendocrine, Paneth, goblet and tuft cells) and absorptive (enterocytes and M cells) lineages. All these cell types generate from a dedicated pool of stem cells at the bottom of crypt structure. Initially named as crypt base columnar (CBC) cells (Cheng and Leblond 1974), ISCs were identified by observations showing the flow of cells that were randomly labeled by mutagenesis from bottom of the crypt to villus (Winton, Blount, and Ponder 1988; M. Bjerknes and Cheng 1999). Subsequent advances in the genetic toolset, specially the advent of lineage tracing methods, allowed finally confirmation that CBCs are indeed stem cells, and LGR5 was discovered as one of the prominent markers of these cells (van de Wetering et al. 2002). It was shown that administration of tamoxifen in offspring of *Lgr5$^{EGFP-IRES-CreERT2}$ > R26R-lacZ* reporter mice promotes Cre-ERT2 fusion enzyme activation and subsequent continuous *lacZ* expression in LGR5$^+$ cells and their descendant cells. In another study activation of Cre resulted in ribbons of lacZ marked cells from bottom to top of the crypt that contained all different cell lineages just in 5 days (Barker et al. 2007). More interestingly, elimination of LGR5$^+$ cells using either irradiation, or injection of diphtheria toxin together with expression of its receptor in these cells, was not persistent, and upon removing of the eliminating factor, LGR5$^+$ cells reappeared in the bottom of the crypt (Dekaney et al. 2009; H. Tian et al. 2011). This suggested that a mechanism existed to ensure replacement of ISCs even after their complete elimination. Indeed further studies using lineage tracing of secretory cells showed that after elimination of LGR5$^+$ cells, DLL$^+$ secretory progenitors populate the empty niche, de-differentiate and act as CBC cells (van Es et al. 2012). There are also reports showing more differentiated cells including Bmi$^+$ EEs can undergo de-differentiation and replace ISC function when necessary (Yan et al. 2017; Jadhav et al. 2017). Hence, the intestinal epithelium has reserve mechanisms in place to ensure regeneration in case of primary ISC-loss.

The position and function of all other mammalian cell types has been investigated in great detail (reviewed in (Clevers 2013; Beumer and Clevers 2021). Proper function of these

cells and also their communication with each other and with other organs of the body ensures that the whole system remains in homeostatic conditions. This has been emphasized by situations in which this composition gets disturbed, including cancer and ageing (reviewed in (Fane and Weeraratna 2020). Changes in the function of ISCs and subsequently other cell types in these situations result in interruption of homeostasis and eventually contribute to age associated phenotypes and death. Major drawbacks of studying turnover in the context of ageing in mammalian systems is the relatively long lifespan of mice and the economic and ethical restrictions of doing large animal cohorts. In recent years, the *Drosophila melanogaster* intestine (or midgut) has become a popular, genetically tractable alternative for studying epithelial turnover during ageing and in disease (reviewed in detail in (Miguel-Aliaga, Jasper, and Lemaitre 2018). Below I will outline the anatomy of this system and highlight key features useful for the study of stem cell biology and ageing.

1.2. *The Drosophila* intestine: anatomy and regionality

The *Drosophila melanogaster* intestine (or midgut) is reminiscent of the mammalian intestine, although, with simpler cellular composition. This similarity, together with the short life time and the availability of an extensive range of sophisticated genetic tools, makes *Drosophila* an excellent model organism to study intestinal biology (Lemaitre and Miguel-Aliaga 2013).

Physiologically, the fly gut consists of a simple epithelium surrounded by visceral muscles, nerve cells and tracheae from outside and a semipermeable layer called peritrophic membrane which consists of chitin and proteins from inside (Figure 2). There is also a very thin layer of mucus covering the inner membrane that is functionally similar to the mammalian intestinal mucus layer. The *Drosophila* intestine is subdivided into three sections with different developmental origins; the foregut and the hindgut which have ectodermal origin, and the midgut with endodermal origin (Lemaitre and Miguel-Aliaga 2013). From these three parts, the midgut is of prime importance, as it is the main part

responsible for digestion and absorption of the food and is also most similar part to the mammalian digestive tract.
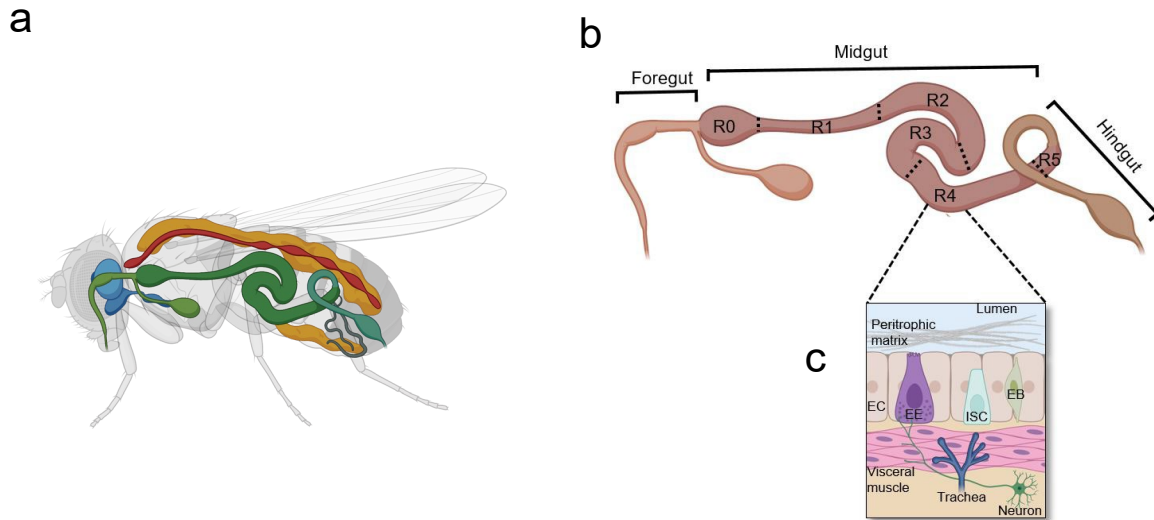
Figure 2. Schematic representation of *Drosophila* digestive system.
a: Digestive tract of D*rosophila* (here showed in green) is situated in the middle section of the body and encompasses the majority of its space. b: *Drosophila* gut consists of three main sections; Foregut, midgut and hindgut. Midgut is the main section responsible for digestion and absorption of food, and can be further divided into subsections (R0 to R5). c: Cellular composition of *Drosophila* midgut. Several tissues including epithelia, muscle, neurons and tracheae are present in the epithelium of the midgut. The peritrophic matrix is in direct contact with the contents of the lumen.

The midgut can be further sub-compartmented to three main sections; anterior, middle and posterior sections. Further molecular and morphological subdivisions have also been made for the midgut, based on either cellular composition (ISC proliferation rate), physiological features (pH) or gene expression profiles (Murakami et al. 1994; Strand and Micchelli 2011; Buchon et al. 2013; Marianes and Spradling 2013; Dutta et al. 2015).

From a cellular perspective, the *Drosophila* intestine has four cell types; ISCs, Enteroblast (EB), Enterocyte (EC) and Enteroendocrine Cell (EE). Upon receiving appropriate proliferation signals, ISCs start to divide. Based on the symmetry of ISC division, it can give rise to two ISCs (symmetric) or one ISC and one progenitor EB cell (asymmetric). Depending on the level of Notch signaling, EBs can either differentiate into absorptive ECs (high Notch signaling), which comprise the majority of cells in the adult midgut and are responsible for producing digestive enzymes and absorption of nutrients, or secretory EEs, which are small cells that are responsible for regulation of food intake, energy

expenditure and glucose and lipid metabolism by producing different hormones (Lemaitre and Miguel-Aliaga 2013).

A host of transcription factors (TFs) and signal transduction pathways determine cell identity, proliferation and compartmentalization of the midgut, and a collection of pan-gut and region-specific TFs are the pillars of this regulation. A good example of the effect of TFs in determining different gut regions is the role of homeobox TFs Labial and Ptx1 which act locally, and the pan-gut TF GATAe in determining so called copper cells in the middle section of the midgut (region R3). Due to activity of H+/V- type proton pumps and other ion transporters/channels in copper cells, this section of the midgut is more acidic (pH~3) compared to the other parts (pH= 7-9) (Buchon et al. 2013; Dubreuil, Grushko, and Baumann 2001; Hoppler and Bienz 1994; Okumura et al. 2007).

It is noteworthy that, despite their important role in determining region specificity in the gut, gene expression is not always sharply regulated throughout the gut, and especially in boundaries of different sections of the gut. Wnt signaling plays an important role in regulating ISC proliferation and differentiation in both mammals and flies (Schuijers and Clevers 2012; Lin, Xu, and Xi 2008). Generation of gradients of Wnt have been reported in many developmental processes, including determination of intestinal boundaries in *Drosophila*. Using a *Fz3-GAL4* Wnt-receptor reporter Buchon et al. showed that a Wnt gradient provides a tissue organization center that determines borders of various sections of the intestine (Buchon et al. 2013). Moreover, they observed changes in EC morphology which was in line with graded Wnt pathway activity in the vicinity of the region boundaries, especially in R5 region of the gut. This emphasized the role of the Wnt signaling pathway in determining gut regionality.

Similar to the mammalian intestine, the composition of cells, and regulation of ISC proliferation in *Drosophila* plays a pivotal role in determining organism homeostasis or disease. In the next section, I will outline some of the key pathways that control ISC proliferation and differentiation in the *Drosophila* midgut in more detail.

1.3. Signaling pathways controlling epithelial turnover through their effect on ISC division and differentiation

Like their mammalian counterparts, *Drosophila* ISC proliferation is regulated by activity of several conserved signaling pathways that stem from various environmental, paracrine, local and systemic cues. Some of the signaling pathways that regulate ISC proliferation and differentiation include: Wg, Notch, JAK/STAT, EGFR, JNK, Tor, Hippo, IL, JH and Ret (reviewed in detail in: Miguel-Aliaga, Jasper, and Lemaitre 2018).

Unlike mammals, in *Drosophila* the rate of ISC proliferation is low under normal homeostatic conditions. However, upon stress, infection, or during ageing, the rate of ISC proliferation increases. This increase is affected by paracrine factors released from differentiated cells in the vicinity of ISCs, including ECs, EEs and also visceral muscle, that all act together to form the ISC niche. One example is the conserved Wg/Wnt signaling that plays crucial role in proliferation of ISCs in both mammals and *Drosophila.* The wg/Wnt gradient dictates the proliferation of ISCs in a dose-dependent manner. It has been shown that in *Drosophila*, the levels of Wg is high in the visceral muscle surrounding the gut (Ai Tian et al. 2016). This provides a gradient similar to the gradient of Wnt and BMP in mammalian crypt structure and determines the proliferative versus differentiated fate of cells in the crypt (Clevers 2013; Beumer et al. 2022). Interestingly, in *Drosophila* the regulation of ISC proliferation by Wg is non-autonomous; When the Wg pathway is activated in absorptive enterocytes, it suppresses JAK-STAT signaling in nearby ISCs, preventing their proliferation (Ai Tian et al. 2016). Moreover, Cordero et al. showed that Wg is required for Myc dependent ISC proliferation in response to damage and during regeneration (Cordero et al. 2012). This shows that even undifferentiated cells play a role in promoting ISC proliferation in challenging situations like tissue damage.

In addition to genetic factors, the environmental factors and specifically certain nutrients in the intestine play important roles in regulating ISC proliferation and subsequent differentiation. A good example is the role of cycles of fasting and refeeding on symmetry of proliferation. In this particular case, re-feeding upon fasting results in an Insulin-like

peptide 3 (DILP3) increase, generated in visceral muscle. This increase results in switching ISCs from asymmetric to symmetric division which increases the midgut's regenerative potential and eventually results in renewed organ growth (O'Brien et al. 2011).

Furthermore, gut regionality affects the rate of ISC proliferation, as different regions have very distinct changes in their proliferative index (Strand and Micchelli 2011). The gastric stem cells reside in the middle section of the *Drosophila* midgut are less proliferative compared to the ISCs in posterior (R4-R5) section. Moreover, the response of ISCs in different regions to signaling pathways also differs. Inactivation of Dpp signaling, for example, causes miss-differentiation of ISCs in middle midgut but not posterior midgut (H. Li, Qi, and Jasper 2013). Another example is the activity of JAK/STAT signaling which in middle midgut results in generation of ectopic EC like cells, but in posterior midgut results in altered ISC proliferation and failure to differentiate beyond the ISC-EB progenitor state (Jiang et al. 2009; H. Li, Qi, and Jasper 2016). Epidermal growth factor receptor (EGFR) signaling also plays role in activation of ISC proliferation. It has been shown that activation of EGFR is not enough to promote ISC proliferation in homeostatic conditions. Combined activation of ERK by EGF and also ROS-induced JNK activation, on the other hand, is sufficient to promote ISC division (Biteau and Jasper 2011).

Finally, it is noteworthy that until recently it was believed that ISCs are the only cell type that are capable of dividing in response to different environmental and physiological demands of the intestine. However, it has become clear now that in addition to ISCs, some of the EE progenitor cells and EBs are also capable of dividing. Tian et al have reported that EBs can undergo mitosis upon upregulation of the epidermal growth factor receptor (EGFR)-Ras signaling pathway. They observed that infection with bacteria results in elevated levels of EGFR-RAS activity. Interestingly, EB-specific ectopic activation of EGFR is enough to promote EB mitosis in a cell autonomous manner (Aiguo Tian et al. 2022). In the case of EEs, Chen et al proposed a model in which transient activation of Scute (Sc) in ICSs induces proliferation towards EE generation. Increased Sc activity in ISC results in asymmetric division and formation an EE progenitor (EEP) and another ISC. In the newly formed EEP Sc acts both as a mitogenic and cell fate

inducer factor, causing EEP to undergo one additional round of division that results in generation of an EE pair. After this final division, accumulation of the EE specific TF, Pros, results in EE maturation and also downregulation of *sc*. In total however, this type of mitosis accounts for a small fraction of proliferative activity in the gut and the bulk of proliferative capacity comes from ISCs (Chen et al. 2018; He et al. 2018).

1.4. Ageing and its effects on the intestine

The turnover of *Drosophila* intestine is slow under homeostatic conditions, and it has been estimated that it completely regenerates only three to four times during the life of a fly (Jiang et al. 2009). Considering that the ISCs are the main drivers of regeneration of the gut, they have been the center of investigation for tissue homeostasis. Much is known about differentiation activity, regulation of proliferation and also maintenance of ISCs, and research on intestinal ageing has also focused on changes of ISC behavior in one way or another (Rodriguez-Fernandez, Tauc, and Jasper 2020). Ageing can be classified into several distinct cellular hallmarks such as decreased proteostasis, DNA damage, altered signaling etc. (Kennedy et al. 2014; López-Otín et al. 2013). The intestine of *Drosophila* shows many of these changes during the ageing process. In this section I will highlight several of the ageing hallmarks and how they manifest in the ageing intestine, and what we have learned from studying these in a whole-organism context.

1.4.1. Uncontrolled ISC proliferation and aberrant differentiation due to dysregulated signaling.

Although the number of proliferative ISCs increases with age, the fraction of healthy functional ISCs decreases. This is due to the fact that ageing disrupts several of the key signaling pathways, such as Notch, EGFR and JAK/STAT (Biteau, Hochmuth, and Jasper 2008; Biteau et al. 2010). Increased Delta-Notch signaling negatively affects the balance between ISC proliferation and differentiation and this dysregulation is in part triggered by

increased stress-related JNK-signaling in the ageing gut (Biteau et al. 2010). Another example is that the decline in functional ISCs is associated with chronic/repeated activation of the nutrient-dependent mammalian Target of Rapamycin (mTOR) signaling pathway throughout life (Haller et al. 2017). As previously mentioned, increased stress pathway signaling activity by e.g. the Unpaired-JAK/STAT pathway and JNK pathways are among the main drivers of many age-related changes in ISC behavior. In the case of JNK, it has been shown that activation of JNK in old intestine is responsible for changes in orientation of mitotic spindle in favor of symmetric ISC division. This in turn will result in over-proliferation of ISCs, instead of asymmetric division, which results in production of differentiating daughter cells that will eventually result in tissue dysplasia (D. J.-K. Hu and Jasper 2019).

1.4.2. Alterations of microbiome abundance and composition lead to increased inflammation and commensal dysbiosis.

Upon infection, inflammatory signals including interleukin-6 like cytokine (Unpaired, Upd) that is produced by ECs or visceral muscle play important role in activation of JAK/STAT in ISCs and subsequently tissue regeneration (Buchon, Broderick, Chakrabarti, et al. 2009; Buchon, Broderick, Poidevin, et al. 2009; Jiang et al. 2009). In young flies, negative regulatory mechanisms ensure the transient activation of inflammatory responses in conditions like injury, and return to homeostasis once the infection is cleared. For instance, the Dpp pathway plays an important role in the response to infection, but its activation is down-regulated when the infection/stress is over (Ayyaz, Li, and Jasper 2015; McClelland, Jasper, and Biteau 2017; Tracy Cai et al. 2019; Biteau, Hochmuth, and Jasper 2008).

Ageing, however, interrupts these signaling feedback mechanisms and results in permanent low-grade signaling activity that leads to organ-level changes in intestinal cell composition and regionality. For instance, altered JAK/STAT signaling leads to trans-differentiation of acid producing "copper" cells into ECs, resulting in loss of acidity and subsequently commensal dysbiosis in old flies (H. Li, Qi, and Jasper 2016). In addition to JAK/STAT, increase in the bacterial population in the gut is accompanied by over-activation of Foxo in ECs and subsequent decrease in expression of genes that encode

class SC of peptidoglycan recognition proteins (PGRP-SC). This in turn negatively regulates the IMD/Rel pathway (Bischoff et al. 2006). Over-expression of PGRP-SC in ECs reverses the abovementioned phenotypes and is able to extend organismal lifespan (L. Guo et al. 2014). Interestingly, many of the age-related changes in the gut including tissue dysplasia, ISC hyper-proliferation and also increase in inflammatory pathways are delayed in flies that lack a microbiome through raising in axenic conditions (L. Guo et al. 2014; H. Li, Qi, and Jasper 2016). This type of increased, dysregulated immune signaling is reminiscent of the phenomenon of Inflammageing (Franceschi et al. 2018), which is the altered, low-grade activation of the immune system due to ageing and over-nutrition, leading to immune system exhaustion and low-grade inflammation in various tissues of the body. Although *Drosophila* does not have an adaptive immune system, a similar phenomenon of increased inflammation and altered immune signaling, coupled with increased bacterial dysbiosis is associated with *Drosophila* intestinal ageing (L. Guo et al. 2014).

1.4.3. Loss of gut structural integrity and metabolic dysfunction.

Next to effects on signaling and the microbiome, ageing also affects intestinal function on an organismal level. Increased gut permeability becomes a problem with advanced age, both in flies and mammals (Thevaranjan et al. 2017) and this is connected with the increased microbial dysbiosis seen in old gut. In *Drosophila*, Septate Junctions (SJs), the fly versions of tight junctions, are the multi-protein structures between cells that form a tight barrier that keeps small molecules and larger particles such as viruses and bacteria from passing into the intercellular space. Increased passage of small molecules and bacterial antigens from the gut into the abdomen space is one of the hallmarks of the ageing intestine (Rera, Clark, and Walker 2012) and can be easily addressed with feeding flies with blue dye-colored food (Smurf assay). Ageing results in a transcriptional down-regulation of many of the core components of the SJ complex and an increased in miss-localization of core SJ-proteins is seen in ageing guts (Resnik-Docampo et al. 2017).

Moreover, many of the key metabolic sensing pathways involved in ageing, including Insulin/IGF1 signaling (IIS)/Foxo, AMP-activated protein kinase (AMPK), mTOR and Calcium signaling are all shown to either influence lifespan in the gut by affecting ISC behavior or in some cases by affecting gut permeability (reviewed in (Rodriguez-Fernandez, Tauc, and Jasper 2020; Jasper 2020). As an example, reduction of IIS signaling in the entire body, in addition to increasing lifespan, results in decreased age related ISC hyper-proliferation and subsequent hyperplasia (Biteau et al. 2010). In another example, Bolukbasi et al. showed that FoxA transcription factor homolog Fork Head (FKH) acts downstream of IIS and its function is essential for the effect of reduced insulin signaling in extending lifespan. Moreover they observed that over-expression of FKH in the gut is associated with improved barrier function and increase life span without affecting ISC behavior (Bolukbasi et al. 2017).

Another example of effects of nutrient sensing pathways in the gut on age associated phenotypes is the role of dFoxo in regulating lipid metabolism. It has been shown that in normal condition activation of Foxo signaling represses the lipase enzymes in ECs. During ageing, elevated activity of JNK signaling results in activation of Foxo. This activation subsequently impairs the lipid metabolism which contributes to the overall decline of lipid levels in the gut in old flies (Karpac, Biteau, and Jasper 2013).

Not surprisingly, various approaches that have been shown to improve lifespan, including drugs such as Rapamycin and regimes like calorie restriction, have positive effects on intestinal homeostasis (Fan et al. 2015; Regan et al. 2016). More recently, we showed that even short term administration of Rapamycin is able to preserve some of the geroprotective effects but without usual side effects that chronic administration causes. We observed that the beneficial effect of early life treatment could last for long period after stopping the administration of drug. This effect is mediated by elevated autophagy in intestinal enterocytes, which is in parallel with increased levels of intestinal LManV and lysozyme (Juricic et al. 2022).

Despite all the progress, one general shortcoming in the field is that so far most of the focus has been on study of effects of ageing (and many other diseases/conditions) only in female intestine. The main reason for this is the fact that the intestine in mated female flies is larger and also has higher turnover rate, which makes it a better system for study of dynamics of cellular and molecular changes. Only recently we began to explore the differences in male and female intestine. Interestingly, it has been shown that cell intrinsic differences between genders determines the size and turnover rate of male and female guts (Hudry, Khadayate, and Miguel-Aliaga 2016). Moreover, it is becoming clear that these differences are among the factors that regulate response of the intestine to dietary interventions (Regan et al. 2018).

1.5. Cell differentiation and intestinal plasticity

Since the identification of ISCs by the Perrimon and Spradling labs in 2006, Notch signaling has been recognized as a main signaling pathway that determines their differentiation into EC and EE cells (Micchelli and Perrimon 2006; Ohlstein and Spradling 2006). In this model, Notch signaling is active in ISC-EB pairs and levels of Notch signaling between ISC and its daughter EB determines the EC or EE fate outcome.

One of the determining steps in cell differentiation, and also in broader sense in developmental processes, is change in cell polarity and symmetry. With having membrane bound receptors and ligands, Notch signaling is well suited to pattern cells and organs in a coordinated fashion. The possibility of modulating Notch receptors and ligands provides a mechanism for lateral inhibition or induction, and finally determines the fate of cells (Reviewed in (Sjöqvist and Andersson 2019). In the case of ISCs differentiation, lateral inhibition by Notch plays a pivotal role. ISCs that express the Notch ligand "Delta" divide and produce two daughter cell. One of these cells will retains ISC properties including *delta* expression, and maintains the ISC population. At the same time Delta activates Notch receptors on its sister cell (EB). Interestingly, it appears that Delta asymmetry is a result of down-regulation of this gene in EBs after mitosis. This asymmetry eventually results in the exit of EBs from the mitotic cell cycle and differentiation to ECs

14

(Ohlstein and Spradling 2007). In contrast, EEs are produced from ISCs with low (or no) cytoplasmic Delta. Lack of Notch signaling in null Notch allele mutant ISC clones leads to production of highly proliferative ISC-like or EE precursor-like cells (Patel et al 2015, Perrimon and Spradling papers). These findings showed that lateral inhibition feedback from daughter cells is a key feature to ensure correct lineage specification.

Differentiation of EE cells is more complicated than that of ECs, mainly because it coincides with molecular mechanisms that regulate stem cell identity and self-renewal and there is not a clearly-defined intermediate progenitor cell such as the EB. Two distinct molecular mechanisms have been specifically implicated in this process, namely Regulation of *achaete-acute* complex (*AS-C*) genes including *asense* (*ase*) and *scute* (*sc*), and the action of Escargot (Esg), a protein that maintains stemness and also affects EE specification through its antagonistic activity with *sc* (Bardin et al. 2010; Korzelius et al. 2014).

In 2010 Bardin and colleagues showed that *achaete-scute* complex genes especially *ase* and *sc* are required for EE differentiation (Bardin et al. 2010). Interestingly, they concluded that these two genes are not required for stemness as their inactivation does not change Delta expression or clonal expansion of ISCs, an argument that was questioned in coming years (Chen et al. 2018).

Later on, *esg* which is expressed in ISC/EB cells, was shown to act as a factor to maintain ISC identity (Korzelius et al. 2014). It has been shown that lack of Esg results in up-regulation of a number of genes that are involved in EE cell fate specification including *achaete-scute* complex genes and also *prospero (pros)*.

In 2017 a paper from Rongwen Xi's lab connected these findings to EE fate determination by proposing a mechanism by which Sc and Esg coordinately regulate expression of *pros* and subsequently determine EE cell fate. Esg acts as a stem cell maintenance factor and prevents EE differentiation, and its inhibition results in activation of Sc and subsequent EE cell differentiation. Using epistasis experiments they showed that Sc acts

antagonistically with Esg in determining the EE cell fate. Moreover, by using chromatin precipitation experiments, they showed that both Sc and Esg bind to a specific region on the promoter of *pros*. Furthermore, other genetic studies using epistasis experiments revealed that Esg acts in parallel with Notch and upstream of Sc to determine EE fate (Y. Li et al. 2017). All in all, these data showed that differentiation of EEs from ISCs requires transient activation of a number of TFs, and this activation needs to be finely tuned in order to keep balance between ISC self-renewal and EE differentiation.

1.6. Enteroendocrine cell differentiation; from enteroendocrine cell precursors to mature enteroendocrine cells

The determination of the EE cell fate from ISCs was initially thought to result only from a lack of Notch signaling upon ISC division, with the EC/EE decision dependent solely on the level of Notch activity in the ISC daughter after division (Ohlstein and Spradling 2007; Perdigoto, Schweisguth, and Bardin 2011). In 2015 Guo and Ohlstein proposed a model in which accumulation of Pros at the apical site of dividing ISC followed by asymmetric ISC division results in formation of EE cells that express Delta (Z. Guo and Ohlstein 2015). This Delta ligand then activates Notch signaling in the adjacent ISC, which leads to retaining of the stem cell identity. In case of ECs however, the direction of Notch signaling is from ISC to EB and eventually to EC. Therefore, the fact that EEs are produced from a different progenitor cell rather than EBs was becoming more evident. Similarly, Zeng and Hou and Biteau and Jasper provided evidence for differentiation of ECs but not EEs from Su(H)GBE+ EB cells (Zeng and Hou 2015; Biteau and Jasper 2014). In line with the findings of Guo and Ohlstein they also identified a subset of EEs that are positive for both Pros and Delta.

These finding shed light on the complexity of EE differentiation and the involvement of other regulators apart from Notch pathway components. Mainly, the Achaete-Scute family members were found to be required in both ISC proliferation and EE differentiation (Bardin et al. 2010; Chen et al. 2018). Wang et al for instance, showed that the BTB

domain-containing transcriptional repressor Ttk69 acts in parallel to Notch signaling by repressing EE cell specification through inactivation of *AS-C* complex genes (C. Wang et al. 2015). Later it was shown that a negative regulatory feedback loop exists between Ttk69, Phyllopod (Phyl) and Sina. Phyl acts as a bridge to connect Ttk69 with Sina (an E3 ubiquitin ligase). Formation of this protein complex leads to degradation of Ttk69 by Sina and subsequently activates *AS-C* genes, resulting in differentiation towards EEs. Intriguingly, they found that activation of *AS-C* genes induces expression of *phyl*, hence strengthening EE commitment and production through a positive regulatory feedback (Yin and Xi 2018).

This work showed that *sc* has a key role in EE differentiation from ISCs. Intriguingly, the regulation of *sc* in ISCs happens through two regulatory feedback loops that ensure transient activation of this gene. A self-stimulatory loop ensures that *sc* expression gradually increases in the ISCs until it reaches a level that is sufficient for inducing ISC mitosis. This increase results in production of an ISC and an EE progenitor cell, and in parallel activates *E(spl)* genes. As constant *sc* expression would result in ISC depletion due to excess differentiation into the EE lineage, a negative feedback loop between *E(spl)* genes and *sc* ensures that *sc* expression returns to basal levels, hence preventing ISC depletion. Together, the intertwining activities of this network of TFs leads to EE differentiation (summarized in Figure 3a). Moreover, it seems that *E(spl)* genes are not the only negative regulators of *sc* expression as their depletion does not result in constant activation of *sc* (Chen et al. 2018). *sc* is additionally regulated indirectly through Tramtrack, which is in turn regulated post-transcriptionally through a proteasome degradation complex with Sina and Phyl proteins (Yin and Xi 2018; C. Wang et al. 2015).

Interestingly, a parallel negative regulatory mechanism was found by Biteau and Jasper through the Slit/Robo signaling pathway. They find that Slit ligands secreted from EEs activate the pathway in the ISCs by binding to Robo2 receptor. This activation results in inhibition of ISCs from differentiating into the EE lineage. Moreover they showed that this happens upstream of Pros and independent of the activation of Notch pathway (Biteau and Jasper 2014).

All in all these findings show the complexity of the gene regulatory network (GRN) controlling EE differentiation with involvement of various regulatory loops and parallel pathways that work in concert to determine EE fate (Figure 3a).

1.7. Parallels with differentiation of the mammalian secretory cell lineage

Despite the fact that the mammalian intestine has more complexity in cell type composition compared to *Drosophila*, several of the key signaling pathways that determine secretory vs absorptive cell fate have been evolutionarily conserved. Figure 3 compares the main differentiation events that take place in *Drosophila* and mammals. Recent studies in mouse, using time-resolved lineage labeling combined with single-cell gene expression analysis, showed that a switch from canonical to PCP/non-canonical Wnt signaling is the earliest event that happens in ISCs to determine secretory lineage specification (Böttcher et al. 2021). After this initial step, Notch signaling plays a pivotal role in determining secretory vs absorptive cell fate decision, similar to the situation in the *Drosophila* midgut. Similar to the midgut, in mammals the Notch target bHLH transcription factors are the most important TFs governing the absorptive versus endocrine fate choice. High levels of Notch activity promote the expression of Hairy and Enhancer of Split 1 (Hes1) bHLH transcription factor which will eventually lead to absorptive cell fate (van Es, van Gijn, et al. 2005; Pellegrinet et al. 2011; VanDussen et al. 2012; Carulli et al. 2015; Fre et al. 2005). On the other hand, Notch has an inhibitory effect on Atoh1/Math1, a bHLH TF related to the *AS-C* genes in *Drosophila*. Depletion of Notch or Hes1 results in cell cycle arrest and commitment to secretory cell lineage differentiation, while inactivation of *Atoh1* results in depletion of three main secretory cell types (Paneth cells, goblet cells and EE cells) in mouse (Q. Yang et al. 2001).

18
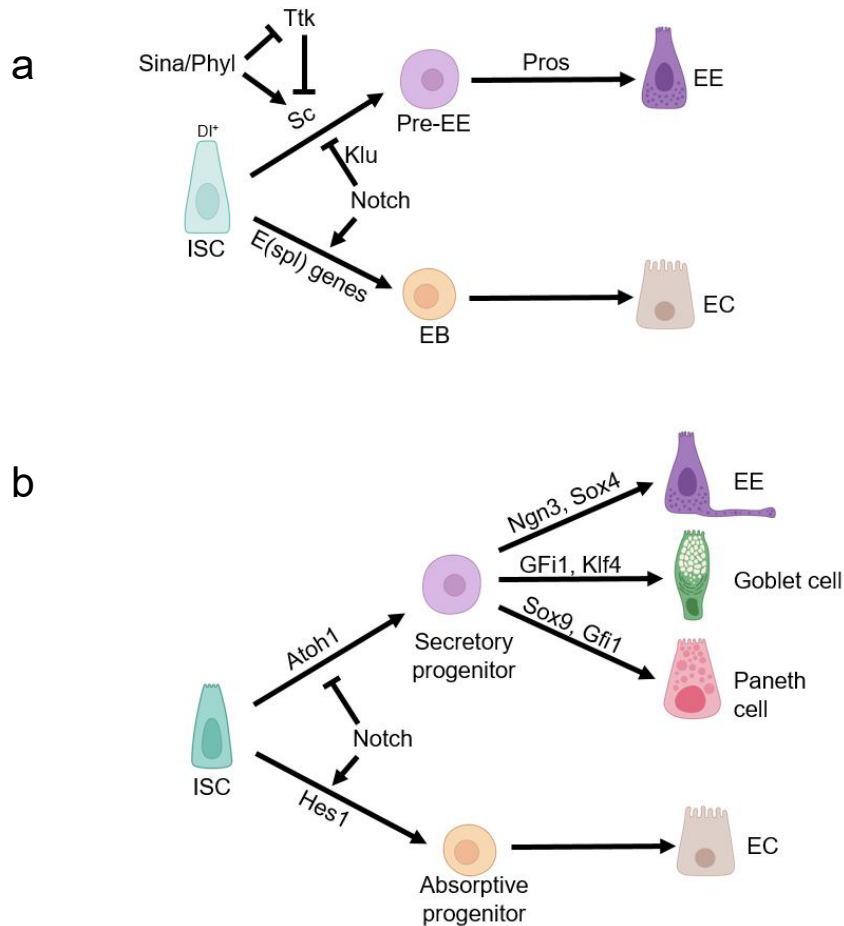
Figure 3. Schematic representation of intestinal cell differentiation in *Drosophila* and mammals.
a: In *Drosophila* depending on Notch activity, delta positive ISCs give rise to two types of progenitor cells; pre-EE cells generate through activity of bHLH TF Scute and EBs form by activation of *E(spl)* gene family. Pre EEs will subsequently mature by activation of Pros. b: In mammals, in the absence of Notch signaling, Atoh1 dictates the lineage commitment for the entire secretory cells. Ngn3 TF then directs EE lineage specification while Klf4 and Sox9 are responsible for goblet and Paneth cell differentiation respectively.

Whereas Atoh1/Math1 acts as a master upstream regulator of secretory fate, the different subtypes of secretory cells, including EE cells, are governed by subsequent downstream activation of other specific TFs.

In the case of goblet cell specification, *Atoh1* activation leads to activation of growth factor independent protein 1 (Gfi1) which together with elevated levels of mitogen-activated protein kinase (MAPK) activity determines the goblet cell fate (Shroyer et al. 2005; Heuberger et al. 2014). Some region-specific TFs also play role in secretory cell differentiation, and one example of such TFs is zinc finger TF Kruppel-like factor 4 (Klf4).

Depletion of Klf4 results in lack of goblet cells in colon, but not in small intestine (Katz et al. 2002).

Paneth cell differentiation starts with activation of Atoh1, but also requires elevated Wnt signaling activity. High-mobility group (HMG) protein Sox9 is the main TF that acts downstream of Wnt signaling to determine Paneth cell fate, and its inactivation results in depletion of Paneth cells in the gut (Mori-Akiyama et al. 2007; van Es, Jay, et al. 2005). Most Paneth cells originate from slowly dividing Label Retaining Cells (LRCs). While in normal homeostatic conditions these Paneth cells support the ISCs, upon injury activation of *Bmi1* and repression of Paneth-specific genes results in their proliferation and regeneration (Roth et al. 2012).

Mammalian EE specification depends on expression of the bHLH family member TF Neurogenin 3 (Ngn3). *ngn3* is exclusively expressed in pre-EE cells and its abundance reduces during the maturation process of EE cells (Gehart et al. 2019; Jenny et al. 2002). In addition to *ngn3*, other TFs including *sox4*, which is a member of the HMG family of TFs, also play role in early stages of EE cell specification in the bottom of crypt structure in the intestine. *sox4* is transiently expressed at the start of EE differentiation process, and its deletion results in loss of all GLP1-positive EEs in duodenum and jejunum, indicating its essential role in differentiation of specific subtypes of EEs.

The negative regulatory interactions by TFs in the GRN controlling secretory differentiation play an important role in cementing cell fate decisions and the directionality of differentiation. A clear example of this is the dual role of *gfi1* which is abundantly expressed in goblet cells and, in addition to determining their fate, inhibits fate conversion of this cells toward the EE lineage (Shroyer et al. 2005; Matthew Bjerknes and Cheng 2010).

Despite the fact that much progress has been made in EE cell lineage commitment in the mammalian intestine, there are still many unknown aspects that need to be investigated. For one, the exact relation between the potency of the different progenitor cell states and mature EE cells is still not fully understood. A recent report showed that, unlike previous assumptions, uni-potent, and not bi- or multi-potent, secretory progenitor cells are responsible for mediating the differentiation of EE and Paneth cells (Buczacki et al. 2013).

1.8. Enteroendocrine cells in the intestine act as a local and systemic signaling hub

The contents of the intestine are made up of ingested nutrients, chemicals and microbes amongst others. This content needs to be scanned for nutritional value, chemical composition and assessed for potential harmful pathogens. This information will then need to be relayed to distant tissues such as the liver, pancreas, brain as well as the immune system. There are multiple cell types at work in the intestine that ensure this happens in a precise and coordinated fashion. These include the nervous system, the enteroendocrine system and also the immune system of the gut. Other reviews excellently cover the gut-brain axis and the role of the immune system in maintaining intestinal health (Mayer, Nance, and Chen 2022; Latorre et al. 2016; Wachsmuth, Weninger, and Duca 2022). As the focus of my thesis, here I will specifically expand on the role of entero-endocrine (EE) cells as a signaling hub for intestinal inter-organ communication.

The entero-endocrine system is responsible for regulating both local and systemic responses to contents of the intestine, hence affecting different physiological and cellular behaviors. As an example of local signals, it has been shown that an EE subtype called G-cells in mice can affect a specific population of gastric stem cells that resides in 4+ region of the crypt and express the gastrin/CCK2 receptor (*cck2r*). While the precursor form of the hormone Gastrin (progastrin) activates this population, amidated gastrin that is secreted from G cells inhibits ISC activation and acts as a tumor suppressor (Chang et al. 2020). A prime example of the systemic regulation of glucose metabolism by EEs is the action of the glucagon-like peptide-1 (GLP-1) secreted from L cells in the gut. This hormone regulates glucose abundance, hence affecting its availability in the body and GLP-1 agonists are used in the clinic as prime candidate for the reduction of Type II diabetes and for weight loss through appetite control (Gribble and Reimann 2021). Another example of the physiological effect of EEs is regulation of stomach acidity by binding of gastrin to Cck2r receptor in parietal cells of the stomach and subsequent acid secretion.

EEs exert many of their main functions in local and inter-organ communication through the production and secretion of peptide hormones in response to various stimuli. Different types of EE cells produce different levels of these hormones. Hence, EE subtype classification has been based on the type of hormone that they predominantly produce. In mammals for instance, there were seven types of EEs which have been shown by letters (D, I, K, L, X, S, N) (Reviewed in: Beumer and Clevers 2021), and based on low-throughput, single time point studies it was believed that each of these cell types are capable of producing only a single hormone. Recent advances in the field of molecular biology, especially single cell transcriptome analysis, changed this "one hormone-one cell type" concept. Now we know that in both mammals and *Drosophila*, depending on the position, age and transcriptional program of the cell, a single EE can produce more than one type of hormone, and one hormone can be produced by multiple types of EE (X. Guo et al. 2019; Beumer et al. 2020). These findings revealed that EE biology is more complicated than previously thought and much is to be learned about the classification and specification of EE subtypes.

In the *Drosophila* midgut, EEs produce 11 different pro-hormone precursors that upon processing give rise to more than 25 different peptides (Nässel and Zandawala 2020). *Drosophila* EE hormones are produced by enteroendocrine cells in a region-specific manner. Table 1 summarizes the hormones that *Drosophila* EEs produce and their place of expression in the gut, as well as their known functions. These hormones regulate a wide range of physiological and cellular functions in *Drosophila*, ranging from local regulation of stem cell proliferation (e.g.Tachykinin (Tk) to more systemic functions including regulation of visceral muscle contraction (for Diuretic Hormone-31 (Dh31), control of metabolism and feeding (for Neuropeptide F (NPF), and even control of circadian rhythm (CCHa2 and NPF). Despite the importance and the range of cellular and physiological functions that EE hormones have, most of the historic focus in insect endocrinology has been on the neuropeptides that originate from the nervous system.

Table 1. *Drosophila* EE peptide hormones.

Regions that they are produced and secreted from, developmental stage in which they have been detected and their function. A: Anterior midgut, M: Middle midgut, P: Posterior midgut, L: Larvae, A: Adult, ?: Unknown or not confirmed function (Nässel and Zandawala 2020).

Peptide	Region	Stage	Function in the midgut
NPF	A, M	L/A	Feeding control, regulate DILPs and IKH, regulate GSCs, lipid metabolism
Orcokinin	M	L/A	?
TK	A, M, P	L/A	Lipid metabolism, ISC proliferation
sNPF	A	L/A	?
CCHa1	P	L/A	Regulate arousability?
CCHa2	A,P	L/A	Signal to IPCs
AstA	P	L/A	Signal to AKH cells and IPCs, regulation of gut contraction, regulation of K^+ absorption
AstB/MIP	M, P	L/A	?
AstC	A, M, P	L/A	?
DH31	P	L/A	Muscle contraction of middle midgut
Bursicon α	P	A	Regulation of AKH, regulate midgut visceral muscle contraction

Hormones require various steps of precursor processing before they are secreted in their final, bio-active form. The processing of hormones is at the beginning of a proteolytic cascade of events resulting in maturation of functional peptide hormones. This is achieved by function of different classes of enzymes including prohormone convertases, carboxypeptidases, and amidating enzymes. In *Drosophila* EEs and also in cells of the nervous system, two main types of prohormone convertases Amontillado (Amon) and Silver (Svr) are responsible for the processing of hormones and their maturation. Amon is responsible for the first processing step of prohormone conversion in *Drosophila* by cutting the C-terminal of canonic mono or dibasic amino acids (including R, KR or RR). It has been shown that expression pattern of Amon in the gut and nervous system matches that of EEs and peptidergic neurons. Importantly, eliminating Amon results in loss of most of the mature EE hormones in the gut (Wegener et al. 2011). The subsequent steps of

this process are carried out by *Silver*, which encodes a carboxypeptidase enzyme. It is evident that prohormone processing in *Drosophila* is much simpler than in mammals which have 4 different pro-hormone convertases in EE cells (Rehfeld et al. 2008).

After maturation, the release of EE hormones is under the control of environmental as well as internal signals. Various types of molecules can trigger release of hormones from EEs: Tk- and Dh31-producing EEs get activated by the presence of protein in the food (Park et al. 2016; Song, Veenstra, and Perrimon 2020). NPF secretion, on the other hand, is regulated by sugar intake from food as well as by the sex peptide (SP) hormone that reaches the gut after mating (Ameku et al. 2018; Yoshinari et al. 2021).

Hence, multiple levels of control over hormone activity exist in the intestine: transcriptional control of their production by different TFs, processing into their final mature peptides and their secretion from EEs can all be regulated by various internal and external inputs. The range of functions exerted by EE hormones is very broad. Some EE hormones control lipid metabolism through affecting carpora cardiaca (CC) or insulin producing cells (IPCs) and subsequently modulation of DILPs or Adipokinetic Hormone (AKH). Bursicon α and NPF can also suppress lipid storage through inactivation of *AKH* , although the mode of action is different for each of them; while Bursicon α regulation of *AKH* is indirect and through *lgr2* expressing neurons, NPF directly suppresses *AKH* by affecting CC cells (Scopelliti et al. 2019; Yoshinari et al. 2021).Tachykinin on the other hand regulates general lipid homeostasis by influencing gut lipid storage (Amcheslavsky et al. 2014). CCHa2 can also act through IPCs in the brain and regulates food intake (Ren et al. 2015; Sano et al. 2015).

1.9. Hormonal plasticity and its relation to enteroendocrine subtype classification

EE cells of the *Drosophila* midgut were initially divided into two classes based on the main hormones that they produce; Class I cells that mainly express AstC and class II cells which express Tk. More recently Guo et al have classified EE cells into three major sub-

types (AstA, AstC and NPF) and 10 different subtypes based on single cell RNA sequencing data (X. Guo et al. 2019). In their dataset, 14 peptide hormones of EEs had expression including *AstA, AstC, Tk, NPF, sNPF, DH31, CCHa1, CCHa2, Mip* and *Orcokinin*. This study also showed that each EE subtype expresses 2-5 different peptide hormones. In addition to hormones, EEs also express genes of the G protein-coupled receptor (GPCR) family that can receive and respond to EE hormones. Interestingly, in most cases the place of production of hormones and its corresponding receptor are different. CCHa1 for example is mostly produced in posterior section of the midgut. Its receptor however has expression in EEs in the middle and anterior parts and also in visceral muscle surrounding the middle section of the midgut.

In both *Drosophila* and mammals the expression, translation, posttranslational modifications and finally secretion of each of EE hormones show great variability in spatiotemporal manner throughout the gut. In *Drosophila* this heterogeneity becomes apparent from single cell analysis that shows almost all EE cells are capable of producing more than one hormone and, more interestingly, that the positioning of EE cells in the gut is a strong determining factor that dictates the type of hormone that the EE cell produces. Table 2. summarizes the spatial distribution of *Drosophila* EE hormones along the midgut axes and lists the TFs active in each of EE cell types in that region.

Table 2. Place of production of EE hormones in *Drosophila* intestine and transcription factors that are associated with them.

TF: transcription factor (adapted from (X. Guo et al. 2019).

Region	Hormone combinations	TF
R2a, R2b	AstC, Orcokinin	Mamo, Exex, Dac
R2a, R2b	sNPF, CCHa2, Orcokinin (low)	Mano, Sug, Fer1
R2	AstC, Orcokinin, CCHa1	Mamo, Fer1
R2	Tk, NPF, DH31 (part of), CCHa1 (part of)	Mirr, Notch
R3	AstC, Orcokinin	Mamo, Exex, Dac
R3	Tk, NPF, Mip (part of), Nplp2 (part of)	Esg,Ptx1, NK7.1
R4	AstC, CCHa1, CCHa2, Mip	Fer1, Sug, Nlp
R4, R5	AstC, CCHa1	Nlp
R4c, R5	AstC, AstA, CCHa1	Drm, Fer1, Nlp
R4c, R5	Tk, CCHa1, DH31, NPF (part of)	Drm, NK7.1, Nlp

Due to the large size of the mammalian intestine, the data regarding the spatial distribution of EEs and the hormones they produce is still far from being complete and needs more investigation (Beumer et al. 2020; Gehart et al. 2019; Haber et al. 2017; Grün et al. 2015). However, it is likely that the classification of EEs in mammals also requires revision in the light of new advances in single cell technology.

A major caveat of single-cell gene expression profiling is that it, too, often classifies cells with a different expression profile as different cell (sub)-types. Cell classification happens either automatically by measuring distance in multi-dimensional space by t-SNE or UMAP, or is done using manual classifiers. Both methods have their disadvantages and can overestimate differences between individual cells. On the other hand, sc-Seq can also miss distinct cell types and cluster them together, although they are functionally

distinct, e.g. sc-Seq analysis of the fly intestine has failed to distinguish ISCs from EBs by clustering alone (Hung et al. 2020), whereas these cells are clearly distinct both in functionality as in morphology. Furthermore, the sequencing depth of most sc-Seq platforms is not sufficient to pick up meaningful differences in e.g. transcription factors, which are often lowly expressed, between individual cells (Wu et al. 2014). Hence, determining the GRN that control sub-type specification will rely on other technologies as well such as bulk RNA-Seq, localization studies and cell-type specific knockdown experiments.

1.10. Regulation of enteroendocrine cell heterogeneity

EE subtype heterogeneity is regulated by both external environmental cues as well as internal cues such as cell type-specific transcriptional factors. Externally, both niche-specific and environmental factors play a role in determining type of hormones that EEs produce. In mammals for instance, morphogen gradients along the crypt-villus axis regulate the type of hormones that EEs produce (Beumer et al. 2018). Specifically, a BMP-signaling gradient along the crypt-villus axis drives hormone "reprograming" in L cells, resulting in decreased GLP-1 production and increase in PYY production, hence changing the identity of so called L cells to I and finally N during maturation along the villus.

In *Drosophila* Notch signaling plays an important role in specifying EE subtypes, in addition to its general role in EE differentiation(X. Guo et al. 2019; Beehler-Evans and Micchelli 2015). Absence of Notch results in depletion of TK$^+$ class II EEs while promoting AstC$^+$ class I formation (X. Guo et al. 2019). Interestingly, newly differentiated EE pairs in the intestine can each produce a separate hormone. For example, one of the cells in an EE pair can be TK$^+$ while the other one is AstC$^+$. Considering the lateral inhibition that is a key mechanism of Notch feedback regulation, it is possible that it regulates specification of each of EEs to class I or II fate at progenitor stage. Unlike Notch, the role of other morphogenic factors including BMP or Wnt signaling in EE hormonal plasticity in *Drosophila* is still unclear and needs further investigation.

In addition to niche-specific signals, nutrients and gut microbiota also play role in determination of type of hormones that EEs produce. In mice for instance, high lipid diet results in a general decrease in the number of EEs with more evident effects on L cell numbers, and systemic reduction of gut hormones. This reduction is accompanied by downregulation of TFs that regulate EE specification including *math1*, *atoh1*, *NEUROD1*, *pax6* and *pax4* (Nässel and Winther 2010; Moran-Ramos, Tovar, and Torres 2012; Richards et al. 2016).

In *Drosophila*, dietary cholesterol changes the level and duration of Notch activity and subsequently ISC differentiation. Reducing cholesterol in the food, or knocking down its receptor *Hr96* in the nucleus, results in reduction of EE cell numbers in the posterior midgut. Interestingly, decrease in the lipid content of the food was associated with increased Notch activity, but not with ISC proliferation changes or cell death rate. These results provide evidence for diet-dependent regulation of Notch and subsequently EE differentiation that is independent of cell proliferation in *Drosophila*. (Obniski, Sieber, and Spradling 2018). On the other hand, and not surprisingly, there are numerous reports of effects of different contents of the food on EE hormone production. For instance, it has been recently shown that sugar in the diet could increase production and secretion of NPF from EEs in the gut (Yoshinari et al. 2021). This gut-derived NPF has an incretin-like function and results in suppression of AKH and enhanced secretion of DILPs, resulting in decreased lipid anabolism.

Despite the potential and diversity of EE hormones, it is hard to distinguish the mode and place of action for many of these, mostly because the necessary tools for studying the midgut EE population are limited or non-specific. Most experiments use the *pros-Gal4* driver to express genes/RNAi's of interest in EEs, but in addition to EE cells of the intestine, *pros* is also expressed in various regions of the brain, including the areas that are responsible for producing neuropeptides that are genetically identical to those produced in the gut. Hence separating gut-derived from brain derived activity of EE hormones remains a challenge. More recently, gut-specific EE drivers have been generated that mostly rely on using promoter regions of the hormones (namely Tk) that are specifically active in the gut but not in the brain (Amcheslavsky et al. 2014). Despite

being an improvement, expression of many of these drivers is restricted to specific subtypes of EEs and cannot be used as a pan-EE diver like *pros*. We have attempted to use pan-neuronal drivers such as *elav* and *syb* to express *Gal80* in the brain, thereby restricting *Gal4* expression to gut EE's only. Unfortunately, *Gal80* expression using these drivers also inhibits EE *Gal4* activity (S. Azami and J. Korzelius, unpublished observations). Hence, finding a pan-EE driver that is restricted to the midgut would be a critical step in gaining more understanding of EE biology both locally and systemically.

1.11. Aims of the project

The gene regulatory network governing ISC differentiation has been the subject of research for more than a decade. This has provided a detailed, but not complete, understanding of events that happen during the process of EE and EC differentiation. Despite this progress, the exact order of events by which the decision between EE and EC is cemented in progenitor cell types has remained unclear.

In the first Results chapter of this thesis, I present the characterization of the Klu TF and how this TF controls fate choice in the enteroblast (EB) progenitor. This work identifies Klu as a factor that acts downstream of Notch, acting to repress *scute* activation in maturing EBs. Transcriptional analysis of Klu target genes has identified potential novel genes that regulate EE differentiation.

The second Results chapter investigates the physiological role of EEs and the hormones produced by these cells in intestinal homeostasis and how EE expression profiles change with ageing. We performed bulk RNA-Seq and sc-Seq of EEs in young and old flies and also focused on the difference between male and female EE cells in our sc-Seq dataset. The main aim of this part of the project is to tackle the changes in EE biology during ageing and between sexes, and to determine the physiological consequences of these changes and how they contribute to organismal ageing.

2.1. Fly work
2.1.1. Fly maintenance

Unless otherwise is stated, fly stocks were fed a conventional sugar/yeast/agar (SYA) (Bass et al. 2007) diet and kept at 65% humidity on a 12:12 hour light:dark cycle. For GAL4 reporter experiments, flies were allowed to mate for two days at 25°C, then transferred onto SYA food with a density of 20 female flies per vial, and kept on 25 °C for the indicated period of time. In order to inhibit expression of UAS-driven RNAi, a temperature-sensitive Gal80 repressor construct (Gal80[ts]) was used. The Gal80[ts] is active at 18°C and can be blocked by transferring flies to 29°C to stimulate Gal4 activity (McGuire et al. 2003). Hence, for these experiments, flies were mated and kept in 18°C and subsequently were transferred to 29°C at a density of 20 female flies per vial for the indicated period of time.

Unless stated otherwise, for all experiments female Gal4 driver flies were crossed with wild type or UAS-construct males.

2.1.2. Fly Lines and Husbandry
The stocks listed below were used in this PhD thesis:

Drosophila Stock Center:

BL28731 (*klu* RNAi on 3rd), BL60469 (*klu* RNAi on 2nd), BL56535 (*UAS-klu[Hto]*), BL1997 (w[*]; P{w[+ mW.hs] = FRT(w[hs])}2A), BL4540 (w[*]; P{w[+mC] = *UAS-FLP.D}JD2*), BL84593 (*AstA-GAL4*), BL84671 (*NPF-GAL4*), BL25800 (*TK* RNAi), BL25866 (*AstA* RNAi), BL25867(*sNPF* RNAi), BL25868 (*AstC* RNAi), BL27237 (*NPF* RNAi), BL25869 (*DSK* RNAi), BL57183 (*CCHa2* RNAi), BL57562 (*CCHa1* RNAi), BL61833 (*orkokinin* RNAi).

VDRC: v27228 (N RNAi).

Other stocks: *klu-Gal4 UAS-GFP, FRT2A kluR51/Tm6B, hs-Flp, Tub-Gal4, UAS-GFP/Fm7;FRT2A, TubGal80ts/Tm2,Ubx* (T. Klein, Düsseldorf),*esg-F/O (w; esg-Gal4, tub-Gal80ts, UAS-GFP; UAS-flp, Act > CD2 > Gal4(UAS-GFP)/TM6B), esg^{ts} (y,w;esg-Gal4, UAS-GFP/CyO;tub-Gal80^{ts}/Tm3), Su(H)^{ts} (w;Su(H)GBE-Gal4,UAS-CD8-GFP/CyO;tub-Gal80ts/TM3), Su(H)-F/O genotype (control) w;Su(H)GBE-Gal4, UAS-CD8-GFP/CyO;tub-Gal80ts/UAS-Flp, Act > CD2 > Gal4, Su(H)-F/O genotype (klu^{RNAi}) w;Su(H)GBE-Gal4,UAS-CD8-GFP/kluRNAi BL60469;tub-Gal80^{ts}/UAS-Flp, Act > CD2 > Gal4, ISC-specific esg^{ts}29 w;esg-GAL4,UAS-2XEYFP/CyO;Su(H)GBEGAL80, tub-Gal80^{ts}/TM3,Sb, w;esg-gal4, tub-Gal80^{ts}, UAS-GFP/CyO,wg-lacZ;P{w [+ mC] = UAS-FLP.D}JD2/Tm6B, w,10XUAS-GFP(attp40)/CyOwglacZ;MKRS/TM6B, w;tub-Gal80^{ts},UAS-GFP/CyO,wgLacZ;Prosv1-Gal4/Tm6B, w;Tk-Gal4* (gut-specific).

For all experiments flies were collected 2-3 days after eclosion, and kept on standard cornmeal food. For induction of RNAi lines using the temperature sensitive Gal80 (Gal80^{ts}) construct, parent flies were crossed and kept at the restrictive temperature of 18ºC. 4-7 days after collection flies were transferred to 29 degrees in order to deactivate Gal80 and initiate Gal4 driven RNAi expression.

2.1.3. Fly Genetics

For all experiments female flies containing the GAL4 driver were crossed with male UAS flies or WT. To generate the temperature-sensitive *pros-GAL4* line, flies containing the *pros^{V1}-GAL4* insertion on the third chromosome were crossed with flies containing *Gal80^{ts}, UAS-GFP* on the second chromosome. Stable stocks were generated that have the following genotype: *w;tub-Gal80ts,UAS-GFP/CyO,wgLacZ;Prosv1-Gal4/Tm6B.*

2.1.4. Backcrossing

For backcrossing of RNAi and UAS over-expression constructs, we backcrossed these in the $w^{Dahomey}$ (w^{Dah}) background. 25 male flies of the desired genotype were crossed to 25 female w^{Dah} flies to start the backcross. 25 virgin flies from this first cross were then mated with 25 male w^{Dah} flies and the process were repeated for at least 6 generations. Finally, to make the desired construct homozygous, backcrossed flies were mated to backcrossed flies of the same w^{Dah} background containing TM6B or CyO balancer chromosomes. For flies from the Perrimon lab/Harvard Medical School TRIP RNAi collection, which are marked by a *vermillion (v)* rescue construct, a $v^{Dahomey}$ background was used for backcrossing.

2.2. Molecular biology

2.2.1. RNA extraction, cDNA synthesis and quantitative real time PCR (qRT-PCR)

Total RNA was extracted by Trizol reagent (Invitrogen) according to the manufacturer's instructions. For the bulk RNA sequencing experiment, Arcturus PicoPure RNA isolation kit (Thermo Fisher scientific) was used according to manufacturer's instructions. To remove genomic DNA, samples were treated with DNase I (ThermoFisher) according to manufacturer's instructions. RNA concentration was measured either by NanoDrop I, or Qubit BR RNA assay (ThermoFisher). cDNA was synthesized using 150ng/µl concentration of extracted mRNA using the SuperScript III first-strand synthesis kit (Invitrogen) and poly T, according to the manufacturer's instructions.

For qRT-PCR, TaqMan Master Mix (ThermoFisher) was used according to the manufacturer's manual and Act5c was used as internal control gene. qRT-PCR was performed using QuantStudio7 (ThermoFisher). Relative expression (fold induction) was calculated using the ΔΔCT method and Act5C was used as a normalization control.

2.2.2. Immunostaining of adult *Drosophila* guts

10-15 guts from adult female flies were dissected in 1x Phosphate-Buffered Saline (PBS) and transferred to fixative comprising of 4% formaldehyde in 1x PBS solution for 45 minutes. A Buffer of 1x PBS containing 0.15% Triton X100 was used as washing buffer. After 30 minutes wash in washing buffer, guts were transferred in blocking solution containing PBT with 0.3% bovine serum albumin for minimum of 30 minutes. Subsequently, guts were incubated in primary antibody at 4°C overnight followed by washing for an hour and incubation at secondary antibody for 2 hours. After second antibody incubation, guts were washed for 45 minutes in washing buffer and finally were mounted on slide using VectaShield Antifade Mounting Medium with DAPI (Vectorlabs). The following primary antibodies were used for the immunostaining:

Chicken anti-GFP (1:1000; ThermoFisher A10262), mouse anti-Prospero (MR1A, 1:50, DSHB), mouse antibeta-galactosidase (40-1a, 1:200; DSHB), mouse anti-Armadillo (N2 7A1, 1:20; DSHB), rabbit antiphosphorylated Histone H3-Ser10 (pH3S10, 1:500, sc8656-R; Santa Cruz Biotechnology), Guinea pig anti-NPF (a gift from Dr. Ryusuke Niwa).

2.2.3. FACS

For scRNA-Seq, males of genotype $pros^{v1}$-GAL4>10xUAS-GFP were crossed to w1118 virgins and male and female progeny were allowed to mate for two days (except for the virgin condition) and kept on normal SY food for the respective time points. 70-100 midguts/genotype were dissected in triplicate, and for each sample (except old male sample) around 5000 live cells were sorted into RNAse-free 1× PBS with 5 mM EDTA using FACS Aria III sorter (BD Biosciences). Cells were subsequently sent for 10X Genomics library preparation according to manufacturer's manual by the Cologne Center for Genomics (CCG). For the FACS analysis of NPF+ cells experiment, 30 anterior midgut/condition were dissected under the same conditions as previously described and used for quantification of GFP+ cells. FACS-plots were generated with FlowJo v10.

2.2.4. Single cell RNA sequencing

More than 9000 live cells were used to prepare 10XGenomics libraries using the manufacturer's manual. In brief, Gemcode single cell platform was used to encapsulate

single cells and gel beads into droplet. Next, cell lysis and barcode transcription were performed in these droplets and subsequently cDNA was amplified to generate to a concentration of around 100ng. Following this step, standard Illumina library preparation was carried out and next generation RNA sequencing was performed using Illumina system (Novogene).

2.2.5. scRNA seq data analysis

Seurat version 4.0.0 (Hao et al. 2021) and Garnett for Monocle3 Version 0.2.8 (Pliner, Shendure, and Trapnell 2019) pipelines were used for analysis, clustering and annotation of single cell data. For clustering of cells and PCA/UMAP generation, cells with fewer than 2 reads were discarded. Most variable features were identified and used for downstream analysis. Data was log normalized, scaled and centered to mean = 0 and variance = 1. Subsequently, linear dimentionality reduction/PCA was performed, and cell clusters were identified using the "Louvain" algorithm. Finally non-linear dimensional reduction (UMAP) was performed.

For cell type annotation analysis, classifier was trained based on preselected marker genes and expression data. Then this trained classifier was used to classify cells into cell types. Finally, differentiation expression was performed between the cell types and clusters using Seurat.

2.3. Microbiology

2.3.1. Ecc15 infection

To induce ISC proliferation in the gut, infection with the pathogen *Erwinia carotovora* (*Ecc15*) was used. Bacteria were grown at 30°C in aeration in Luria-Bertani medium (LB) over night. The following day medium containing the bacteria were centrifuged at 4000g for 15 minutes. Supernatant was removed and the bacterial pellet was re-suspended in 1ml solution of 5% sucrose in water. 1ml of 5% sucrose in water solution was used as control. 600 µl of bacterial or sucrose suspension was dispensed on Whatmann filter

paper in empty vials and 15-20 adult females were added. Flies were kept on Ecc15 or sucrose control food for 16 hours followed by immediate dissection.

2.4. Microscopy

Series of 2-4μm stacks were obtained for each gut using a Leica Sp8 DLS confocal microscope. For imaging of the entire length of the gut, the tilescan module of the Leica microscope was used. The same settings were used across different age/sex, unless otherwise is stated. All images were processed with FIJI/imageJ software. First, maximum intensity z-stack projections were obtained for each image. For quantification of GFP+ cells in NPF experiments, anterior and middle midgut region where GFP+ cells were located was cropped from the image and the quantification was conducted using the Find Maxima tool in ImageJ. The following settings were used for quantification of GFP+ NPF and Pros+ EEs; Output type: point selection, prominence for GFP signal: 190, prominence for Pros signal: 35. For quantification of pH3+ cells guts were directly observed under either Leica DLS confocal or Leica DMI6000b microscopes and the number of pH+/gut was counted. The same settings were used for all conditions in each experiment.

2.5. Statistical analysis

Statistical analysis was performed using GraphPad Prism software. Paired t-test was used for paired comparisons of different conditions. For multiple comparison, one way ANOVA with post-hoc testing was used. The relevant statistical test is indicated in the legend of each figure. P values < 0.05 were considered as significant. *$P<0.05$, **$P<0.01$, ***$P<0.001$ and ****$P<0.0001$.

3. Results

3.1. Investigating the mechanism of differentiation from ISC to enteroendocrine cell: the role of transcription factor Klumpfuss

The first aim of this PhD project was to investigate the role of the transcription factor Klumpfuss (Klu) in controlling EE differentiation in *Drosophila* gut. Klu is a member of the Early Growth Response family of zinc-finger transcription factors and has similarities with Wilms' Tumor 1(WT1) which is a mammalian tumor suppressor (Klein and Campos-Ortega 1997). In flies, over expression of *Klu* in neuroblast stem cells results in cellular overgrowth and formation of tumor like tissue in the brain (Xiao, Komori, and Lee 2012; Berger et al. 2012; X. Yang et al. 1997).

Our preliminary data showed that knockdown of *klu* with RNAi in ISCs/EBs or only EB cells (using *esg-GAL4* or *Su(H)-GAL4* respectively) results in an excess number of EE cells, suggesting a role for Klu in repressing EE fate. These data also showed that *Klu* expression is restricted to EB cells. In order to dissect the function of Klu in EE differentiation in more detail, we performed lineage tracing experiments using mosaic analysis with a repressible cell marker (MARCM) and FlipOut (F/O) systems. Moreover, we analyzed changes in ISC proliferation in *klu* overexpression conditions compared to respective control. Finally, epistasis experiments between Klu and the known Notch transcriptional effector Suppressor of Hairless (Su(H)) showed that Klu acts downstream of Notch signaling and regulates EC vs EE cell fate.

3.1.1. The WT1-like transcription factor Klumpfuss maintains lineage commitment of enterocyte progenitors in the Drosophila intestine.

Some of the results presented in this chapter were used in the already published article "(Korzelius et al. 2019)". The detailed explanation of contribution of Sina Azami as well as the published version of the article can be found in the publication section of this thesis.

3.1.2. Loss of Klu in EBs is sufficient to induce EE cell differentiation.

The phenotype that motivated us to take a closer look at the role of Klu in intestinal cell differentiation was the increase in number of Pros+ EEs in the absence of Klu from ISC/EBs. For these initial experiments we used the *esg-GAL4^{ts}* driver to induce *klu^{RNAi}*. As *esg* is a transcription factor that is expressed in both ISCs and EBs (Korzelius et al. 2014), it is not an appropriate driver to differentiate between the roles of each these cell types in the observed phenotype. Furthermore, our expression data with the *klu-Gal4*, *UAS-GFP* reporter line showed that *klu* was exclusively expressed in the EB, but not the ISC. Hence, we used EB specific *Su(H)GBE-Gal4^{ts}* driver to induce *klu^{RNAi}* only in EBs. This showed that elimination of Klu in EBs is sufficient to increase the number of Pros$^+$ EE cells. In order to confirm this result, and to trace the fate of EBs expressing *klu^{RNAi}*, we used a *Su(H)GBE>*Actin-FlipOut lineage tracing strategy combined with *klu^{RNAi}* to trace the fate of EBs after 10 days of induction of the RNAi. Due to the fact that the basal turnover of ISCs in *Drosophila* gut is low, we infected flies with *Ecc15* pathogen for 16 hours to promote gut turnover. It has been shown that *Ecc15* infection promotes gut turnover and increases ISC proliferation (Buchon, Broderick et al. 2009), hence scaling up the rate of proliferation increases our ability to detect changes in ISC differentiation and clone formation.
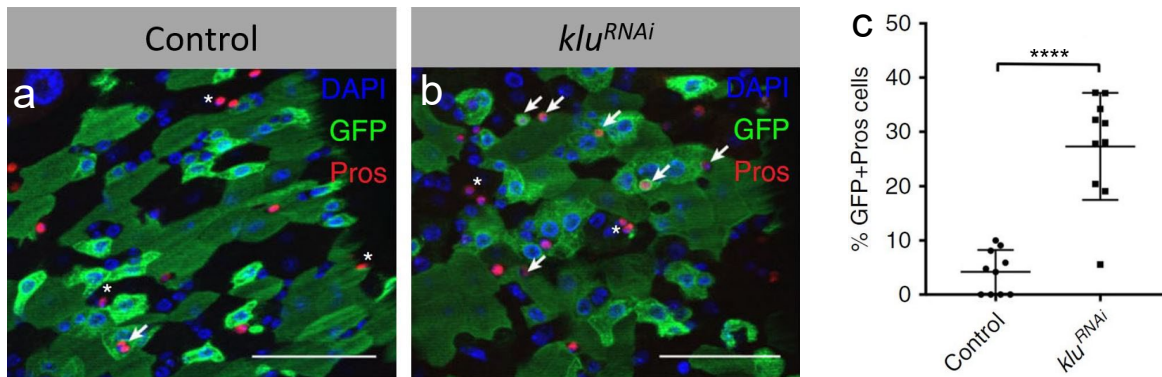
Figure 4. Loss of Klu resulted in increased EE differentiation.
a and b: Number of Pros positive EE cells in clonal area was increased compared to the control condition. Su(H)-GBE FlipOut was used to drive expression of klu^{RNAi} under *Ecc15* infection condition. c: Quantification of GFP/Pros double positive cells/ROI in conditions stated in A. n= 10 guts per condition. Error bars represent mean +/- SD. t-test. Scale bar: 50µm.

We observed a significant increase in number of GFP/Pros double-positive cells in klu^{RNAi} flies compared with their respective controls (Figure 4). Despite the significant increase in ratio of Pros+ EEs in *Su(H)GBE* generated EB clones in the klu^{RNAi} condition, EEs are not exclusively found in these clones, which is in line with observations from others showing that EBs mostly turn into EC fate rather than EE differentiation (Zeng and Hou 2015). These results confirmed our preliminary data regarding the role of Klu in repressing EE fate in EB cells and further solidified our hypothesis that Klu loss in EBs results in a partial reversion of EBs to EE fate.

3.1.3. Klu acts in a cell autonomous manner.

To further confirm our data on excess EE differentiation in absence of Klu and to determine if the phenotype is cell autonomous, we performed MARCM experiment using *klu RNAi* (*FRT40A; klu^{RNAi}*). Our analysis of the klu^{R51} MARCM null allele demonstrated that these flies had an increased number of EE cells compared to control FRT40A animals (J.Korzelius and H.Jasper, unpublished observation), likely due to the heterozygous nature of the klu^{R51} MARCM null allele strain. Therefore, by generating klu^{RNAi} clones in an otherwise wild-type background, we generated mosaic tissue containing two cell types in the intestine of the same animal. Clones with *gfp* expression also co-express *klu RNAi*, and the surrounding tissue that is GFP- is wild type for *klu* (Figure 5).
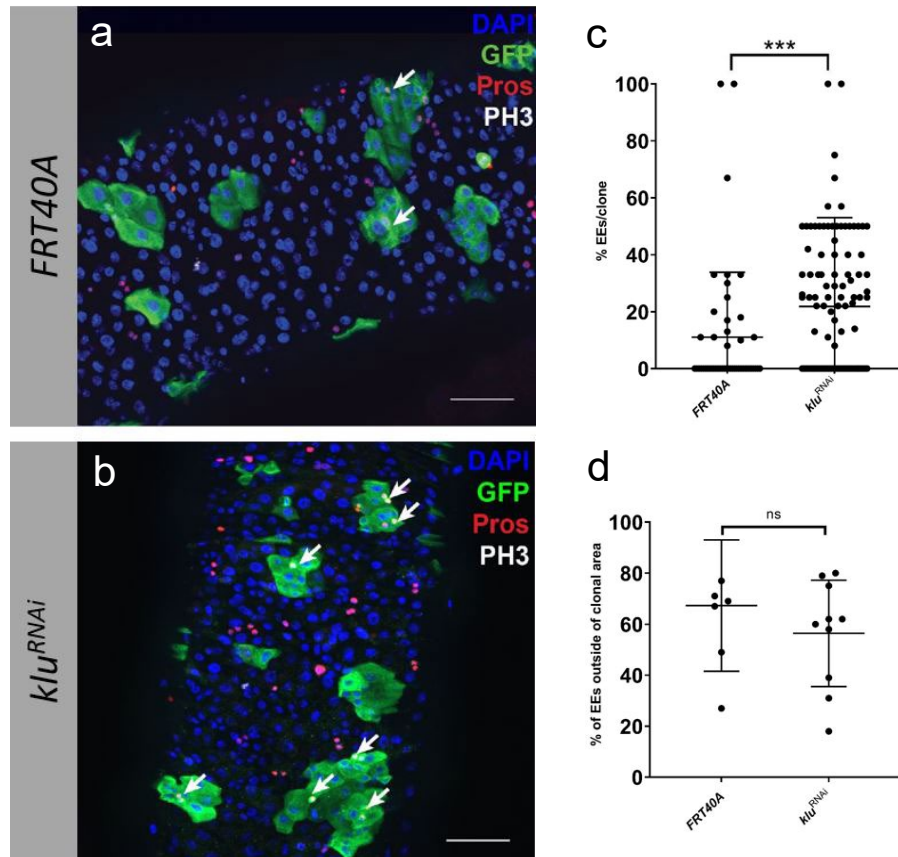
Figure 5. Loss of Klu in EBs was not associated with cell extrinsic effects on EE differentiation.
a and b: Representation of posterior midgut section of *klu^RNAi* and FRT40A control guts. The average percentage of EE/clone (white arrows) was significantly lower in control (7.5%) compared to *klu^RNAi* (23%). Interestingly, the percentage of EE cells outside clonal area was not different in control versus *klu^RNAi* (d). c and d: quantifications of percentage of EE per clone. Error bars represent Mean +/- SD. t-test. Scale bar: 50µm.

We observed an increase in number of EEs only in GFP⁺ clones but not in the surrounding wild type tissue (Figure 5, quantifications). This observation indicated two things: first it confirmed our preliminary data showing that lack of Klu leads to excess EE cells. Second it showed that effect of loss of Klu is cell autonomous and does not affect EE differentiation in a systemic manner.

3.1.4. Overexpression of *klu* in ISCs results in significant reduction of proliferation

Based on our previous experiments, the loss of *klu* expression results in excess EE differentiation from ISCs. Hence, we hypothesized that ectopic *klu* expression should have the opposite effect and block EE differentiation. To test this idea, we used *UAS-klu* construct to over-express full length *klu* in ISCs using the FlipOut system under control of *esg* in combination with *Ecc15* infection. While in wild type conditions *esg-F/O* clones expand in most parts of the posterior midgut seven days after induction, ectopic *klu* expression in ISCs resulted in smaller clone size, indicating an arrest of cell differentiation and proliferation (Figure 6).
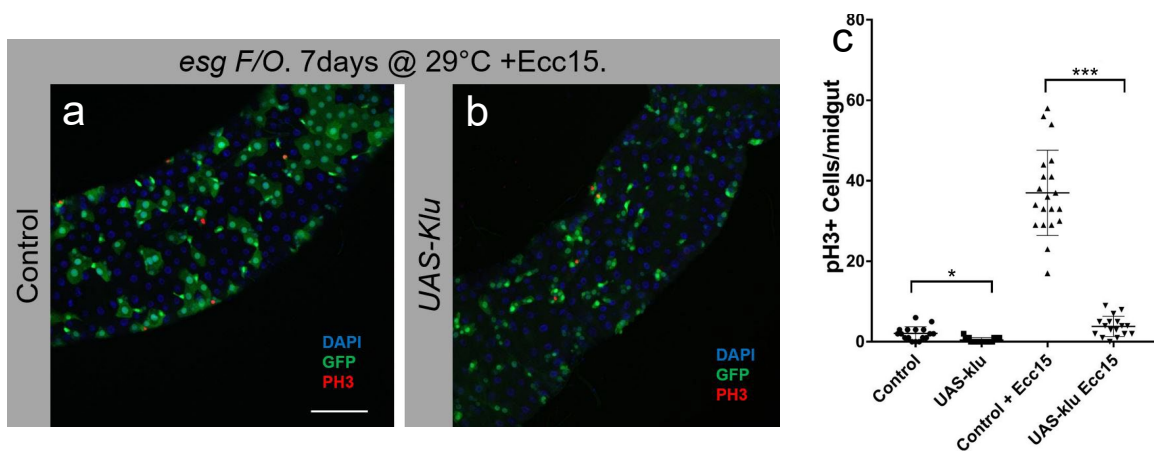
Figure 6. Ectopic *klu* expression resulted in reduction of proliferation and cell arrest.
a and b: Representative pictures of *esg F/O* guts for control and *UAS-klu* in ECC15 infection condition. Number of pH3+ proliferative ISCs was significantly lower in *UAS-klu* condition compared to control both in presence and absence of *Ecc15* infection (c). Error bars represent Mean +/- SD. n = 20. t-test. Scale bar: 50µm.

The decrease in ISC proliferation in *UAS-klu* expressing *esg-F/O* clones was confirmed by quantifying the number of pH3 positive cells per gut (Figure 6c). The negative role of *klu* expression on ISC proliferation and clonal growth were exacerbated by *Ecc15* infection. Whereas control *esg-F/O* intestines showed a significant increase in proliferation upon *Ecc15*, *esg-F/O > UAS-klu* flies showed no increase in proliferation upon *Ecc15* challenge. Altogether, this data showed that ectopic expression of *klu* is sufficient to inhibit ISC proliferation and differentiation in fly gut.

Thus far, we demonstrated that inhibition of *klu* leads to change in the ratio of differentiated cells toward EEs, and that ectopic *klu* activity in the ISC/EB population leads to reduced proliferation. In order to better understand the role of Klu in cell differentiation, we performed lineage tracing experiment using the EB-specific *Su(H)GBE>Actin-FlipOut* system to continuously express *klu* in EB cells. EB cells almost exclusively differentiate into Pdm1-positive enterocytes (ECs) (Biteau and Jasper 2014, Zeng and Hou, 2015). We used Pdm1 staining *Su(H)GBE-F/O* clones to determine the effect of continuous *klu* expression on EB differentiation.
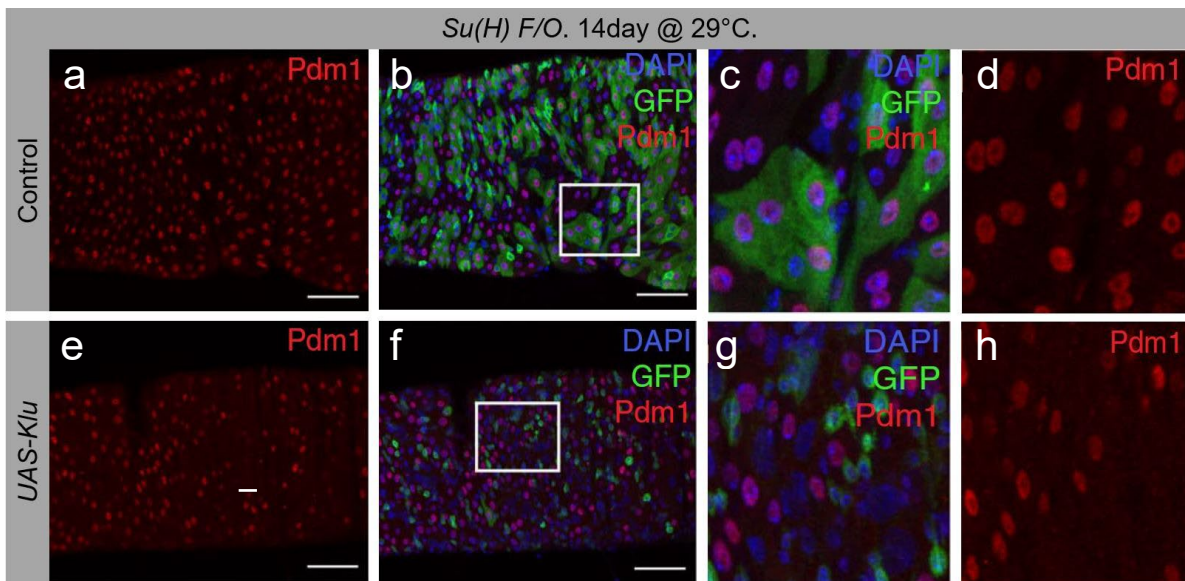
Figure 7. Ectopic *klu* activity resulted in differentiation defects.
Number of GFP/Pdm1 double positive cells was significantly lower in *Su(H)-F/O>UAS-klu* (e-h) compared to the respective control (a-d). c, d and g, h are close ups. N = 7 midgut/genotype. Scale bar: 50μm

We observed that continuous *klu* expression leads to a loss of GFP-Pdm1 double-positive clonal cells when compared to control *Su(H)GBE-F/O* clones (Figure 7, Figure 8a). Quantification of Pdm1 staining showed that continuous expression of *klu* in EBs leads to reduced formation of Pdm1-positive mature ECs (Figure 8a). The observed smaller clonal size also suggested impaired proliferation, as observed when we ectopically expressed

klu in *esg-F/O* clones (Figure 6) expressed in ISCs. This suggested that apart from its role in repressing EE differentiation in EB progenitors, Klu also needs to be downregulated in order for EBs to properly differentiate into mature, *pdm-1* expressing ECs.

In line with our findings on ISC proliferation, we also observed decrease in pH3 positive cells upon constant expression of *klu* in EB population using $Su(H)^{ts}$ driver (Figure 8b). This also highlights dual role of Klu in restricting proliferation and differentiation simultaneously.
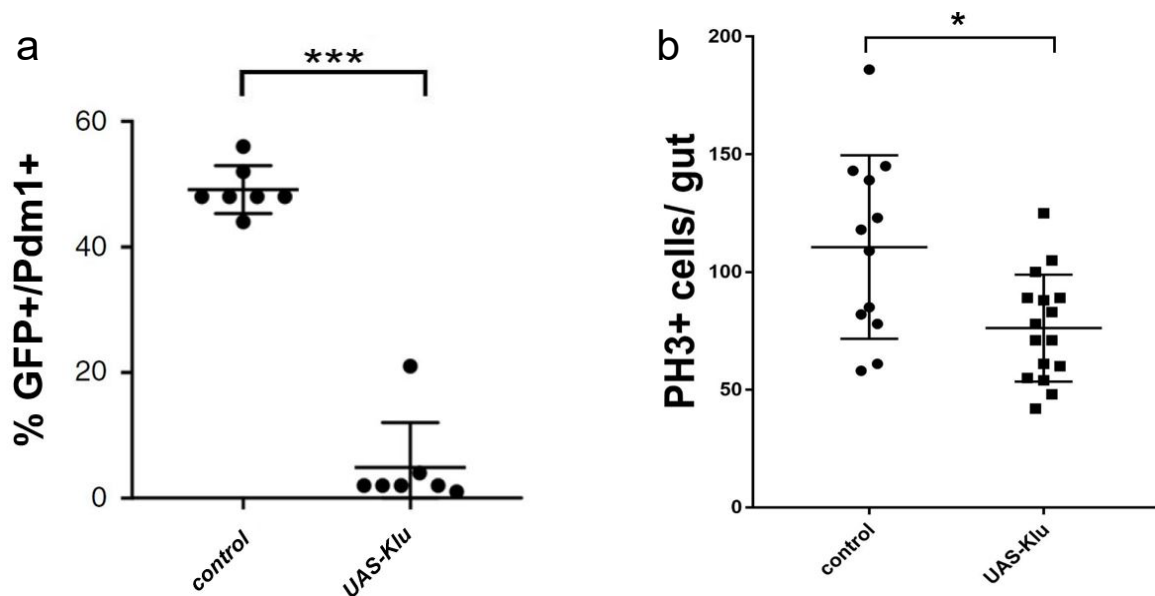
Figure 8. Ectopic Klu activity resulted in differentiation defects (quantification).
a: Quantification of *klu* overexpression condition compared to respective control in EBs using *Su(H)-F/O>UAS-klu*. Error bars = mean+/- Sd. n = 7. b: Quantification of number of proliferative ISCs *klu* over expression compared to control in EBs using the same F/O system. Error bars = mean+/- Sd. n = 12-17. t-test.

3.1.6. Combined inhibition of *Su(H)* and *klu* in ISCs and EBs results in decreased ISC proliferation and clone size

Notch signaling has a pivotal role in EE versus EC fate decision in intestinal cells (Bardin et al. 2010). Previous work from the Bray lab has demonstrated that *klu* is a Su(H) target

gene and acts together with Notch to regulate hemocyte differentiation (Terriente-Felix et al. 2013). To investigate the genetic interaction between Notch signaling and Klu in this context we performed epistasis experiments. We investigated the effect of loss of Klu, Su(H) or the combination of both on number of Pros^{+} EE cells in the gut, and used *esg-F/O* to drive expression of *klu*[RNAi] or *Su(H)*[RNAi]. As expected, inhibition of *klu* resulted in a decrease in Pros[+] EEs in posterior section of the midgut (Figure 9b). Knockdown of *Su(H)* led to a Notch loss-of-function phenotype, characterized by the formation of tumors consisting of a mixture of mitotic ISCs and Pros-expressing cells (Patel et al., 2015, Bardin et al., 2010) (Figure 9c).
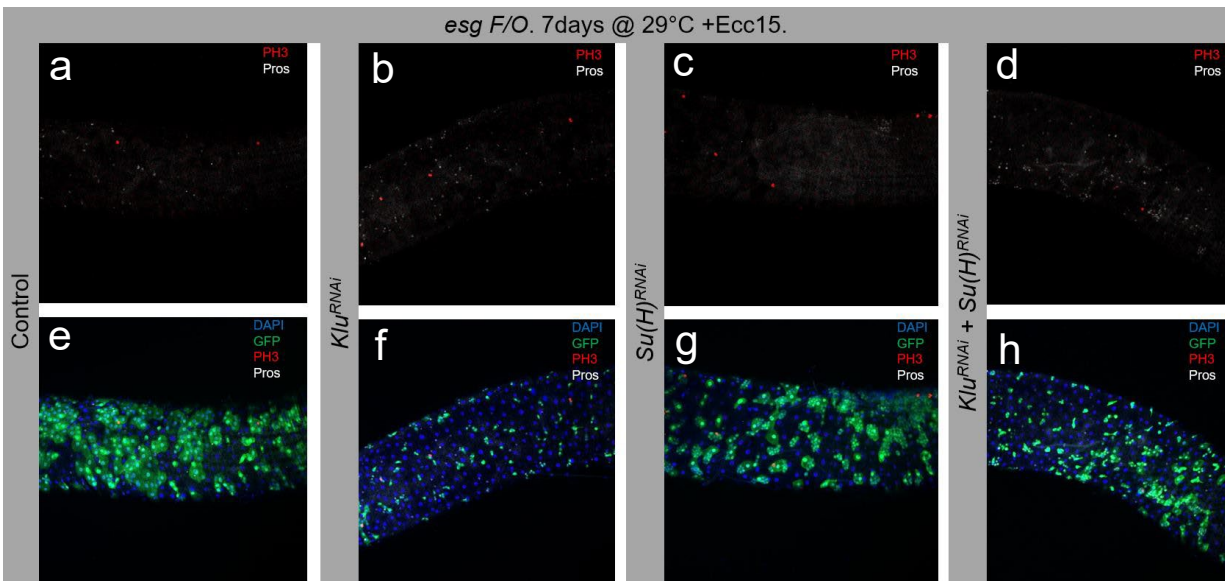
Figure 9. Klu acted downstream of Notch and repressed ISC proliferation.
esg-F/O was used to express *klu*[RNAi], *Su(H)*[RNAi] or combination of both in ISC/EB cells. Size of GFP+ clones in *klu*[RNAi] and combined condition was significantly smaller compared to control and *Su(H)*[RNAi] alone. This indicated that Klu probably acts downstream of Su(H) and hence Notch in regulation of cell fate. ROI: posterior midgut. Scale bar: 50µm.

Interestingly, the combined inhibition of *klu* and *Su(H)* showed a prominent increase of Pros^{+} cells in the tumors at the cost of mitotic, pH3-positive cells (Figure 9d). Hence, the combined inhibition of *klu* and *Su(H)* shunted the growth of Notch tumors that have been associated with loss of Su(H) (Figure 9g versus 9h). It is noteworthy that tumor formation in our *Su(H)* RNAi condition was generally milder compared to our previous studies of loss of Notch using *Notch* RNAi, which might be related to RNAi efficiency or Su(H)-

independent roles of Notch signaling. Together these data suggest that Klu acts downstream of Notch signaling.

In order to quantify the effects of combined loss of Notch and Klu on ISC proliferation and tumor growth, we quantified pH3 cell/midgut for each of the genotypes. As expected and line with previous publications, loss of Notch resulted in an increased mitotic rate for each of the midguts examined. Interestingly, the combined inhibition of *Notch* and *klu* rescued this phenotype and decreased the proliferation rate very close to that of control and *klu^{RNAi}* conditions (Figure 10). Hence, the loss of Klu in Notch-deficient progenitor cells skews the balance towards Pros expression and EE differentiation. Expression of the transcription factor *pros* has been shown to inhibit proliferation by direct inhibition of mitotic gene expression during neuroblast differentiation (Choksi et al. 2006), Hence, excess EE differentiation upon loss of Klu is able to push the Notch-LOF progenitor tumors into a post-mitotic state, thereby preventing their further outgrowth.
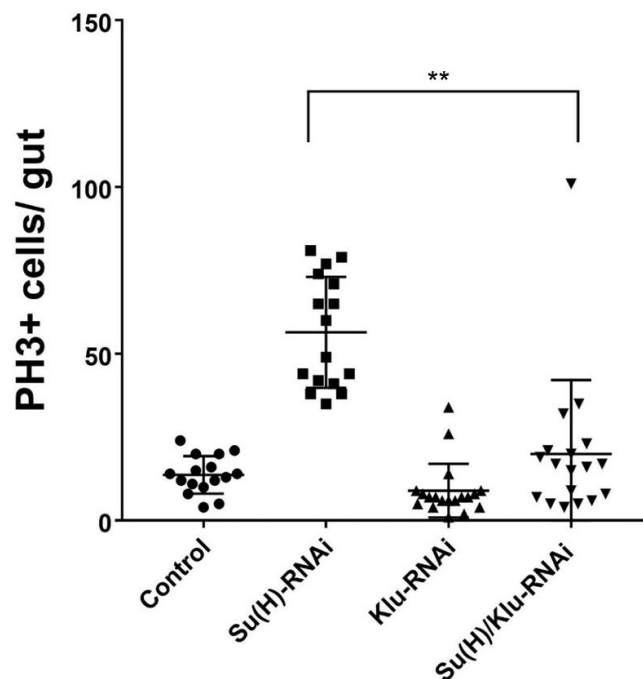
Figure 10. Quantification of Klu and Su(H) epistasis experiments.
*esg-F/*O was used to express respective RNAi constructs in ISC/EB cells. Number of pH3+ proliferative ISCs is significantly lower in *klu^{RNAi}* conditions compared to *Su(H)^{RNAi}*. n = 16-18 guts/condition. Error bars: mean +/- SD. One-way ANOVA with Tukey's post-hoc test.

3.2. Single cell RNA sequencing analysis of EE cells

The intestine is a highly responsive tissue that needs to react to dietary changes and infections. The EE cells are one of the primary cell types that detect and respond to these changes by secreting hormones with local and systemic roles but the exact changes of EE cells during challenges and during the process of ageing process has not been well-investigated thus far. Moreover, differences of EE cells in male and female flies and changes that these cells harbor during the ageing process has not been explored so far.

In recent years, single cell RNA sequencing paved the way to understanding cellular heterogeneity in different tissues, and the dynamics of changes in tissue cell types over time or between different conditions. More recently, the single cell transcriptome of entire organisms have been published through global collaborations such as *Tabula Muris* for *Mus musculus* and *Tabula Drosophilae* for *Drosophila melanogaster* (Schaum et al. 2018; H. Li et al. 2022). These datasets provide gene expression information at single-cell level for tissues that have been poorly characterized before, and have identified new cell populations in tissues, and also provided the possibility of direct comparison of similar cell types in different tissues.

This section of my PhD project aims to shed light on these aspects and give a detailed catalogue of changes in EE gene expression in young versus old and male versus female flies.

3.2.1. Knock down of some of the EE hormones and hormone processing enzymes Amon and Silver result in changes of ISC proliferation

To understand the changes in transcriptome of EE cells during ageing, we first generated bulk RNA-seq data of FACS-sorted EEs from young (7-day) and old (60-day) flies in triplicate populations using the *pros^{v1}-Gal4* driver to mark EE cells with *UAS-GFP*. Interestingly, Differential Expression (DE) analysis of young and old samples indicated

changes in pathways related to ISC identity, proliferation and differentiation (Figure 11a). For instance, we observed an increase in activity of Notch and Wnt signaling pathways, and changes in genes that are related to the mitotic cell cycle and DNA replication, processes normally associated with the mitotic ISC population (Figure 11c). This is suggestive of a shift towards ISC-like features in older EE cells. Moreover, many of the EE hormones showed up or down regulation in old versus young samples (Figure 11b). Of note, expression of *NPF* was decreased in old EEs compare to their young counterparts. In contrast, expression of *CCHa2* and *sNPF* were up-regulated in old samples (Figure 11c) More recently, Tauc et al. reported that activation of *Polycomb* (*Pc*) target genes results in increase in the number the of the EE progenitor cell population in old flies (Tauc et al. 2021).

c

Up regulated in old vs. young

- Alzheimer disease-presenilin pathway (P00004)
- Angiogenesis (P00005)
- Apoptosis signaling pathway (P00006)
- Cell cycle (P00013)
- EGF receptor signaling pathway (P00018)
- Endothelin signaling pathway (P00019)
- FGF signaling pathway (P00021)
- Hedgehog signaling pathway (P00025)
- Huntington disease (P00029)
- Integrin signalling pathway (P00034)
- Lipoate_biosynthesis (P02750)
- Nicotinic acetylcholine receptor signaling pathway (P00044)
- Notch signaling pathway (P00045)
- P53 pathway feedback loops 1 (P04392)
- Pyrimidine Metabolism (P02771)
- Pyruvate metabolism (P02772)
- TCA cycle (P00051)
- Wnt signaling pathway (P00057)
- p53 pathway feedback loops 2 (P04398)
- p53 pathway (P00059)

d

Down regulated in old vs. young

- 5-Hydroxytryptamine degredation (P04372)
- Alzheimer disease-amyloid secretase pathway (P00003)
- Alzheimer disease-presenilin pathway (P00004)
- Apoptosis signaling pathway (P00006)
- Formyltetrahydrofolate biosynthesis (P02743)
- Gamma-aminobutyric acid synthesis (P04384)
- Parkinson disease (P00049)
- Toll pathway-drosophila (P06217)
- Toll receptor signaling pathway (P00054)
- Vasopressin synthesis (P04395)

Figure 11. Gene expression and gene ontology analysis of differentially expressed genes in bulk RNA sequencing experiment.
Volcano plots show up (red) and down (blue) regulated genes in old versus young samples. a: The right plot shows some examples of up regulated genes that are related to signaling pathways and cell cycle (*cycE*, *sna*, *dpn*, *dl*, *ase*). b: some examples of EE hormones that are up (*sNPF*, *CCHa1*, *CCHa2*, *AstA*), or down (*NPF*, *AstC*) regulated in old versus young samples. Adjusted P value significance threshold: 1. c and d show GO enrichment of up and down regulated genes in Bulk RNA samples. Pathways that are highlighted with red box are the ones that are related to cell cycle, proliferation and differentiation.

Considering the changes that we observed in expression of signaling pathway genes that are related to cell proliferation and differentiation, and also the versatility of the hormones that EEs produce, we asked the question to what extend each of the EE hormones can affect gut homeostasis and subsequently ageing. We evaluated ISC proliferation by immunostaining for the pH3 antibody. Flies that carried an RNAi construct against each of the hormones were used for the experiment. Because the rate of proliferation in normal condition is very low, a separate group of flies with the same genotype were infected with Ecc15, promotes gut turnover and increases ISC proliferation (Buchon, Broderick, Poidevin, et al. 2009), hence increasing study power for detecting changes in ISC mitosis. While in the control conditions knock down of only one hormone, *AstA*, increased ISC proliferation, in the *Ecc15*-infected condition knock down of four of these hormones (*CCHa1, CCHa2, AstA and sNPF*) induced changes in ISC proliferation. Interestingly, AstA knock down in normal condition caused increased ISC proliferation, but in infected condition the effect was reversed. For the other three hormones (*CCHa1, CCHa2* and *sNPF*), knock down under *Ecc15* infection caused decrease in ISC proliferation (Figure 12).
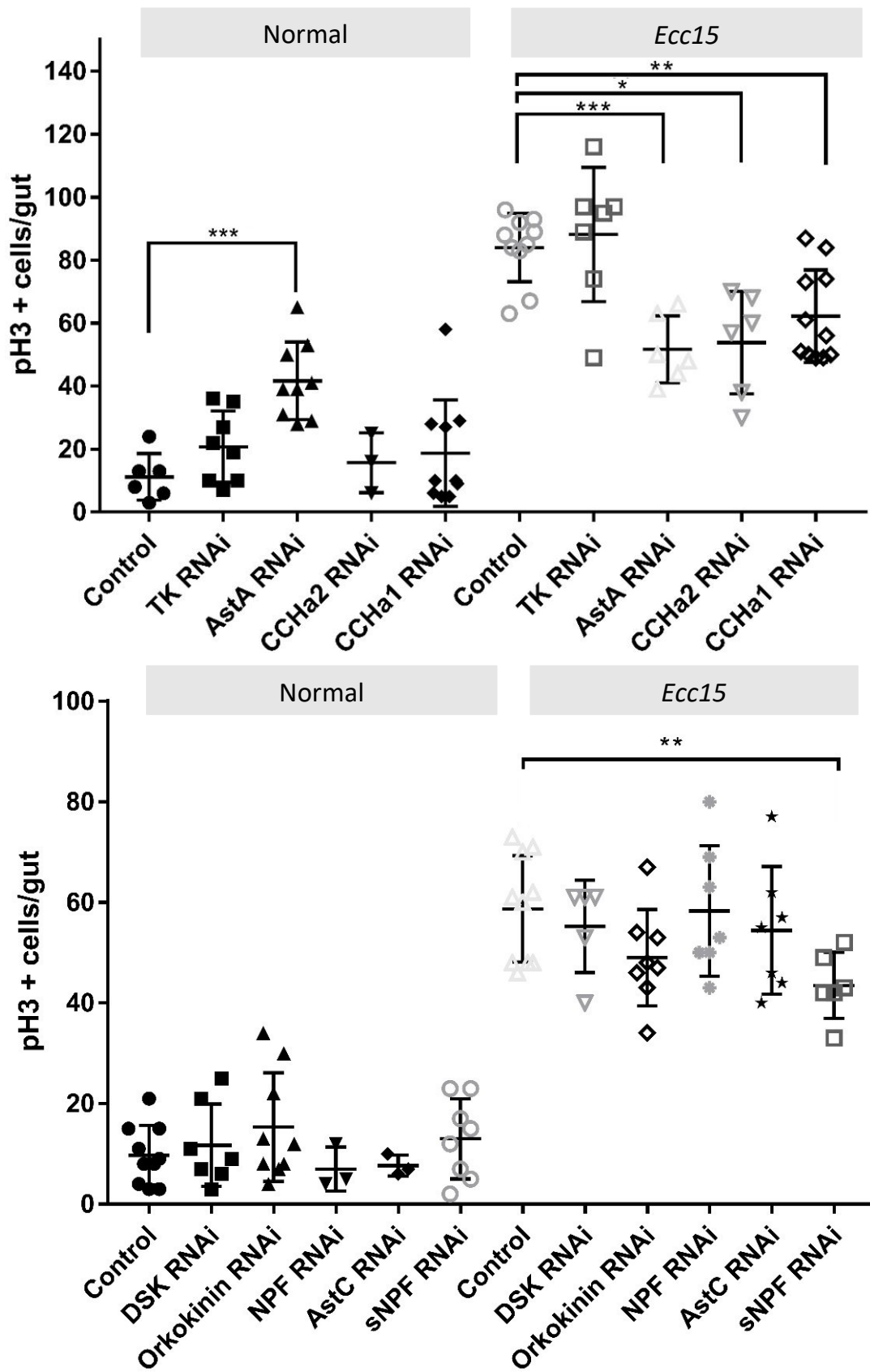
Figure 12. Knock down of EE hormones using *pros-Gal4ts* driver for 7 days.

From these 4 hormones, we focused our efforts on CCHa1, as its function in EE biology was unknown at this point. First, we assessed the expression of *CCHa1* and its receptor. Our GAL4 reporter experiments with the *CCHa1* receptor (*CCHa1-r*), (*CCHa1-r-GAL4>UAS-GFP*) showed that *CCHa1-r* has expression in some EE cells in middle and anterior midgut and, more interestingly, in the visceral muscle surrounding the copper cell region (CCR or R3-region). To assess the role of CCHa1 signaling in the CCR, we performed subsequent experiments using *CCHa1* and *CCHa1-r* RNAi lines. We initially observed that upon knock down of *CCHa1* or its receptor, the acidity of the CCR was reduced. This phenotype was accompanied by loss of copper cells which are responsible for producing acid in the middle midgut (data not shown). Despite these promising initial results, our subsequent studies using different *CCHa1* and *CCHa1-r* RNAi lines and backcrossed *CCHa1* and *CCHa1-r* mutant lines did not confirm the loss of acidity phenotype. Hence we decided to abandon this project.

So far we observed that absence of single EE hormones affect ISC proliferation, especially when the gut is challenged with *Ecc15* infection. To investigate the combinatorial effect of loss of all EE hormone activity on ISC proliferation, we next eliminated expression of *amon* and *svr*, two of the known prohormone processing enzymes in *Drosophila* specifically in EE cells using *pros-GAL4^{ts}* driver. We observed significant decreases in ISC proliferation upon induction of RNAi of *amon* and *svr* (Figure 13).
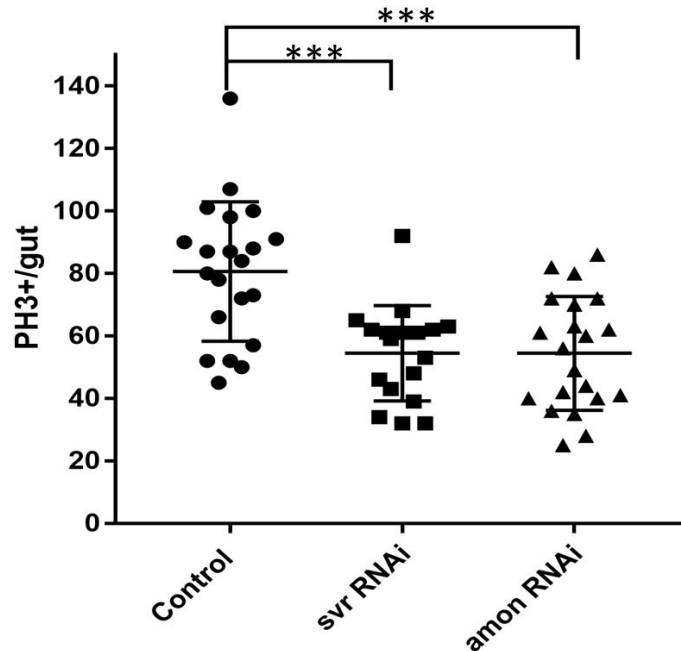
Figure 13. Quantification of ISC proliferation in absence of Silver and Amontillado. *pros-GAL4^{ts}* driver was used to express *svr* and *amon* RNAi for 7 days in presence of Ecc15 infection. Number of pH3+ proliferative ISCs is significantly lower in both RNAi conditions compared to control. n = 17-21 guts/condition. Error bars: mean +/- SD. One-way ANOVA with Dunnett's post-hoc test.

These results are in line with our data regarding single hormone knock down experiments in which we observe decrease of ISC proliferation in absence of several EE-derived hormones when flies are infected with *Ecc15*. This demonstrates that EE hormones not only play important systemic roles, but also signal locally in response to disturbed homeostasis by *Ecc15* infection. Whether these effects are indirect or act directly on ISC proliferation remains to be determined.

3.2.2. scRNA-seq experimental design and clustering of conditions/cell types

In order to gain a more detailed overview of changes in the EE population during ageing at single cell resolution, we performed single cell RNA sequencing using the 10X Genomics platform. We FACS-sorted EE cells from young and old flies that had GFP expression under control of the *pros^{v1}-Gal4* driver. In total five different conditions were

used for this experiment including young (7 days) and old (60 days) female, young and old male, and young virgin flies (Figure 14)
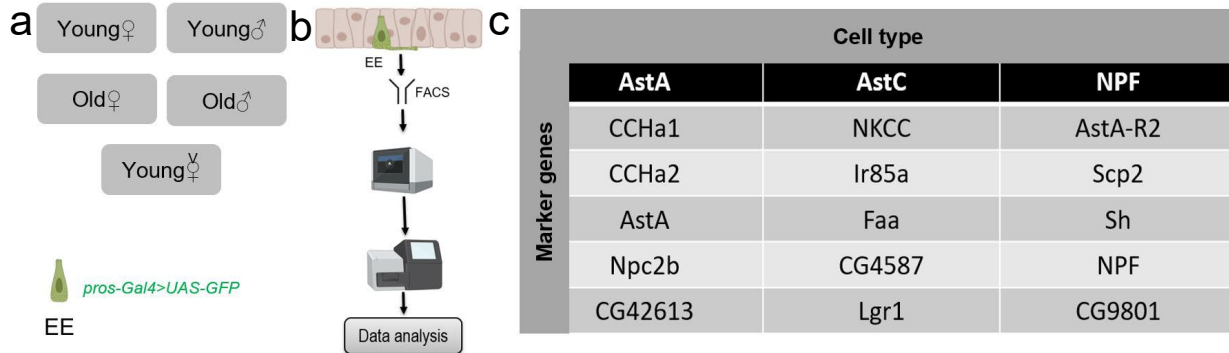
Figure 14. Summary of the scRNA-seq experiment steps and markers used for clustering of cells.
a and b: EEs that expressed endogenous GFP (*pros-Gal4>UAS-GFP*) were FACS sorted from five different conditions, and Chromium 10X platform was used for subsequent single cell generation and library preparation. c: table of the marker genes used for identifying each EE cluster.

We included young virgin samples in the experiment, because mating changes the physiology of female gut drastically, by increasing its size and also turnover rate (Ameku et al. 2018). As there are several reports showing that mating influences EE hormone production and secretion, we reasoned that it would be informative to include both mated and unmated female guts and ascertain the effect of mating on EE cell biology and hormone production.

After filtering out low quality cells (cells with less than 2 reads) we included more than 9000 cells for analysis on the flowcell. The range in cell number was quite large, ranging from 3315 in control mated females to 185 in old males (Table 3). This is striking, as roughly the same number of animals was dissected for males and females. This could be due to the smaller size of the male guts, making the dissociation procedure more prone to over-digestion of the sample and subsequent loss of cells. From the cells that passed the quality threshold, average depth of sequencing was 8,130 reads/cell and average number of genes/cell was 1,650.

Table 3. Details of the scRNA-seq experiment for each condition.
After filtering out low quality cells a total of 9827 cells were sequenced and subsequently used for clustering.

	Young_female	Old_female	Young_male	Old_male	Young-virgin
Number of cells	3315	3009	1110	185	2208
Average depth of reads/cell	8366	11454	7766	6079	7014
Average number of genes per cell	1622	2031	1691	1351	1564

The transcriptome of each cell was analyzed using the Seurat algorithm (Hao et al. 2021), and specific known EE subtype markers from a previous scRNA-seq study were used to cluster different types of EEs based on unique genes highly expressed in each specific subtype which have no/very low expression in the other subtypes (Hung et al. 2020). Based on this clustering, for each condition four different cell types were identified (AstA, AstC, NPF and unknown) (Figure 15).
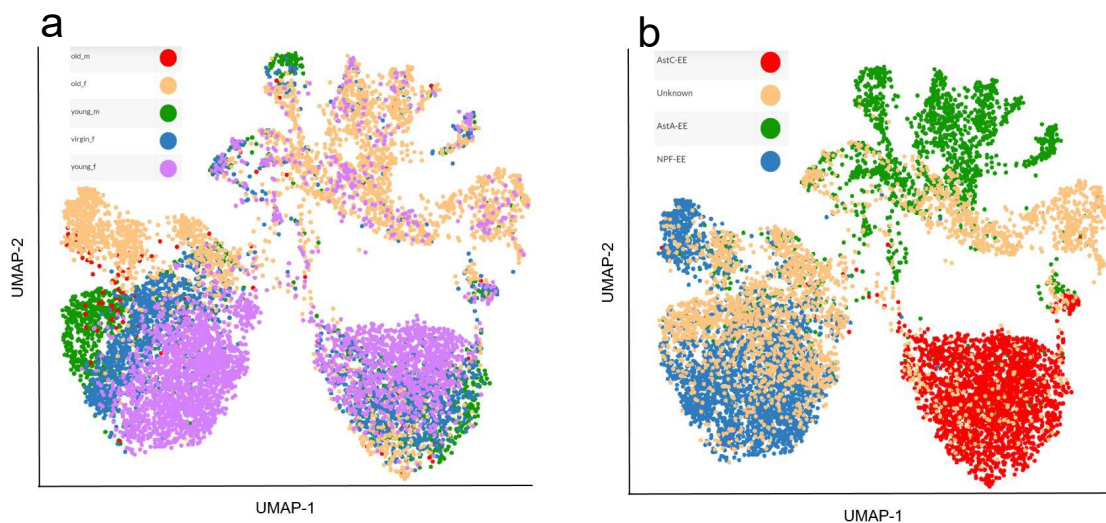
Figure 15. UMAP of the scRNA-seq experiment for each condition.
a: Clustering of the different samples of the study. In general young and old samples were separated clearly. Moreover, young male, female and virgin samples were also separately clustered. Due to low number of old male samples it was difficult to draw conclusions regarding their clustering. b: Clustering based on different EE subtypes using supervised clustering with known EE markers. Four major clusters were identified.

3.2.3. The unknown cell type cluster represents the EE precursor cell type

Our supervised clustering readily identified the three main sub-types of EE cells, but also yielded a cluster of unknown identity. We speculated that the unknown cell cluster could represent the undifferentiated precursor EE cells, whose number increases in the ageing intestine (Tauc et al., 2021). Therefore, we checked for expression of EE precursor cell markers including *Delta* (*Dl*) and *asense* (*ase*), *worniu* (*wor*) and *deadpan* (*dpn*). We confirmed that these genes had higher expression in the unknown cell type compared to the rest of the clusters (Figure 16). Furthermore, cell cycle regulators such as Cyclin E (CycE) and String (*stg*) also showed enrichment in this cluster (data not shown). Therefore, we concluded that the majority of cells in this cluster are EE precursor cells.
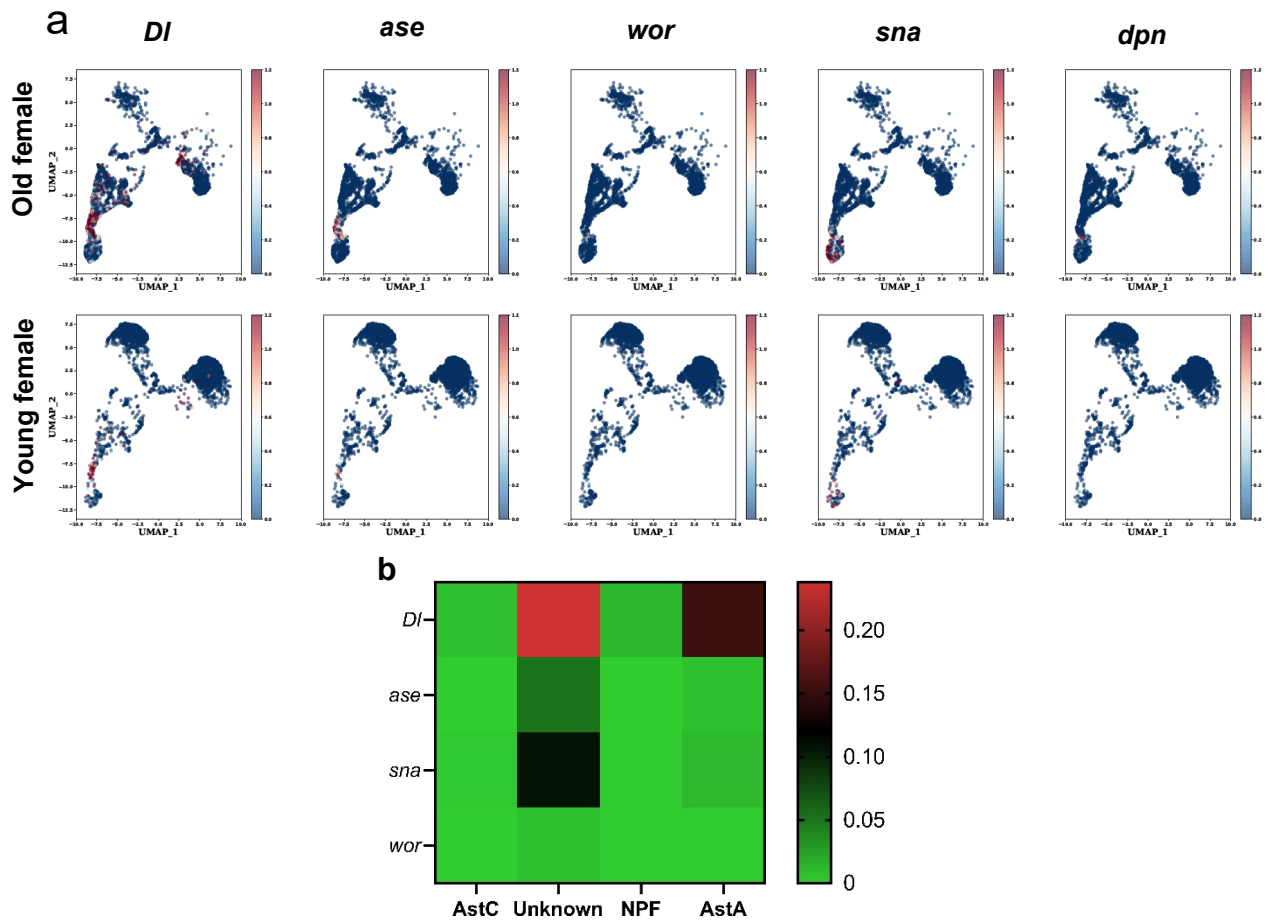
Figure 16. Determining the identity of unknown cluster.
a: Expression of five know EE progenitor and pro-neural marker genes in old and young female samples.
b: Heat map of the same marker genes in different cell types. The unknown cluster had higher expression in almost all markers that are shown indicating that this cluster represents the pre-EE cell population.

Comparing the pre-EE cluster in young and old female samples, we observed an increase in abundance of these cells in old versus young guts. This is in line with findings of Tauc et al., showing an increase in proportion of pre-EE cells in old versus young flies. Similar to their findings, and in addition to the increased number of EE progenitor cells, we also observed an increase in the level of expression of some of proneural genes including *snail* and *wor* and *ase*, in EE progenitor cells in old female samples (Figure 16a).

3.2.4. *esg* is highly expressed in female EEs

One of the interesting findings of this experiment was expression of the stem/progenitor marker gene *esg* in the EE cells. Esg is responsible for maintaining stemness state in ISCs, and its expression is restricted to ISC/EB cells of the midgut based on GAL4 reporter lines and *gfp* knock-in of *sfGFP* in the *esg*-locus (Micchelli and Perrimon 2006; Ohlstein and Spradling 2006; Korzelius et al. 2014). Our results, however, showed that *esg* mRNA was also abundantly detected in EE cells, with higher expression in female EEs (Figure 17). We also observed a decrease in *esg* expression in old female versus young female samples.
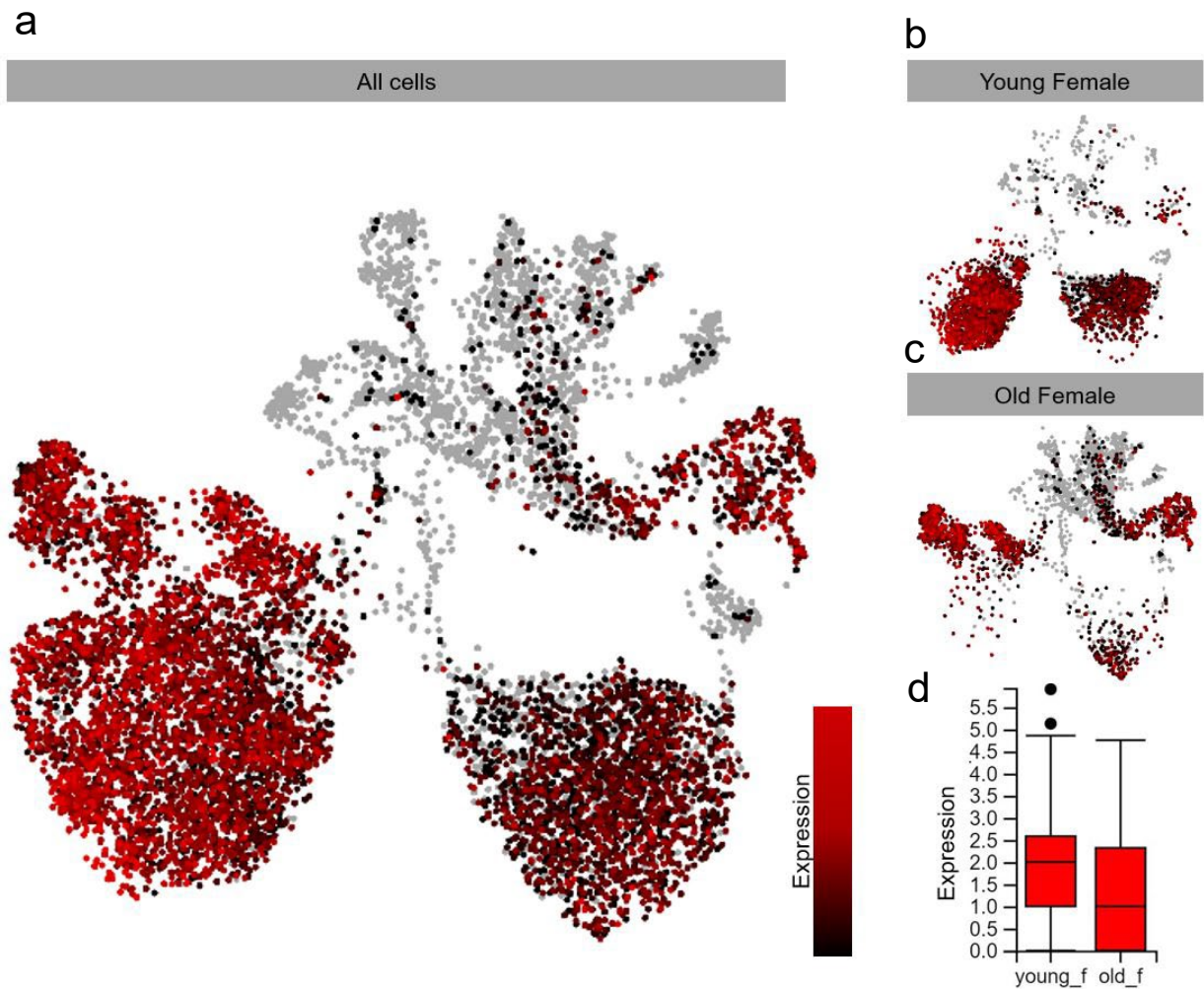
Figure 17. Expression of *esg* in scRNA seq dataset.
a: expression pattern of *esg* in all cell types, young female and old female samples (a, b and c respectively). *esg* expression was lower in old female cells compared to their young counterparts (d).

Guo et al. and Hung et al. have also reported the expression of *esg* in the EE cell clusters in their scRNA seq experiments. It seems that Esg, in addition to acting in ISC maintenance, could also be involved in regulation of EE subtype differentiation. One explanation for this observation could be post-transcriptional regulation of *esg* mRNA that prevents translation of the mRNA, hence blocking its function in these cells. Indeed, it has been shown that miR-8/miR-200 antagonize *esg* effect in EBs and promotes terminal differentiation in response to local cell loss (Antonello et al. 2015). Whether similar miRNA-based mechanisms of expression control are active in EEs remains to be investigated.

One of the main advantages of scRNA-seq analysis of cell populations is that it provides the possibility of tracking changes of cell types/clusters over time or between different experimental conditions. Interestingly, in our dataset we observed that the ratio of different EE-subtypes changed based on the age and/or gender of the flies. One such difference is the substantial shift from a small number of pre-EE cells in young females to higher numbers in old female samples (Figure 15). This finding is in line with findings of Tauc et al regarding the increase in pre-EE/ISC like cells in ageing gut (Tauc et al. 2021).

We also observed shifts in other identified EE-subtype populations in our dataset. This shift is most noticeable between young and old female samples (Figure 18a) in which the percentage of AstA cells increases with age while the percentage of AstC and NPF cells decreases. We observed an increase in the AstA population from 8% in young to 38% in old female guts, and decrease in AstC and NPF populations from 30% and 39% in young to 7% to 14% respectively in old samples (Figure 18a). Interestingly, the expression of *AstA* and *NPF* hormones in the respective cell cluster followed a similar trend, which shows that in addition to changes in number of cells expressing each of these hormones, their mRNA expression level also changes.
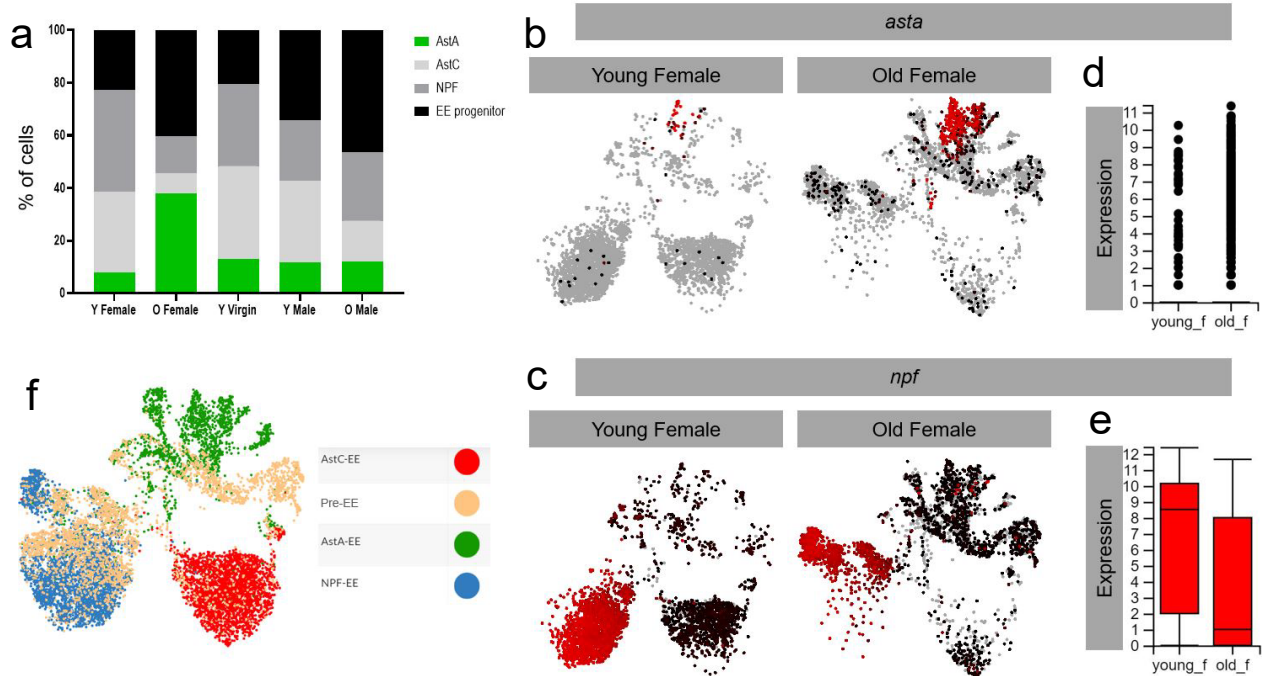
Figure 18. The proportion of different EE cell types in each condition.
EE cell type proportion changed with age (a), and is more evident in female samples. Two particularly interesting EE cell clusters that changed with age were AstA and NPF. Expression patterns of *AstA* and *NPF* hormones (b and c UMAPs respectively, quantified in d and e) followed a similar trend to the proportion of their respective cell clusters. UMAP of all cell types is shown in f as a reference. Expression quantifications are sum of relative raw expression for all cells in each condition.

3.2.6. Number of AstA+ EEs does not change during ageing

One of the findings of the scRNA-seq experiment was the increased proportion of the AstA cell cluster in old versus young female samples (Figure 18b). To confirm the observed shifts and the changes in hormone mRNA transcription with age, we obtained GAL4 reporter lines for several of the hormones that were used for subtype identification. These lines were crossed with *10XUAS-GFP*, and the number of GFP positive cells in young and old flies in both genders was quantified.

First, we used *AstA-Gal4>UAS-GFP* flies to investigate the expression pattern changes of the AstA population. Surprisingly, and in contrast to our scRNA-seq results, we observed a decrease in the total number of GFP+ cells in old versus young female guts (Figure 19a, b). To correct for the total number of EE cells, we normalized AstA+ cells to

the total number of Pros+ EEs per gut (Figure 19c). This revealed that there was no significant change in the AstA-population with age. Hence, we were not been able to confirm scRNA-seq findings regarding the change in AstA cluster proportion using *AstA-Gal4* reporter gene analysis. One possible explanation for this could be non-specific nature of the *Gal4* driver used for this experiment, as it was initially generated for neuroendocrine studies and may not recapitulate the actual expression of *AstA* in EE cells of the gut.
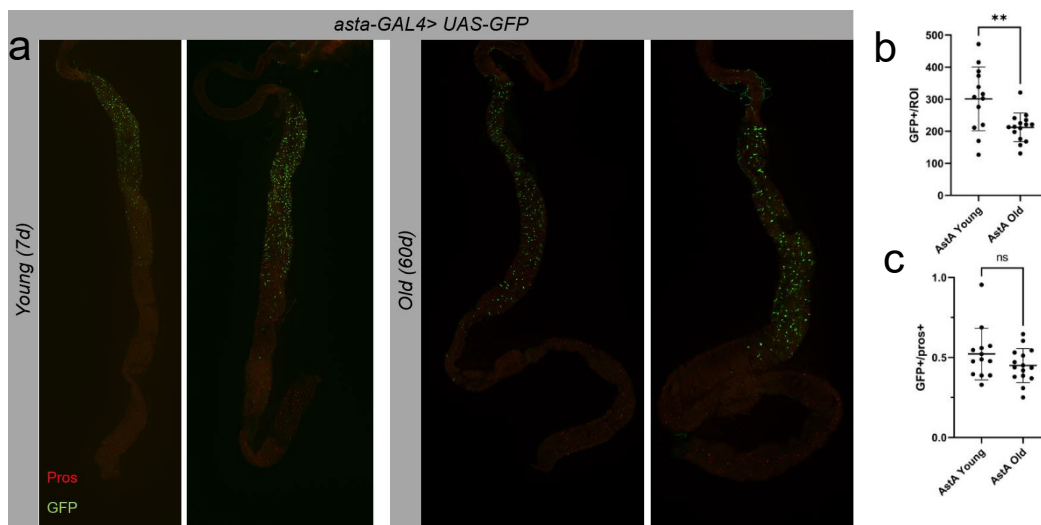
Figure 19. Expression pattern of *AstA-Gal4* in young and old intestine.
a: A *Gal4* reporter line of the AstA hormone was combined with *UAS-GFP* to visualize the expression of this hormone in the gut in female young and old flies. Pros staining was used to normalize the number of AstA-positive cells to the total number of EEs. b: quantifications of raw and normalized (b and c respectively) numbers of GFP positive EEs. n = 13-16, Error bars: mean +/- SD. Scale bar: 100µm, t-test.

3.2.7. Number of NPF+ cells decreases with age in both genders

Next, we wanted to confirm the decrease in NPF cell population during ageing using *NPF-Gal4>UAS-GFP* reporter flies. We observed a clear reduction in GFP+ EEs in old female flies compared to their younger counterparts (Figure 20).
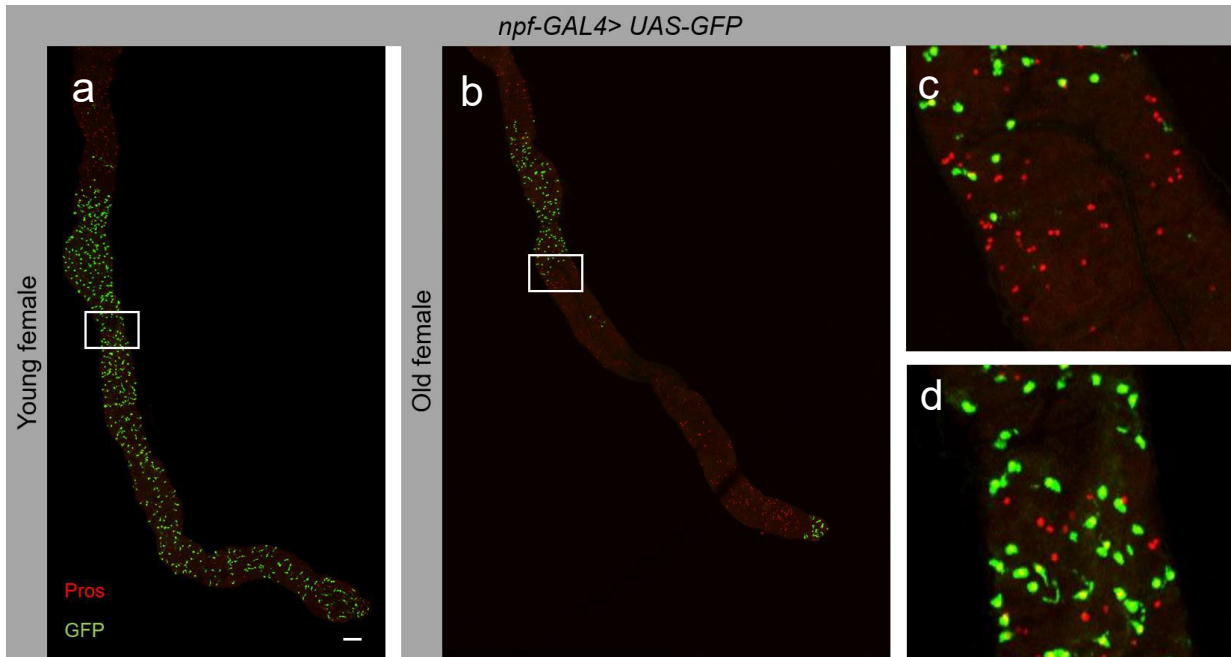
Figure 20. Expression pattern of NPF in female midgut.
A *NPF-Gal4* reporter line was combined with *UAS-GFP* to visualize the expression of *NPF* in the midgut of female, young (a) and old (b) flies. While in young samples GFP$^+$ cells existed in all parts of middle and anterior midgut, in old guts this pattern was lost in most of anterior region. Pros staining was used to normalize the number of NPF positive cells to the total number of EEs. c and d show close ups of old and young samples respectively. ROI: Anterior and middle midgut. Scale bar: 100µm.

The decrease was especially apparent in the anterior portion (anterior of the R3/CCR middle midgut region) of the female midgut. In the case of male flies, a reduction in abundance of NPF+ EE cells was also observed but, in contrast to the females, this change was mostly evident in the middle midgut (Figure 21).
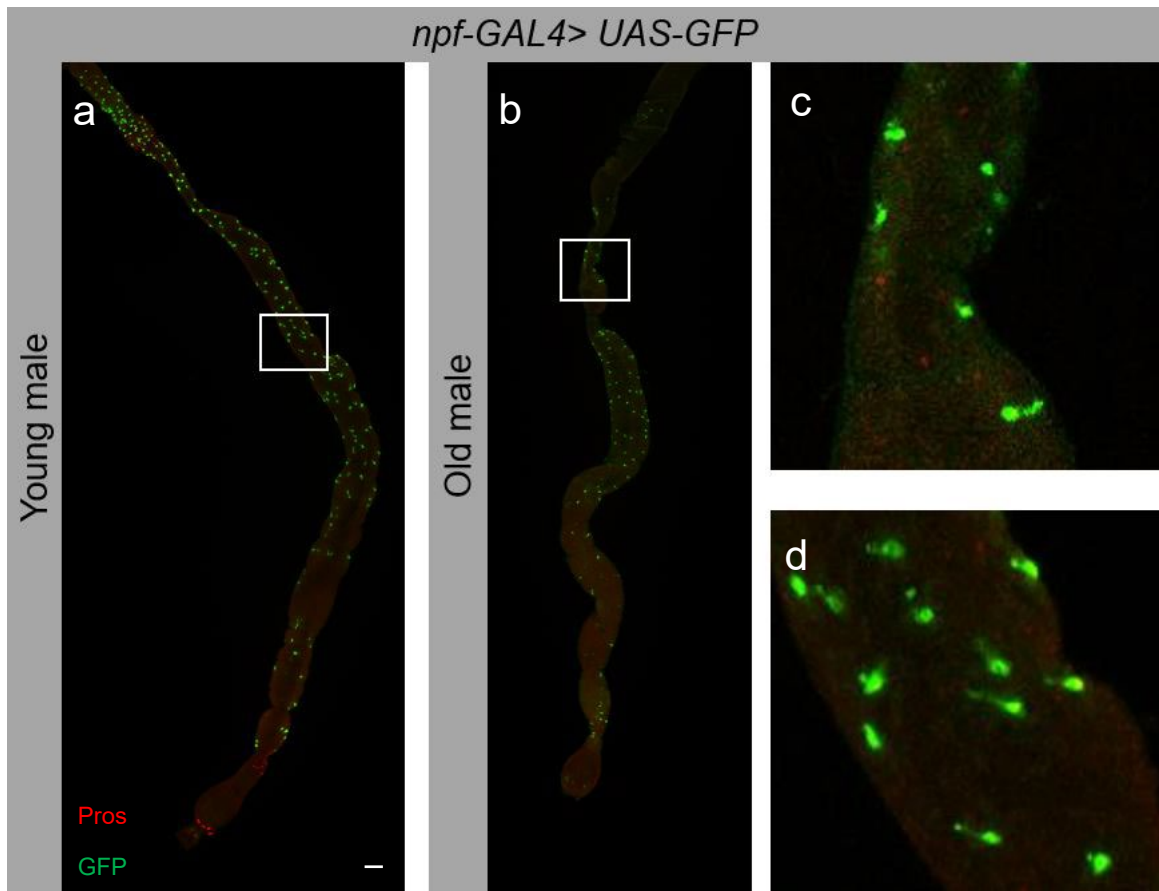
Figure 21. Expression pattern of *NPF* in male midgut.
Expression pattern of a *NPF-Gal4* reporter line combined with *UAS-GFP* to visualize the expression of *NPF* in the midgut of male, young (a) and old (b) flies. Interestingly, lack of GFP$^+$ EE cells in old samples happened in different regions of the gut in male and female samples (compare to figure 20 a and b); while in female samples anterior section was affected in male samples middle section of the midgut had fewer GFP$^+$ cells. Pros staining was used to normalize the number of NPF positive cells to the total number of EEs. c and d show close ups of old and young samples respectively. ROI: Anterior and middle midgut. Scale bar: 100µm.

We did not observe any difference in abundance of NPF+ EEs between young female and virgin flies (data not shown). Quantification of the number of GFP+ cells showed that the total number of NPF producing EEs in both female and male samples decreased with age (Figure 22). Quantification of virgin female samples confirmed no significant change when compared to mated young female flies, indicating that the effect is probably not dependent on mating. Next, we normalized the *NPF-Gal4* GFP+ cells to the total number of Pros+ EEs per gut. This confirmed the decrease in the proportion of NPF+ cells for both old females and males, confirming that the number of NPF producing cells in the midgut decreases with age.
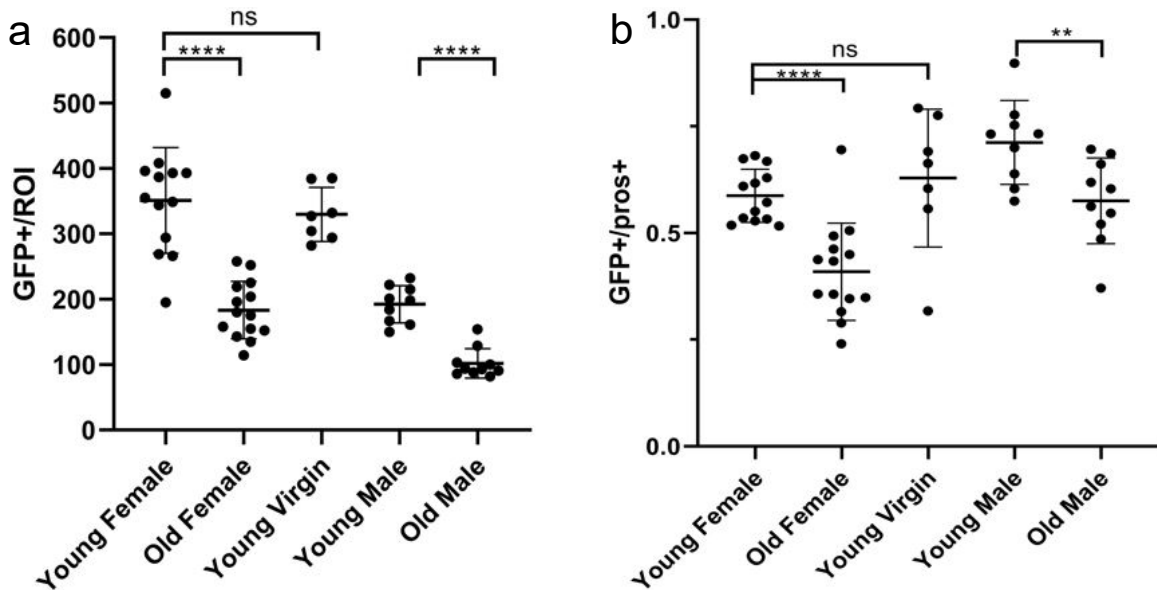
Figure 22. Quantification of number of NPF positive EEs in the gut.
a: Number of NFP+ cells/Region of Interest (ROI) for the indicated conditions. b: NPF+ cells normalized against Pros+ cells for each ROI in (A). n = 10-15 per condition, Error bars: mean +/- SD, One-way ANOVA with Dunnett's post-hoc test for female, and t-test for male samples.

3.2.8. Changes in NPF+ EEs in does not happen in the same region of the gut in male and female flies

In addition to decrease of NPF+ cells in old samples of both male and female flies, we observed that this reduction happened in different regions of the gut for each gender. The decrease in females was more evident in the anterior midgut of old females, while in case of males it was more evident in middle midgut. In order to quantify this, we counted the number of NPF+ cells in the middle and anterior section of the midgut separately. This confirmed that in female flies the R1 and R2 sections of anterior midgut are most affected, and in male flies decrease happens exclusively in R3 section (Figure 23).
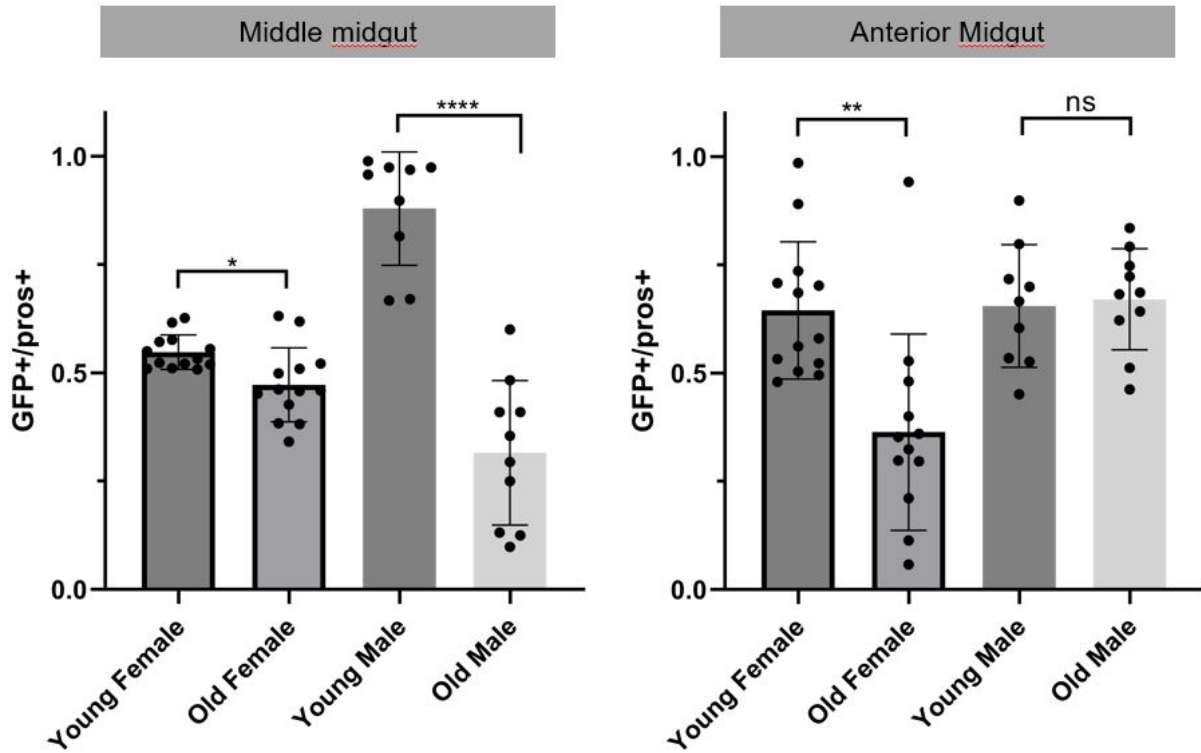
Figure 23. Region specific quantification of number of NPF-positive EEs in the gut.
Number of GFP-positive/Pros-positive cells in *NPF-GAL4>UAS-GFP* flies were quantified in middle and anterior sections of the midgut (a and b respectively). Data is shown for young and old samples from both male and female flies. n = 10-15, Error bars: mean +/- SD, t-test.

Therefore, we showed that despite general change in the number of *NPF*-expressing cells in the middle and anterior section of the gut in old and young flies in both sexes, the region responsible for this difference is not the same in male and female guts.

4. Discussion

4.1. Role of the transcription factor Klumpfuss in intestinal cell differentiation.

Since the identification of ISCs in the *Drosophila* intestine, much effort has been dedicated to unravel the regulatory mechanisms that determine differentiation of various cell types from these progenitor cells. The bulk of our knowledge in this field comes initially from lineage tracing experiments combined with cell type/cell marker identifications. Advances in understanding of the role of signaling pathways in this process has also played an important role in our understanding of cellular differentiation in this epithelium. In this section of my PhD project, I investigated the role of the transcription factor Klumpfuss as one of the molecular players in determining EC versus EE cell fate decision and its effects on stem cell proliferation in *Drosophila* intestine. I confirmed that loss of Klu in EBs is sufficient to shift differentiation towards the EE lineage in a cell autonomous manner. Moreover, I investigated the role of ectopic *klu* expression on EB cell fate and found that *klu* over expression results in a cell arrest state by preventing further differentiation of EB to EC. Finally, I provided evidence for the hierarchy of *klu* activity by showing that it acts downstream of Notch signaling.

4.1.1. *klu* is expressed in EBs and restricts EB to EE differentiation.

It has been previously shown that Klu is a regulator of asymmetric division of the self-renewing neuroblast and maintains the type I and II brain neuroblast stem cell fate (Xiao, Komori, and Lee 2012). However, its role in the intestine has not been addressed in detail. Our preliminary data showed that *klu* is expressed exclusively in EBs. We used different

lineage tracing methods to confirm this finding and showed that inhibition of *klu* in EBs shifts the differentiation in favor of the EE lineage. The ratio of EC/EE production in the intestine is greatly skewed towards ECs as these are the main cell types that make intestinal tissue in *Drosophila*. Hence, the tight control of this ratio is of great importance for intestinal homeostasis and survival of the organism. It has been shown that *achaete-acute* complex genes including *ase* and *sc* play pivotal roles in determining EE cell fate from ISC/EB cells. Therefore, it might be possible that Klu acts to suppress these genes in the EB, hence prevents EE formation in this EC-precursor. Our subsequent investigations using Klu DamID in Esg+ stem-progenitor cells did not show any binding of Klu in or near the regulatory regions of *sc.* Despite this finding, we observed binding sites of Klu near regulatory regions of genes acting upstream in the control of *sc*, including *sina* (Korzelius et al. 2019). It has been shown that Sina, Sinah and the adaptor protein Phyllopod together form a complex that is able to promote proteasome degradation of transcription repressor Tramtrack, which is a repressor of EE fate (Chen et al. 2018; Yin and Xi 2018). Hence repression of *sina* by Klu could potentially result in blockage of EE fate. Interestingly our subsequent RNA-seq data showed that expression of *sina* is 2.2 fold upregulated in *klu^{RNAi}* condition. Moreover, expression of *phyl* was also increased by 8 fold in *klu^{RNAi}* and downregulated 15-fold in *klu* overexpression condition. Hence we propose that EE suppression by Klu takes place in EBs, upstream of Scute through repression of Sina and subsequent stabilization of Tramtrack (Korzelius et al. 2019).

4.1.2. *klu* overexpression results in cell arrest.

To determine the role of Klu in lineage differentiation in more detail, we induced its expression ectopically using a *UAS-klu* construct in ISCs and EBs. In both cases *klu* overexpression resulted in formation of smaller sized clones compared to respective controls. We also observed decreased ISC proliferation when *klu* was ectopically expressed. Based on these observations we speculated that Klu could potentially hinder

cell cycle progression and put cells in a cell cycle-arrested state. Indeed, our subsequent RNA-seq and Dam-ID data supported this hypothesis, showing that Klu has binding peaks at *cyclin B* (*CycB*) and *cyclin E* (*CycE*) loci. Both of these proteins are essential for cell cycle progression, with the first one being involved in G1-S and the second one in G2-M phases of cell cycle (Shcherbata et al. 2004). Moreover, we observed that *CycE* expression is up-regulated in the *klu* RNAi condition. Next to G1-S regulation, CycE is essential for endocycle regulation, which is part of the EB-to-EC differentiation process (Zielke et al. 2011; Xiang et al. 2017). Cumulatively, these data suggest a regulatory role for Klu in determining cell cycle progression by blocking the mitotic cell fate and promoting endo-replicating cell cycles in EBs/differentiating ECs.

As another dimension of Klu activity, Reiff et al. showed that Klu can also determine the fate of EBs through activation of apoptosis and subsequent removal of the excessively formed EBs in the gut. This mechanism ensures that on the one hand there are always enough cells available in the gut to maintain homeostasis, and on the other hand it removes the extra EBs from the repertoire of the gut cells (Reiff et al. 2019).

4.1.3. Klu acts downstream of Notch signaling to regulate EB fate

Notch is one the most important signaling pathways in cell fate determination in *Drosophila* and mammalian ISCs. In addition to intestine, Notch also plays a pivotal role in differentiation of cells during development and in many other organs including nervous system and respiratory system (Lathia, Mattson, and Cheng 2008). In the respiratory epithelial tissue, dysregulation of Notch results in a wide range of respiratory problems including pulmonary artery hypertension, interstitial pulmonary fibrosis and lung cancer (reviewed in (Kiyokawa and Morimoto 2020).

In the intestine, Notch signaling takes place through reciprocal communication of stem cells that have Delta ligand and surrounding daughter cells that express Notch (reviewed in (Noah and Shroyer 2013; Demitrack and Samuelson 2016). Activation of Notch in EBs starts a cascade of signaling molecules that will eventually result in differentiation into

EC. This signaling is regulated in various stages, and interestingly the asymmetry of *Delta*-expressing cells is also a result of downregulation of regulatory genes including gene in EBs after mitosis. This asymmetry eventually results in exit of EBs from mitotic cell cycle and differentiation to ECs. We observed that Klu acts downstream of Su(H) in EBs to determines cell fate and cell cycle regulation. Based on these observations, it is not surprising that in our subsequent transcriptomic study we also saw changes in many genes that are involved in Notch signaling including *E(Spl)* genes in both *klu^RNAi* and overexpression lines. Moreover, we observed binding peaks of Klu in the proximal end of the *E(Spl)* locus, which includes the *E(Spl)-mδ*, *E(Spl)-mγ* and *E(Spl)m8-HLH* genes. Interestingly, it has been shown that E(Spl)m8-HLH and scute form a regulatory loop that promotes ISCs to directly differentiate into EE precursor cells (Chen et al. 2018).

One striking finding of our DamID was that Klu also binds to its own locus. This can be an indication of a negative auto-regulatory loop which ensures transient activation of *klu* and together with its effects on Notch signaling regulators, restrict the duration of the Notch transcriptional response in EBs.

As an additional mode of action, it has been shown by Reiff et al. that Klu activation in EB can result in an apoptotic response. In addition to regulating the ratio of EC to EEs, this response results in EB life/death decisions through antagonistic interaction with EGFR signaling, eventually influences the amount of differentiated cells that are present in the gut independent of ISC proliferation (Reiff et al. 2019). Finally, after we published our results, Hung et al. also reported the role of Klu in EC versus EE fate determination, which further confirms our findings (Hung et al. 2020).

Interestingly it has been shown that Wt1, which is a zinc finger transcription factor with structural similarities to Klu, is transiently expressed in nephric and hematopoietic lineages of progenitor cells (Hastie 2017) similar to the expression pattern of *klu* in the intestine. Hence it would be interesting to test if Wt1 has a similar role, as Klu does in *Drosophila*, in differentiation choice of secretory intestinal cell lineage in mammals. In order to test this, we used mouse intestinal organoids system. Results of immunofluorescence staining of primary cultured small intestine organoids (data not shown here) using anti-Wt1 antibody did not provide any evidence for the presence of

Wt1. Moreover we did not observe expression of *wt1* in RNA sequencing of the small intestine of young C57Bl/6 mouse. This might indicate that role of these TFs is to a great extent context dependent. For instance, expression of *klu* in the brain stem cells (neuroblasts) result in stem cell maintenance and its overexpression leads to formation of brain tumours (Xiao, Komori, and Lee 2012), but in the gut, it promotes cell fate determination and its over expression restricts ISC proliferation (our data).

4.2. Single cell analysis of EE cells

In recent years, the advent of single cell Omics technologies paved the way for a better understanding of cellular heterogeneity, cell type identification and cellular states present in the tissue, and effects of different treatments/study conditions at single cell level. In the second part of my PhD project I used bulk and scRNA sequencing to investigate transcriptional changes in EE cells at different ages and between genders.

I observed up-regulation of genes related to cell cycle and differentiation in old intestine along with changes in transcription of different EE hormones in the bulk RNA seq data. Moreover, I investigated the effect each of these EE hormones or their processing enzymes on ISC proliferation

In the scRNA-seq approach, I used supervised clustering of cell types based on previously published data (Hung et al. 2020). With this method, I identified 4 major EE clusters in the experimental conditions. I observed significant changes in the proportion of different EE cell clusters between young and old time points especially in female samples. Furthermore, I used Gal4 reporter lines of some of the EE hormones to confirm these changes in EE cell type ratios during the ageing process and between different genders in more detail.

Additionally, in the scRNA-seq data I observed widespread expression of transcription factor *esg* in EEs in almost all conditions of the experiment, a finding that is in contrast with the Gal4-based expression pattern seen for this gene, which is normally restricted to ISC and EB (Korzelius et al. 2014; Antonello et al. 2015).

67

In *Drosophila* ISCs, Esg acts as a transcriptional regulator of stem cell fate by repression of EC and EE differentiation, and so far it was thought that it is mainly expressed in progenitor cells, including Delta[+] ICSs and Su(H)[+] EBs. In these cells Esg represses the transcription of a number of genes including *nubbin/Pdm1* and *pros*, which are main regulators of differentiation to EC and EE respectively (Korzelius et al. 2014). Interestingly, ectopic *Pdm1* expression in progenitor cells is associated with decreased *esg* transcription. This could be an indication of the type of negative feedback loop between Esg and its target genes that eventually results in regulation of decision between preserving stem cell state or differentiation.

In case of EEs however there are discrepancies. DamID experiments on Drosophila neuroblasts showed that Pros has a binding site in the *esg* locus (Choksi et al. 2006). Interestingly, Li et al. showed that transient inactivation of *esg* in ISCs, but not EBs, promotes EE differentiation (Y. Li et al. 2017). They showed that inactivation of Notch and subsequent up-regulation of *sc* on the one hand results in direct activation of *pros* and one the other hand by antagonizing Esg prevents its inhibitory effect on *pros*. The outcome of this regulatory loop is specification of EEs through activation of *pros* in the absence of Notch signaling.

Moreover, most studies so far have focused on either *Gal4* or *lacZ*-based reporter genes and the probable effects of post-transcriptional regulation on *esg* function has remained understudied. In line with our observations, Guo et al and Hung et al reported the expression of *esg* in EEs that reside in the R3 region of the gut (X. Guo et al. 2019; Hung et al. 2020). Interestingly they observed that *esg* modulated expression of some of the hormones that are produced in EE cells in this region. Hence it is clear that in addition to maintaining ISC stemness, Esg also plays role in region-specific regulation of EE hormone production. One of the hormones that based on Guo et al. is regulated by Esg in the middle midgut is NPF (X. Guo et al. 2019). Interestingly, in our dataset expression

of both *esg* and *NPF* decrease with age. It is possible that the decrease in *NPF* transcription is to some extent due to lack of Esg in old guts.

In our dataset, we observed that both the number of Esg^{+} cells and the expression of *esg* increases in old EEs. Interestingly, Biteau et al. also reported accumulation of Esg^{+} cells in old guts, but they attributed this to the accumulation of ISCs in old gut, which is considered as a hallmark of ageing intestine. As they did not measure changes in Pros/Esg double positive EE cell numbers, it is difficult to conclude what proportion of this change in the number of Esg^{+} cells comes from ISCs and what proportion comes from increased pre-EE cells. (Biteau, Hochmuth, and Jasper 2008).

Further studies are needed to test this hypothesis and others regarding role of Esg in EE cell biology especially during ageing. In case of the effect of Esg on EE hormone production for instance, temporally controlled RNAi knockdown of *esg* and subsequent measurements of NPF transcript and protein levels could give direct insight into role of Esg on EE hormone production. Moreover, it has been reported that microRNAs such as miR-8 promote terminal differentiation of ISC/EBs by antagonizing Esg effects (Antonello et al. 2015). It would be interesting to know how much the increase in *esg* in old flies is compensated by miRs and to what extent the excess *esg* transcript level results in increased protein levels and functional output in old flies, or how much is buffered by post-transcriptional methods of regulation.

4.2.2 EE hormone production and cell type ratios change with in the ageing intestine

In recent years, it has become increasingly evident that production of hormones in EE cells is a dynamic process that changes depending on different environmental factors. EE hormone secretion is regulated by spatial placement of EE cells within the intestinal lumen, both along the A-P axis and crypt-villi axis (Dutta et al. 2015; Beumer et al. 2018). Furthermore, EE differentiation state and the type of nutrients play a role in determining the hormone(s) that EE cell produces. In mammals for instance GLP-1 is released from EEs in response to dietary sugar and subsequently regulates glucose metabolism

(Baggio and Drucker 2007). Bursicon α in *Drosophila* is another example of EE hormones that are produced and secreted upon availability of sugar in the food and represses AKH hormone in CC. Therefore, lack of Bursicon α signaling leads to lipodystrophy and hypoglycemia (Scopelliti et al. 2019). Preprocessing events also play important roles in maturation and functionality of hormones, which shows the importance of control of EE hormones in different levels, from transcription to translation and subsequently maturation by peptide processing (reviewed in (Reiher et al. 2011). Moreover, release of hormones from EE cells provides another level of control in EE hormone biology. A good example of control of hormone function by secretion in EE cells of *Drosophila* gut is release of NPF from EEs in response to activation by the seminal-fluid protein sex peptide (SP) upon mating (Ameku et al. 2018).

Advances in methods that are used to investigate endocrine biology, especially single cell sequencing, has resulted in the concept of EE hormonal plasticity; The type of hormone that an EE cell produces changes over time. Our scRNA-seq data provides evidence for these changes in the proportion of different EE cells in the context of age and sex. Due to the higher number of sequenced cells in female samples in our experiment, this difference is most reliably evident in young versus old female flies. We observed a clear decrease in proportion of NPF cells in older samples and increases in the AstA and pre-EE cell populations.

In the case of AstA population we observed an increase from 8% in young to 38% in old female guts, but our follow up experiment with a GAL4 reporter line for *AstA* did not confirm our scRNA-seq data. This could be due to the fact that the Gal4 line used for this experiment does not fully recapitulate the endogenous expression pattern of the gene in this tissue, as indicated by the lab that has generated this line (Tayler et al. 2012). Alternatively, as the AstA hormone is only one of the markers that we used for identifying the AstA EE subtype, we cannot exclude the possibility that other genes that we used as marker are main drivers of the observed increase in the AstA cell cluster. Unfortunately, due to lack of reagents including antibodies and reporter lines for these markers, it was not possible for us to further characterize the observed phenotype. Therefore further studies are needed to confirm this change and subsequently look for its probable effects

on local, tissue-level and systemic ageing. In particular, generating Gal4 reporter lines for other AstA cluster markers such as *lgr1*, *faa* and *sh* could help to accurately measure the changes of the identified cell clusters during ageing. Moreover, these reporters could give clues regarding the spatial distribution of each EE subtype in the gut, and subsequent changes in this distribution over time. This spatial information cannot be extrapolated using purely singe cell transcriptome approaches.

The change in EE progenitor populations with age in female fly sample is evident by increase in proportion of cells that express ISC-associated markers including *Dl*, *ase*, *sna*, and *wor*. We observed an increase of these cells from 21% (of total cells) in young female samples to 40% in old guts. Interestingly, Tauc et al reported a similar increase in EE progenitor cells in old flies while they were studying effects of chromatin remodeling on ISC differentiation potential (Tauc et al. 2021). They showed that in old guts, the promoter region of many of the genes that are targets of *Polycomb* (Pc), become more accessible. This results in higher expression of genes that are specific to EE cells including *ase* and *synaptotagmin 4*, and also regulators of EE fate like *sc* and *phyl* (X. Guo et al. 2019; Tauc et al. 2021). Moreover, preventing this mis-differentiation phenotype by inhibiting Pc results in phenotype reversal and improves gut health in old flies (Tauc et al. 2021). The increase in expression of EE-progenitor specific genes in aged ISCs is associated with a general increase in H3K27 di-methylation levels in aged ISCs. It is noteworthy that the level of this histone modification is in general higher in EEs compared to ISCs. Therefore, the fact that older ISC get higher H3K27me2 marks could be an indication of the mechanism by which activation of Pc genes results in increased pre-EE cell numbers seen in old guts. It was shown that H3K27me2 is responsible for repressing aberrant gene activation by affecting enhancers in mammals (Ferrari et al. 2014). In flies H3K27me2 represses the accessibility of DNA to RNA pol II and associated transcription factors (Lee et al. 2015). Interestingly, there are reports indicating the role of H3K27me2 in aged populations of hematopoietic stem cells and muscle stem cells (L. Liu et al. 2013; Sun et al. 2014).

In case of mammals, it has been shown that *Bmi1*, which is a member of Polycomb genes, is involved in ISC self-renewal and proliferation (López-Arribillaga et al. 2015). Bmi1 is expressed in ISCs and acts downstream of Notch, and is co-regulated by Notch and beta-Catenin. Inhibition of *Bmi1* results in reduced ISC proliferation and differentiation toward goblet cell fate, a phenotype that partially resembles Notch loss of function (López-Arribillaga et al. 2015, 1). More interestingly, a population of Bmi1$^+$ cells express markers of EEs including *prox1*, the *pros* orthologue in mice. These cells show colony formation potential *in-vitro* and are key to re-establishing tissue homeostasis in the intestine after injury, hence acting as a reserve-ISC reservoir for the intestine (Yan et al. 2017). This is another indication of existence of proliferative reservoirs among EE cell population that upon injury or in some cases even in homeostatic conditions could replace ISC function. These studies altogether show the close similarity, both functionally and transcriptionally, between ISC and pre-EE fates and that these cellular states can exhibit a remarkable plasticity that becomes especially apparent during stress and ageing.

4.2.3. *NPF* expression decreases with age

NPF is the *Drosophila* orthologue of mammalian neuropeptide Y (*NPY*), and similar to its mammalian counterpart, regulates a wide range of physiological activities including food intake, circadian rhythms, courtship, mating dependent cell proliferation and alcohol sensitivity (Brown et al. 1999; Y. Hu et al. 1996; Wen et al. 2005; W. Liu et al. 2019). Wen et al. for instance, showed that NPF signaling in the brain causes alcohol sensitivity. They observed that flies that lack NPF or its receptor show decreased sensitivity to ethanol sedation, while flies that overexpress *NPF* have higher sensitivity compared to controls (Wen et al. 2005). NPF also affects courtship in male flies. Knock down of *NPF* in a subset of neurons results in sexual hyper-activation of male flies and prompts mating behavior even in the absence of optimal stimuli (W. Liu et al. 2019). NPF release from EEs is also controlled by mating. It has been shown that NPF release from EEs in the midgut is triggered by presence of sex peptide upon mating. The released NPF subsequently promotes germline stem cell proliferation through paracrine activity in ovaries (Ameku et al. 2018).

One of the interesting findings of our scRNA-seq dataset was the decrease in proportion of NPF cells from 39% of all cell types in young female samples to around 14% in old guts. We found decreased expression of *NPF* in both our bulk and scRNA-seq datasets. We confirmed this finding by quantifying the number of NPF+ cells in young and old flies with a Gal4 knock-in reporter line of *NPF* (*NPF-Gal4*) combined with *UAS-GFP*. We observed loss of NPF+ cells with age in both male and female flies, although the region of the gut that was affected by this phenotype was different in each gender. In male flies, the middle section of the midgut was mainly responsible for the phenotype while in female samples, both anterior and middle midgut regions lost their NPF+ cell population.

Like many other neuropeptides that have expression in EE cells in addition to nervous system, most experiments so far have focused on the NPF hormone that originates from the brain, and until very recently not much was known about the role of NPF that is produced and secreted by the gut. In 2018 Ameku et al, showed that in addition to previous reports regarding effects of brain derived NPF on courtship behavior in flies (Ameku et al. 2018), gut derived NPF is also under control of mating in *Drosophila*. It has been shown that sex peptide originating from seminal fluid promotes enhanced secretion, but not enhanced production, of NPF from midgut EEs in female flies. Midgut-derived NPF subsequently activates germline stem cell proliferation. This was an interesting example of endocrine function of midgut-derived NPF, but also could be a probable explanation for the loss of NPF population phenotype that we observed, considering that the old flies in our experiment have mated only for a few days at the beginning of the experiment, and since then have been kept in vials without male flies. To test this, we used young virgin female flies and did the NPF quantification using the Gal4 driver line. We did not observe any difference in number or distribution of NPF$^+$ cells in virgin versus female flies.

In addition to similarities to NPY, there are reports showing that NPF acts in a similar way to incretin-like hormones in mammals to regulate energy homeostasis. Incretin refers to entero-endocrine hormones that stimulate secretion of insulin and/or glucagon in

mammals. Two widely-studied examples of incretin hormones are glucose-dependent insulinotropic polypeptide (GIP) and GLP-1 (Baggio and Drucker 2007). Like NPF, regulation of these hormones happens at different levels (Gribble and Reimann 2019). For instance, carbohydrate and lipid contents in the food stimulates the secretion of both hormones. Once released from the cell, incretin hormones stimulate secretion of insulin and simultaneously repress glucagon. NPF is the first and only reported incretin-like hormone in *Drosophila.*

Yoshinari et al. showed that NPF could regulate energy homeostasis by modulating insulin signaling on the one hand and adipokinetic hormone (AKH) on the other (Yoshinari et al. 2021). The *Drosophila* genome encodes 8 different insulin like peptides (*dIlps* or *DILPs* 1-8). From these, DILP 2, 3 and 5 have been shown to be particularly essential for regulating haemolymph glucose levels and fat storage, and also affect longevity (Grönke et al. 2010). The *Drosophila* genome also encodes *AKH*, which functionally acts similarly to glucagon. AKH is secreted from corpora cardiaca (CC) and through affecting fat body promotes lipolysis which leads to availability of energy to the body (Ahmad, He, and Perrimon 2020). Gut derived NPF is received by NPF receptor in two separate sections of the brain; one is insulin producing cells, in which NPF increases insulin signaling, and the other is CC, which produces AKH (Yoshinari et al. 2021). Interestingly, loss of NPF, similar to the loss of incretin function in mammals, leads to significant metabolic dysfunction, accompanied by lipodystrophy, hyperphagia and hypoglycemia. We observed a significant decrease in expression of *NPF* in old flies. Our unpublished data also indicated that NPF protein abundance reduces with age in $W^{Dahomey}$ flies. It would be particularly interesting to test if in addition to systemic effects on lipid content of the body, lack of NPF also affects local fat storage in the gut. This could be investigated by staining and quantification of fat droplets that cover the outer surface of the intestine.

Importantly, GLP-1 receptor agonists have been recently emerged as an approved and effective treatment for Type 2 diabetes and weight loss. Considering the fact that ageing is the primary risk factor for Type 2 diabetes, it would be interesting to test if increasingly lower levels of incretin-like hormones such as NPF could be predictive to the onset of

diabetes. Lowering insulin signaling activity is one of the best-established lifespan extending mechanisms that is conserved between different organisms from flies to mice. It would be interesting to test if overexpression of *NPF* (as an incretin-like hormone) in old gut rescues some of the metabolic hallmarks of ageing, or improve the lifespan of flies in general. In mammals there are various reports showing that GLP-1 and its agonists could have beneficial effects on age related phenotypes. Direct administration of GLP-1 in rats for instance, rescues age related glucose intolerance and also restores reduced insulin response to glucose in old animals (Y. Wang et al. 1997). More recently it has been shown that GLP-1 receptor agonists could reverse age related transcriptional changes of the brain cells, and also reduce transcriptional signatures of Alzheimer disease in macroglia that happens in old mice (Z. Li et al. 2021). Moreover, considering the fact that *NPY*, mammalian orthologue of *NPF*, also affects insulin secretion from pancreatic cells, and has role in regulating appetite (Imai et al. 2007), finding a similar change in proportion of NPY producing EEs in old mammals could also be of great scientific and therapeutic interest. Altogether, incretin and incretin-like hormones would make novel interesting candidates for improving age related phenotypes and should be considered as candidates with therapeutic potential for longevity intervention.

5. List of Figures

6. List of Tables

7. Contributions

Dr. Jerome Korzelius and Prof. Dr. Heinrich Jasper designed the Klumpfuss project. I conducted crossing, dissection, immunostaining, imaging and analysis of the sections that are mentioned in chapter 3.1. Dr. Jerome Korzelius conducted the bulk RNA sequencing experiment. Dr. Thomas Leech helped with the dissection of flies for the single cell RNA sequencing experiment. Ayesha Iqbal analyzed the single cell RNA sequencing data. Dr. Jerome Korzelius and Prof. Dr. Linda Partridge supervised the thesis projects.

8. References

Ahmad, Muhammad, Li He, and Norbert Perrimon. 2020. "Regulation of Insulin and Adipokinetic Hormone/Glucagon Production in Flies." *WIREs Developmental Biology* 9 (2): e360. https://doi.org/10.1002/wdev.360.

Amcheslavsky, Alla, Wei Song, Qi Li, Yingchao Nie, Ivan Bragatto, Dominique Ferrandon, Norbert Perrimon, and Y. Tony Ip. 2014. "Enteroendocrine Cells Support Intestinal Stem-Cell-Mediated Homeostasis in Drosophila." *Cell Reports* 9 (1): 32–39. https://doi.org/10.1016/j.celrep.2014.08.052.

Ameku, Tomotsune, Yuto Yoshinari, Michael J. Texada, Shu Kondo, Kotaro Amezawa, Goro Yoshizaki, Yuko Shimada-Niwa, and Ryusuke Niwa. 2018. "Midgut-Derived Neuropeptide F Controls Germline Stem Cell Proliferation in a Mating-Dependent Manner." *PLoS Biology* 16 (9): e2005004. https://doi.org/10.1371/journal.pbio.2005004.

Antonello, Zeus A., Tobias Reiff, Esther Ballesta-Illan, and Maria Dominguez. 2015. "Robust Intestinal Homeostasis Relies on Cellular Plasticity in Enteroblasts Mediated by MiR-8-Escargot Switch." *The EMBO Journal* 34 (15): 2025–41. https://doi.org/10.15252/embj.201591517.

Ayyaz, Arshad, Hongjie Li, and Heinrich Jasper. 2015. "Haemocytes Control Stem Cell Activity in the Drosophila Intestine." *Nature Cell Biology* 17 (6): 736–48. https://doi.org/10.1038/ncb3174.

Baggio, Laurie L., and Daniel J. Drucker. 2007. "Biology of Incretins: GLP-1 and GIP." *Gastroenterology* 132 (6): 2131–57. https://doi.org/10.1053/j.gastro.2007.03.054.

Bardin, Allison J., Carolina N. Perdigoto, Tony D. Southall, Andrea H. Brand, and François Schweisguth. 2010. "Transcriptional Control of Stem Cell Maintenance in the Drosophila Intestine." *Development (Cambridge, England)* 137 (5): 705–14. https://doi.org/10.1242/dev.039404.

Barker, Nick, Johan H. van Es, Jeroen Kuipers, Pekka Kujala, Maaike van den Born, Miranda Cozijnsen, Andrea Haegebarth, et al. 2007. "Identification of Stem Cells in Small Intestine and Colon by Marker Gene Lgr5." *Nature* 449 (7165): 1003–7. https://doi.org/10.1038/nature06196.

Bass, Timothy M., Richard C. Grandison, Richard Wong, Pedro Martinez, Linda Partridge, and Matthew D. W. Piper. 2007. "Optimization of Dietary Restriction Protocols in Drosophila." *The Journals of Gerontology. Series A, Biological Sciences and Medical Sciences* 62 (10): 1071–81. https://doi.org/10.1093/gerona/62.10.1071.

Beehler-Evans, Ryan, and Craig A. Micchelli. 2015. "Generation of Enteroendocrine Cell Diversity in Midgut Stem Cell Lineages." *Development (Cambridge, England)* 142 (4): 654–64. https://doi.org/10.1242/dev.114959.

Berger, Christian, Heike Harzer, Thomas R. Burkard, Jonas Steinmann, Suzanne van der Horst, Anne-Sophie Laurenson, Maria Novatchkova, Heinrich Reichert, and Juergen A. Knoblich. 2012. "FACS Purification and Transcriptome Analysis of Drosophila Neural Stem Cells Reveals a Role for Klumpfuss in Self-Renewal." *Cell Reports* 2 (2): 407–18. https://doi.org/10.1016/j.celrep.2012.07.008.

Beumer, Joep, Benedetta Artegiani, Yorick Post, Frank Reimann, Fiona Gribble, Thuc Nghi Nguyen, Hongkui Zeng, Maaike Van den Born, Johan H. Van Es, and Hans Clevers. 2018. "Enteroendocrine Cells Switch Hormone Expression along the Crypt-to-Villus BMP Signalling Gradient." *Nature Cell Biology* 20 (8): 909–16. https://doi.org/10.1038/s41556-018-0143-y.

Beumer, Joep, and Hans Clevers. 2021. "Cell Fate Specification and Differentiation in the Adult Mammalian Intestine." *Nature Reviews. Molecular Cell Biology* 22 (1): 39–53. https://doi.org/10.1038/s41580-020-0278-0.

Beumer, Joep, Jens Puschhof, Julia Bauzá-Martinez, Adriana Martínez-Silgado, Rasa Elmentaite, Kylie R. James, Alexander Ross, et al. 2020. "High-Resolution MRNA and Secretome Atlas of Human Enteroendocrine Cells." *Cell* 181 (6): 1291-1306.e19. https://doi.org/10.1016/j.cell.2020.04.036.

Beumer, Joep, Jens Puschhof, Fjodor Yousef Yengej, Lianzheng Zhao, Adriana Martinez-Silgado, Marloes Blotenburg, Harry Begthel, et al. 2022. "BMP Gradient along the Intestinal Villus Axis Controls Zonated Enterocyte and Goblet Cell States." *Cell Reports* 38 (9): 110438. https://doi.org/10.1016/j.celrep.2022.110438.

Bischoff, Vincent, Cécile Vignal, Bernard Duvic, Ivo G Boneca, Jules A Hoffmann, and Julien Royet. 2006. "Downregulation of the Drosophila Immune Response by Peptidoglycan-Recognition Proteins SC1 and SC2." *PLoS Pathogens* 2 (2): e14. https://doi.org/10.1371/journal.ppat.0020014.

Biteau, Benoît, Christine E. Hochmuth, and Heinrich Jasper. 2008. "JNK Activity in Somatic Stem Cells Causes Loss of Tissue Homeostasis in the Aging Drosophila Gut." *Cell Stem Cell* 3 (4): 442–55. https://doi.org/10.1016/j.stem.2008.07.024.

Biteau, Benoît, and Heinrich Jasper. 2011. "EGF Signaling Regulates the Proliferation of Intestinal Stem Cells in Drosophila." *Development (Cambridge, England)* 138 (6): 1045–55. https://doi.org/10.1242/dev.056671.

———. 2014. "Slit/Robo Signaling Regulates Cell Fate Decisions in the Intestinal Stem Cell Lineage of Drosophila." *Cell Reports* 7 (6): 1867–75. https://doi.org/10.1016/j.celrep.2014.05.024.

Biteau, Benoît, Jason Karpac, Stephen Supoyo, Matthew DeGennaro, Ruth Lehmann, and Heinrich Jasper. 2010. "Lifespan Extension by Preserving Proliferative Homeostasis in Drosophila." *PLoS Genetics* 6 (10): e1001159. https://doi.org/10.1371/journal.pgen.1001159.

Bjerknes, M., and H. Cheng. 1999. "Clonal Analysis of Mouse Intestinal Epithelial Progenitors." *Gastroenterology* 116 (1): 7–14. https://doi.org/10.1016/s0016-5085(99)70222-2.

Bjerknes, Matthew, and Hazel Cheng. 2010. "Cell Lineage Metastability in Gfi1-Deficient Mouse Intestinal Epithelium." *Developmental Biology* 345 (1): 49–63. https://doi.org/10.1016/j.ydbio.2010.06.021.

Bolukbasi, Ekin, Mobina Khericha, Jennifer C. Regan, Dobril K. Ivanov, Jennifer Adcott, Miranda C. Dyson, Tobias Nespital, Janet M. Thornton, Nazif Alic, and Linda Partridge. 2017. "Intestinal Fork Head Regulates Nutrient Absorption and Promotes Longevity." *Cell Reports* 21 (3): 641–53. https://doi.org/10.1016/j.celrep.2017.09.042.

Böttcher, Anika, Maren Büttner, Sophie Tritschler, Michael Sterr, Alexandra Aliluev, Lena Oppenländer, Ingo Burtscher, et al. 2021. "Non-Canonical Wnt/PCP Signalling Regulates Intestinal Stem Cell Lineage Priming towards Enteroendocrine and Paneth Cell Fates." *Nature Cell Biology* 23 (1): 23–31. https://doi.org/10.1038/s41556-020-00617-2.

Brown, M. R., J. W. Crim, R. C. Arata, H. N. Cai, C. Chun, and P. Shen. 1999. "Identification of a Drosophila Brain-Gut Peptide Related to the Neuropeptide Y Family." *Peptides* 20 (9): 1035–42. https://doi.org/10.1016/s0196-9781(99)00097-2.

Buchon, Nicolas, Nichole A. Broderick, Sveta Chakrabarti, and Bruno Lemaitre. 2009. "Invasive and Indigenous Microbiota Impact Intestinal Stem Cell Activity through Multiple Pathways in Drosophila." *Genes & Development* 23 (19): 2333–44. https://doi.org/10.1101/gad.1827009.

Buchon, Nicolas, Nichole A. Broderick, Mickael Poidevin, Sylvain Pradervand, and Bruno Lemaitre. 2009. "Drosophila Intestinal Response to Bacterial Infection: Activation of Host Defense and Stem Cell Proliferation." *Cell Host & Microbe* 5 (2): 200–211. https://doi.org/10.1016/j.chom.2009.01.003.

Buchon, Nicolas, Dani Osman, Fabrice P.A. David, Hsiao Yu Fang, Jean-Philippe Boquete, Bart Deplancke, and Bruno Lemaitre. 2013. "Morphological and Molecular Characterization of Adult Midgut Compartmentalization in Drosophila." *Cell Reports* 3 (5): 1725–38. https://doi.org/10.1016/j.celrep.2013.04.001.

Buczacki, Simon J. A., Heather Ireland Zecchini, Anna M. Nicholson, Roslin Russell, Louis Vermeulen, Richard Kemp, and Douglas J. Winton. 2013. "Intestinal Label-Retaining Cells Are Secretory Precursors Expressing Lgr5." *Nature* 495 (7439): 65–69. https://doi.org/10.1038/nature11965.

Carulli, Alexis J., Theresa M. Keeley, Elise S. Demitrack, Jooho Chung, Ivan Maillard, and Linda C. Samuelson. 2015. "Notch Receptor Regulation of Intestinal Stem Cell Homeostasis and Crypt Regeneration." *Developmental Biology* 402 (1): 98–108. https://doi.org/10.1016/j.ydbio.2015.03.012.

Chang, Wenju, Hongshan Wang, Woosook Kim, Yang Liu, Huan Deng, Haibo Liu, Zhengyu Jiang, et al. 2020. "Hormonal Suppression of Stem Cells Inhibits Symmetric Cell Division and Gastric Tumorigenesis." *Cell Stem Cell* 26 (5): 739-754.e8. https://doi.org/10.1016/j.stem.2020.01.020.

Chen, Jun, Na Xu, Chenhui Wang, Pin Huang, Huanwei Huang, Zhen Jin, Zhongsheng Yu, Tao Cai, Renjie Jiao, and Rongwen Xi. 2018. "Transient Scute Activation via a Self-Stimulatory Loop Directs Enteroendocrine Cell Pair Specification from Self-Renewing Intestinal Stem Cells." *Nature Cell Biology* 20 (2): 152–61. https://doi.org/10.1038/s41556-017-0020-0.

Cheng, H., and C. P. Leblond. 1974. "Origin, Differentiation and Renewal of the Four Main Epithelial Cell Types in the Mouse Small Intestine. V. Unitarian Theory of the Origin of the Four Epithelial Cell Types." *The American Journal of Anatomy* 141 (4): 537–61. https://doi.org/10.1002/aja.1001410407.

Choksi, Semil P., Tony D. Southall, Torsten Bossing, Karin Edoff, Elzo de Wit, Bettina E. Fischer, Bas van Steensel, Gos Micklem, and Andrea H. Brand. 2006. "Prospero Acts as a Binary Switch between Self-Renewal and Differentiation in Drosophila Neural Stem Cells." *Developmental Cell* 11 (6): 775–89. https://doi.org/10.1016/j.devcel.2006.09.015.

Clevers, Hans. 2013. "The Intestinal Crypt, a Prototype Stem Cell Compartment." *Cell* 154 (2): 274–84. https://doi.org/10.1016/j.cell.2013.07.004.

Cordero, Julia B, Rhoda K Stefanatos, Alessandro Scopelliti, Marcos Vidal, and Owen J Sansom. 2012. "Inducible Progenitor-Derived Wingless Regulates Adult Midgut Regeneration in Drosophila." *The EMBO Journal* 31 (19): 3901–17. https://doi.org/10.1038/emboj.2012.248.

Dekaney, Christopher M., Ajay S. Gulati, Aaron P. Garrison, Michael A. Helmrath, and Susan J. Henning. 2009. "Regeneration of Intestinal Stem/Progenitor Cells Following Doxorubicin Treatment of Mice." *American Journal of Physiology. Gastrointestinal and Liver Physiology* 297 (3): G461-470. https://doi.org/10.1152/ajpgi.90446.2008.

Demitrack, Elise S., and Linda C. Samuelson. 2016. "Notch Regulation of Gastrointestinal Stem Cells." *The Journal of Physiology* 594 (17): 4791–4803. https://doi.org/10.1113/JP271667.

Dubreuil, R. R., T. Grushko, and O. Baumann. 2001. "Differential Effects of a Labial Mutation on the Development, Structure, and Function of Stomach Acid-Secreting Cells in Drosophila Melanogaster Larvae and Adults." *Cell and Tissue Research* 306 (1): 167–78. https://doi.org/10.1007/s004410100422.

Dutta, Devanjali, Adam J. Dobson, Philip L. Houtz, Christine Gläßer, Jonathan Revah, Jerome Korzelius, Parthive H. Patel, Bruce A. Edgar, and Nicolas Buchon. 2015. "Regional Cell-Specific Transcriptome Mapping Reveals Regulatory Complexity in the Adult Drosophila Midgut." *Cell Reports* 12 (2): 346–58. https://doi.org/10.1016/j.celrep.2015.06.009.

Es, Johan H. van, Marielle E. van Gijn, Orbicia Riccio, Maaike van den Born, Marc Vooijs, Harry Begthel, Miranda Cozijnsen, et al. 2005. "Notch/Gamma-Secretase Inhibition Turns Proliferative Cells in Intestinal Crypts and Adenomas into Goblet Cells." *Nature* 435 (7044): 959–63. https://doi.org/10.1038/nature03659.

Es, Johan H. van, Philippe Jay, Alex Gregorieff, Marielle E. van Gijn, Suzanne Jonkheer, Pantelis Hatzis, Andrea Thiele, et al. 2005. "Wnt Signalling Induces Maturation of Paneth Cells in Intestinal Crypts." *Nature Cell Biology* 7 (4): 381–86. https://doi.org/10.1038/ncb1240.

Es, Johan H. van, Toshiro Sato, Marc van de Wetering, Anna Lyubimova, Annie Ng Yee Nee, Alex Gregorieff, Nobuo Sasaki, et al. 2012. "Dll1+ Secretory Progenitor Cells Revert to Stem Cells upon Crypt Damage." *Nature Cell Biology* 14 (10): 1099–1104. https://doi.org/10.1038/ncb2581.

Fan, Xiaolan, Qing Liang, Ting Lian, Qi Wu, Uma Gaur, Diyan Li, Deying Yang, et al. 2015. "Rapamycin Preserves Gut Homeostasis during Drosophila Aging." *Oncotarget* 6 (34): 35274–83. https://doi.org/10.18632/oncotarget.5895.

Fane, Mitchell, and Ashani T. Weeraratna. 2020. "How the Ageing Microenvironment Influences Tumour Progression." *Nature Reviews Cancer* 20 (2): 89–106. https://doi.org/10.1038/s41568-019-0222-9.

Ferrari, Karin J., Andrea Scelfo, Sriganesh Jammula, Alessandro Cuomo, Iros Barozzi, Alexandra Stützer, Wolfgang Fischle, Tiziana Bonaldi, and Diego Pasini. 2014. "Polycomb-Dependent H3K27me1 and H3K27me2 Regulate Active Transcription and Enhancer Fidelity." *Molecular Cell* 53 (1): 49–62. https://doi.org/10.1016/j.molcel.2013.10.030.

Franceschi, Claudio, Paolo Garagnani, Paolo Parini, Cristina Giuliani, and Aurelia Santoro. 2018. "Inflammaging: A New Immune-Metabolic Viewpoint for Age-Related Diseases." *Nature Reviews. Endocrinology* 14 (10): 576–90. https://doi.org/10.1038/s41574-018-0059-4.

Fre, Silvia, Mathilde Huyghe, Philippos Mourikis, Sylvie Robine, Daniel Louvard, and Spyros Artavanis-Tsakonas. 2005. "Notch Signals Control the Fate of Immature Progenitor Cells in the Intestine." *Nature* 435 (7044): 964–68. https://doi.org/10.1038/nature03589.

Gehart, Helmuth, Johan H. van Es, Karien Hamer, Joep Beumer, Kai Kretzschmar, Johanna F. Dekkers, Anne Rios, and Hans Clevers. 2019. "Identification of Enteroendocrine Regulators by Real-Time Single-Cell Differentiation Mapping." *Cell* 176 (5): 1158-1173.e16. https://doi.org/10.1016/j.cell.2018.12.029.

Gribble, Fiona M., and Frank Reimann. 2019. "Function and Mechanisms of Enteroendocrine Cells and Gut Hormones in Metabolism." *Nature Reviews. Endocrinology* 15 (4): 226–37. https://doi.org/10.1038/s41574-019-0168-8.

———. 2021. "Metabolic Messengers: Glucagon-like Peptide 1." *Nature Metabolism* 3 (2): 142–48. https://doi.org/10.1038/s42255-020-00327-x.

Grönke, Sebastian, David-Francis Clarke, Susan Broughton, T. Daniel Andrews, and Linda Partridge. 2010. "Molecular Evolution and Functional Characterization of Drosophila Insulin-like Peptides." *PLoS Genetics* 6 (2): e1000857. https://doi.org/10.1371/journal.pgen.1000857.

Grün, Dominic, Anna Lyubimova, Lennart Kester, Kay Wiebrands, Onur Basak, Nobuo Sasaki, Hans Clevers, and Alexander van Oudenaarden. 2015. "Single-Cell Messenger RNA Sequencing Reveals Rare Intestinal Cell Types." *Nature* 525 (7568): 251–55. https://doi.org/10.1038/nature14966.

Guo, Linlin, Jason Karpac, Susan L. Tran, and Heinrich Jasper. 2014. "PGRP-SC2 Promotes Gut Immune Homeostasis to Limit Commensal Dysbiosis and Extend Lifespan." *Cell* 156 (1–2): 109–22. https://doi.org/10.1016/j.cell.2013.12.018.

Guo, Xingting, Chang Yin, Fu Yang, Yongchao Zhang, Huanwei Huang, Jiawen Wang, Bowen Deng, Tao Cai, Yi Rao, and Rongwen Xi. 2019. "The Cellular Diversity and Transcription Factor Code of Drosophila Enteroendocrine Cells." *Cell Reports* 29 (12): 4172-4185.e5. https://doi.org/10.1016/j.celrep.2019.11.048.

Guo, Zheng, and Benjamin Ohlstein. 2015. "Stem Cell Regulation. Bidirectional Notch Signaling Regulates Drosophila Intestinal Stem Cell Multipotency." *Science (New York, N.Y.)* 350 (6263): aab0988. https://doi.org/10.1126/science.aab0988.

Haber, Adam L., Moshe Biton, Noga Rogel, Rebecca H. Herbst, Karthik Shekhar, Christopher Smillie, Grace Burgin, et al. 2017. "A Single-Cell Survey of the Small Intestinal Epithelium." *Nature* 551 (7680): 333–39. https://doi.org/10.1038/nature24489.

Haller, Samantha, Subir Kapuria, Rebeccah R. Riley, Monique N. O'Leary, Katherine H. Schreiber, Julie K. Andersen, Simon Melov, et al. 2017. "MTORC1 Activation during Repeated Regeneration Impairs Somatic Stem Cell Maintenance." *Cell Stem Cell* 21 (6): 806-818.e5. https://doi.org/10.1016/j.stem.2017.11.008.

Hao, Yuhan, Stephanie Hao, Erica Andersen-Nissen, William M. Mauck, Shiwei Zheng, Andrew Butler, Maddie J. Lee, et al. 2021. "Integrated Analysis of Multimodal Single-Cell Data." *Cell* 184 (13): 3573-3587.e29. https://doi.org/10.1016/j.cell.2021.04.048.

Hastie, Nicholas D. 2017. "Wilms' Tumour 1 (WT1) in Development, Homeostasis and Disease." *Development (Cambridge, England)* 144 (16): 2862–72. https://doi.org/10.1242/dev.153163.

He, Li, Guangwei Si, Jiuhong Huang, Aravinthan D. T. Samuel, and Norbert Perrimon. 2018. "Mechanical Regulation of Stem-Cell Differentiation by the Stretch-Activated Piezo Channel." *Nature* 555 (7694): 103–6. https://doi.org/10.1038/nature25744.

Heuberger, Julian, Frauke Kosel, Jingjing Qi, Katja S. Grossmann, Klaus Rajewsky, and Walter Birchmeier. 2014. "Shp2/MAPK Signaling Controls Goblet/Paneth Cell Fate Decisions in the Intestine." *Proceedings of the National Academy of Sciences of the United States of America* 111 (9): 3472–77. https://doi.org/10.1073/pnas.1309342111.

Hoppler, S., and M. Bienz. 1994. "Specification of a Single Cell Type by a Drosophila Homeotic Gene." *Cell* 76 (4): 689–702. https://doi.org/10.1016/0092-8674(94)90508-8.

Hu, Daniel Jun-Kit, and Heinrich Jasper. 2019. "Control of Intestinal Cell Fate by Dynamic Mitotic Spindle Repositioning Influences Epithelial Homeostasis and Longevity." *Cell Reports* 28 (11): 2807-2823.e5. https://doi.org/10.1016/j.celrep.2019.08.014.

Hu, Y., B. T. Bloomquist, L. J. Cornfield, L. B. DeCarr, J. R. Flores-Riveros, L. Friedman, P. Jiang, et al. 1996. "Identification of a Novel Hypothalamic Neuropeptide Y Receptor Associated with Feeding Behavior." *The Journal of Biological Chemistry* 271 (42): 26315–19.

Hudry, Bruno, Sanjay Khadayate, and Irene Miguel-Aliaga. 2016. "The Sexual Identity of Adult Intestinal Stem Cells Controls Organ Size and Plasticity." *Nature* 530 (7590): 344–48. https://doi.org/10.1038/nature16953.

Hung, Ruei-Jiun, Yanhui Hu, Rory Kirchner, Yifang Liu, Chiwei Xu, Aram Comjean, Sudhir Gopal Tattikota, et al. 2020. "A Cell Atlas of the Adult Drosophila Midgut." *Proceedings of the National Academy of Sciences of the United States of America* 117 (3): 1514–23. https://doi.org/10.1073/pnas.1916820117.

Imai, Yumi, Hiral R. Patel, Evan J. Hawkins, Nicolai M. Doliba, Franz M. Matschinsky, and Rexford S. Ahima. 2007. "Insulin Secretion Is Increased in Pancreatic Islets of Neuropeptide Y-Deficient Mice." *Endocrinology* 148 (12): 5716–23. https://doi.org/10.1210/en.2007-0404.

Jadhav, Unmesh, Madhurima Saxena, Nicholas K. O'Neill, Assieh Saadatpour, Guo-Cheng Yuan, Zachary Herbert, Kazutaka Murata, and Ramesh A. Shivdasani. 2017. "Dynamic Reorganization of Chromatin Accessibility Signatures during Dedifferentiation of Secretory Precursors into Lgr5+ Intestinal Stem Cells." *Cell Stem Cell* 21 (1): 65-77.e5. https://doi.org/10.1016/j.stem.2017.05.001.

Jasper, Heinrich. 2020. "Intestinal Stem Cell Aging: Origins and Interventions." *Annual Review of Physiology* 82 (February): 203–26. https://doi.org/10.1146/annurev-physiol-021119-034359.

Jenny, Marjorie, Céline Uhl, Colette Roche, Isabelle Duluc, Valérie Guillermin, Francois Guillemot, Jan Jensen, Michèle Kedinger, and Gérard Gradwohl. 2002. "Neurogenin3 Is Differentially Required for Endocrine Cell Fate Specification in the Intestinal and Gastric Epithelium." *The EMBO Journal* 21 (23): 6338–47. https://doi.org/10.1093/emboj/cdf649.

Jiang, Huaqi, Parthive H. Patel, Alexander Kohlmaier, Marc O. Grenley, Donald G. McEwen, and Bruce A. Edgar. 2009. "Cytokine/Jak/Stat Signaling Mediates Regeneration and Homeostasis in the Drosophila Midgut." *Cell* 137 (7): 1343–55. https://doi.org/10.1016/j.cell.2009.05.014.

Juricic, Paula, Yu-Xuan Lu, Thomas Leech, Lisa F. Drews, Jonathan Paulitz, Jiongming Lu, Tobias Nespital, et al. 2022. "Full Geroprotection from Brief Rapamycin Treatment by Persistently Increased Intestinal Autophagy." bioRxiv. https://doi.org/10.1101/2022.04.20.488884.

Karpac, Jason, Benoit Biteau, and Heinrich Jasper. 2013. "Misregulation of an Adaptive Metabolic Response Contributes to the Age-Related Disruption of Lipid Homeostasis in Drosophila." *Cell Reports* 4 (6): 1250–61. https://doi.org/10.1016/j.celrep.2013.08.004.

Katz, Jonathan P., Nathalie Perreault, Bree G. Goldstein, Catherine S. Lee, Patricia A. Labosky, Vincent W. Yang, and Klaus H. Kaestner. 2002. "The Zinc-Finger Transcription Factor Klf4 Is Required for Terminal Differentiation of Goblet Cells in the Colon." *Development (Cambridge, England)* 129 (11): 2619–28. https://doi.org/10.1242/dev.129.11.2619.

Kennedy, Brian K., Shelley L. Berger, Anne Brunet, Judith Campisi, Ana Maria Cuervo, Elissa S. Epel, Claudio Franceschi, et al. 2014. "Geroscience: Linking Aging to Chronic Disease." *Cell* 159 (4): 709–13. https://doi.org/10.1016/j.cell.2014.10.039.

Kiyokawa, Hirofumi, and Mitsuru Morimoto. 2020. "Notch Signaling in the Mammalian Respiratory System, Specifically the Trachea and Lungs, in Development, Homeostasis, Regeneration, and Disease." *Development, Growth & Differentiation* 62 (1): 67–79. https://doi.org/10.1111/dgd.12628.

Klein, T., and J. A. Campos-Ortega. 1997. "Klumpfuss, a Drosophila Gene Encoding a Member of the EGR Family of Transcription Factors, Is Involved in Bristle and Leg Development." *Development (Cambridge, England)* 124 (16): 3123–34. https://doi.org/10.1242/dev.124.16.3123.

Korzelius, Jerome, Sina Azami, Tal Ronnen-Oron, Philipp Koch, Maik Baldauf, Elke Meier, Imilce A. Rodriguez-Fernandez, Marco Groth, Pedro Sousa-Victor, and Heinrich Jasper. 2019. "The WT1-like Transcription Factor Klumpfuss Maintains Lineage Commitment of Enterocyte Progenitors in the Drosophila Intestine." *Nature Communications* 10 (1): 4123. https://doi.org/10.1038/s41467-019-12003-0.

Korzelius, Jerome, Svenja K. Naumann, Mariano A. Loza-Coll, Jessica Sk Chan, Devanjali Dutta, Jessica Oberheim, Christine Gläßer, et al. 2014. "Escargot Maintains Stemness and Suppresses Differentiation in Drosophila Intestinal Stem Cells." *The EMBO Journal* 33 (24): 2967–82. https://doi.org/10.15252/embj.201489072.

Lathia, Justin D., Mark P. Mattson, and Aiwu Cheng. 2008. "Notch: From Neural Development to Neurological Disorders." *Journal of Neurochemistry* 107 (6): 1471–81. https://doi.org/10.1111/j.1471-4159.2008.05715.x.

Latorre, R., C. Sternini, R. De Giorgio, and B. Greenwood-Van Meerveld. 2016. "Enteroendocrine Cells: A Review of Their Role In Brain-Gut Communication." *Neurogastroenterology and Motility : The Official Journal of the European Gastrointestinal Motility Society* 28 (5): 620–30. https://doi.org/10.1111/nmo.12754.

Lee, Hun-Goo, Tatyana G. Kahn, Amanda Simcox, Yuri B. Schwartz, and Vincenzo Pirrotta. 2015. "Genome-Wide Activities of Polycomb Complexes Control Pervasive Transcription." *Genome Research* 25 (8): 1170–81. https://doi.org/10.1101/gr.188920.114.

Lemaitre, Bruno, and Irene Miguel-Aliaga. 2013. "The Digestive Tract of *Drosophila Melanogaster*." *Annual Review of Genetics* 47 (1): 377–404. https://doi.org/10.1146/annurev-genet-111212-133343.

Li, Hongjie, Jasper Janssens, Maxime De Waegeneer, Sai Saroja Kolluru, Kristofer Davie, Vincent Gardeux, Wouter Saelens, et al. 2022. "Fly Cell Atlas: A Single-Nucleus Transcriptomic Atlas of the Adult Fruit Fly." *Science (New York, N.Y.)* 375 (6584): eabk2432. https://doi.org/10.1126/science.abk2432.

Li, Hongjie, Yanyan Qi, and Heinrich Jasper. 2013. "Dpp Signaling Determines Regional Stem Cell Identity in the Regenerating Adult Drosophila Gastrointestinal Tract." *Cell Reports* 4 (1): 10–18. https://doi.org/10.1016/j.celrep.2013.05.040.

———. 2016. "Preventing Age-Related Decline of Gut Compartmentalization Limits Microbiota Dysbiosis and Extends Lifespan." *Cell Host & Microbe* 19 (2): 240–53. https://doi.org/10.1016/j.chom.2016.01.008.

Li, Yumei, Zhimin Pang, Huanwei Huang, Chenhui Wang, Tao Cai, and Rongwen Xi. 2017. "Transcription Factor Antagonism Controls Enteroendocrine Cell Specification from Intestinal Stem Cells." *Scientific Reports* 7 (1): 988. https://doi.org/10.1038/s41598-017-01138-z.

Li, Zhongqi, Xinyi Chen, Joaquim S. L. Vong, Lei Zhao, Junzhe Huang, Leo Y. C. Yan, Bonaventure Ip, et al. 2021. "Systemic GLP-1R Agonist Treatment Reverses Mouse Glial and Neurovascular Cell Transcriptomic Aging Signatures in a Genome-Wide Manner." *Communications Biology* 4 (1): 1–6. https://doi.org/10.1038/s42003-021-02208-9.

Lin, Guonan, Na Xu, and Rongwen Xi. 2008. "Paracrine Wingless Signalling Controls Self-Renewal of Drosophila Intestinal Stem Cells." *Nature* 455 (7216): 1119–23. https://doi.org/10.1038/nature07329.

Liu, Ling, Tom H. Cheung, Gregory W. Charville, Bernadette Marie Ceniza Hurgo, Tripp Leavitt, Johnathan Shih, Anne Brunet, and Thomas A. Rando. 2013. "Chromatin Modifications as Determinants of Muscle Stem Cell Quiescence and Chronological Aging." *Cell Reports* 4 (1): 189–204. https://doi.org/10.1016/j.celrep.2013.05.043.

Liu, Weiwei, Anindya Ganguly, Jia Huang, Yijin Wang, Jinfei D. Ni, Adishthi S. Gurav, Morris A. Aguilar, and Craig Montell. 2019. "Neuropeptide F Regulates Courtship in Drosophila through a Male-Specific Neuronal Circuit." *ELife* 8 (August): e49574. https://doi.org/10.7554/eLife.49574.

López-Arribillaga, Erika, Verónica Rodilla, Luca Pellegrinet, Jordi Guiu, Mar Iglesias, Angel Carlos Roman, Susana Gutarra, et al. 2015. "Bmi1 Regulates Murine Intestinal Stem Cell Proliferation and Self-Renewal Downstream of Notch." *Development (Cambridge, England)* 142 (1): 41–50. https://doi.org/10.1242/dev.107714.

López-Otín, Carlos, Maria A. Blasco, Linda Partridge, Manuel Serrano, and Guido Kroemer. 2013. "The Hallmarks of Aging." *Cell* 153 (6): 1194–1217. https://doi.org/10.1016/j.cell.2013.05.039.

Marianes, Alexis, and Allan C Spradling. 2013. "Physiological and Stem Cell Compartmentalization within the Drosophila Midgut." *ELife* 2 (August): e00886. https://doi.org/10.7554/eLife.00886.

Mayer, Emeran A., Karina Nance, and Shelley Chen. 2022. "The Gut–Brain Axis." *Annual Review of Medicine* 73 (1): 439–53. https://doi.org/10.1146/annurev-med-042320-014032.

McClelland, Lindy, Heinrich Jasper, and Benoît Biteau. 2017. "Tis11 Mediated MRNA Decay Promotes the Reacquisition of Drosophila Intestinal Stem Cell Quiescence." *Developmental Biology* 426 (1): 8–16. https://doi.org/10.1016/j.ydbio.2017.04.013.

McGuire, Sean E., Phuong T. Le, Alexander J. Osborn, Kunihiro Matsumoto, and Ronald L. Davis. 2003. "Spatiotemporal Rescue of Memory Dysfunction in Drosophila." *Science (New York, N.Y.)* 302 (5651): 1765–68. https://doi.org/10.1126/science.1089035.

Micchelli, Craig A., and Norbert Perrimon. 2006. "Evidence That Stem Cells Reside in the Adult Drosophila Midgut Epithelium." *Nature* 439 (7075): 475–79. https://doi.org/10.1038/nature04371.

Miguel-Aliaga, Irene, Heinrich Jasper, and Bruno Lemaitre. 2018. "Anatomy and Physiology of the Digestive Tract of *Drosophila Melanogaster*." *Genetics* 210 (2): 357–96. https://doi.org/10.1534/genetics.118.300224.

Moran-Ramos, Sofia, Armando R. Tovar, and Nimbe Torres. 2012. "Diet: Friend or Foe of Enteroendocrine Cells--How It Interacts with Enteroendocrine Cells." *Advances in Nutrition (Bethesda, Md.)* 3 (1): 8–20. https://doi.org/10.3945/an.111.000976.

Mori-Akiyama, Yuko, Maaike van den Born, Johan H. van Es, Stanley R. Hamilton, Henry P. Adams, Jiexin Zhang, Hans Clevers, and Benoit de Crombrugghe. 2007. "SOX9 Is Required for the Differentiation of Paneth Cells in the Intestinal Epithelium." *Gastroenterology* 133 (2): 539–46. https://doi.org/10.1053/j.gastro.2007.05.020.

Murakami, Ryutaro, Ayako Shigenaga, 1Akira Matsumoto, Ikuo Yamaoka, and Teiichi Tanimura. 1994. "Novel Tissue Units of Regional Differentiation in the Gut Epithelium of Drosopbila, as Revealed by P-Element-Mediated Detection of Enhancer." *Roux's Archives of Developmental Biology* 203 (5): 243–49. https://doi.org/10.1007/BF00360519.

Nässel, Dick R., and Asa M. E. Winther. 2010. "Drosophila Neuropeptides in Regulation of Physiology and Behavior." *Progress in Neurobiology* 92 (1): 42–104. https://doi.org/10.1016/j.pneurobio.2010.04.010.

Nässel, Dick R., and Meet Zandawala. 2020. "Hormonal Axes in Drosophila: Regulation of Hormone Release and Multiplicity of Actions." *Cell and Tissue Research* 382 (2): 233–66. https://doi.org/10.1007/s00441-020-03264-z.

Noah, Taeko K., and Noah F. Shroyer. 2013. "Notch in the Intestine: Regulation of Homeostasis and Pathogenesis." *Annual Review of Physiology* 75 (1): 263–88. https://doi.org/10.1146/annurev-physiol-030212-183741.

Obniski, Rebecca, Matthew Sieber, and Allan C. Spradling. 2018. "Dietary Lipids Modulate Notch Signaling and Influence Adult Intestinal Development and Metabolism in Drosophila." *Developmental Cell* 47 (1): 98-111.e5. https://doi.org/10.1016/j.devcel.2018.08.013.

O'Brien, Lucy Erin, Sarah S. Soliman, Xinghua Li, and David Bilder. 2011. "Altered Modes of Stem Cell Division Drive Adaptive Intestinal Growth." *Cell* 147 (3): 603–14. https://doi.org/10.1016/j.cell.2011.08.048.

Ohlstein, Benjamin, and Allan Spradling. 2006. "The Adult Drosophila Posterior Midgut Is Maintained by Pluripotent Stem Cells." *Nature* 439 (7075): 470–74. https://doi.org/10.1038/nature04333.

———. 2007. "Multipotent Drosophila Intestinal Stem Cells Specify Daughter Cell Fates by Differential Notch Signaling." *Science (New York, N.Y.)* 315 (5814): 988–92. https://doi.org/10.1126/science.1136606.

Okumura, Takashi, Reiko Tajiri, Tetsuya Kojima, Kaoru Saigo, and Ryutaro Murakami. 2007. "GATAe-Dependent and -Independent Expressions of Genes in the Differentiated Endodermal Midgut of Drosophila." *Gene Expression Patterns: GEP* 7 (1–2): 178–86. https://doi.org/10.1016/j.modgep.2006.07.001.

Park, Jeong-Ho, Ji Chen, Sooin Jang, Tae Jung Ahn, KyeongJin Kang, Min Sung Choi, and Jae Young Kwon. 2016. "A Subset of Enteroendocrine Cells Is Activated by Amino Acids in the Drosophila Midgut." *FEBS Letters* 590 (4): 493–500. https://doi.org/10.1002/1873-3468.12073.

Pellegrinet, Luca, Veronica Rodilla, Zhenyi Liu, Shuang Chen, Ute Koch, Lluis Espinosa, Klaus H. Kaestner, Raphael Kopan, Julian Lewis, and Freddy Radtke. 2011. "Dll1- and Dll4-Mediated Notch Signaling Are Required for Homeostasis of Intestinal Stem Cells." *Gastroenterology* 140 (4): 1230-1240.e1-7. https://doi.org/10.1053/j.gastro.2011.01.005.

Perdigoto, Carolina N., Francois Schweisguth, and Allison J. Bardin. 2011. "Distinct Levels of Notch Activity for Commitment and Terminal Differentiation of Stem Cells in the Adult Fly Intestine." *Development (Cambridge, England)* 138 (21): 4585–95. https://doi.org/10.1242/dev.065292.

Pliner, Hannah A., Jay Shendure, and Cole Trapnell. 2019. "Supervised Classification Enables Rapid Annotation of Cell Atlases." *Nature Methods* 16 (10): 983–86. https://doi.org/10.1038/s41592-019-0535-3.

Regan, Jennifer C., Mobina Khericha, Adam J. Dobson, Ekin Bolukbasi, Nattaphong Rattanavirotkul, and Linda Partridge. 2016. "Sex Difference in Pathology of the Ageing Gut Mediates the Greater

Response of Female Lifespan to Dietary Restriction." *ELife* 5 (February): e10956. https://doi.org/10.7554/eLife.10956.

Regan, Jennifer C., Yu-Xuan Lu, Ekin Bolukbasi, Mobina Khericha, and Linda Partridge. 2018. "Ras Inhibition by Trametinib Treatment in Drosophila Attenuates Gut Pathology in Females and Extends Lifespan in Both Sexes." bioRxiv. https://doi.org/10.1101/356295.

Rehfeld, Jens F., Jens R. Bundgaard, Jens Hannibal, Xiaorong Zhu, Christina Norrbom, Donald F. Steiner, and Lennart Friis-Hansen. 2008. "The Cell-Specific Pattern of Cholecystokinin Peptides in Endocrine Cells versus Neurons Is Governed by the Expression of Prohormone Convertases 1/3, 2, and 5/6." *Endocrinology* 149 (4): 1600–1608. https://doi.org/10.1210/en.2007-0278.

Reiff, Tobias, Zeus A. Antonello, Esther Ballesta-Illán, Laura Mira, Salvador Sala, Maria Navarro, Luis M. Martinez, and Maria Dominguez. 2019. "Notch and EGFR Regulate Apoptosis in Progenitor Cells to Ensure Gut Homeostasis in Drosophila." *The EMBO Journal* 38 (21): e101346. https://doi.org/10.15252/embj.2018101346.

Reiher, Wencke, Christine Shirras, Jörg Kahnt, Stefan Baumeister, R. Elwyn Isaac, and Christian Wegener. 2011. "Peptidomics and Peptide Hormone Processing in the Drosophila Midgut." *Journal of Proteome Research* 10 (4): 1881–92. https://doi.org/10.1021/pr101116g.

Ren, Guilin R., Frank Hauser, Kim F. Rewitz, Shu Kondo, Alexander F. Engelbrecht, Anders K. Didriksen, Suzanne R. Schjøtt, et al. 2015. "CCHamide-2 Is an Orexigenic Brain-Gut Peptide in Drosophila." *PLOS ONE* 10 (7): e0133017. https://doi.org/10.1371/journal.pone.0133017.

Rera, Michael, Rebecca I. Clark, and David W. Walker. 2012. "Intestinal Barrier Dysfunction Links Metabolic and Inflammatory Markers of Aging to Death in Drosophila." *Proceedings of the National Academy of Sciences of the United States of America* 109 (52): 21528–33. https://doi.org/10.1073/pnas.1215849110.

Resnik-Docampo, Martin, Christopher L. Koehler, Rebecca I. Clark, Joseph M. Schinaman, Vivien Sauer, Daniel M. Wong, Sophia Lewis, Cecilia D'Alterio, David W. Walker, and D. Leanne Jones. 2017. "Tricellular Junctions Regulate Intestinal Stem Cell Behaviour to Maintain Homeostasis." *Nature Cell Biology* 19 (1): 52–59. https://doi.org/10.1038/ncb3454.

Richards, Paul, Ramona Pais, Abdella M. Habib, Cheryl A. Brighton, Giles S. H. Yeo, Frank Reimann, and Fiona M. Gribble. 2016. "High Fat Diet Impairs the Function of Glucagon-like Peptide-1 Producing L-Cells." *Peptides* 77 (March): 21–27. https://doi.org/10.1016/j.peptides.2015.06.006.

Rodriguez-Fernandez, Imilce A., Helen M. Tauc, and Heinrich Jasper. 2020. "Hallmarks of Aging Drosophila Intestinal Stem Cells." *Mechanisms of Ageing and Development* 190 (September): 111285. https://doi.org/10.1016/j.mad.2020.111285.

Roth, Sabrina, Patrick Franken, Andrea Sacchetti, Andreas Kremer, Kurt Anderson, Owen Sansom, and Riccardo Fodde. 2012. "Paneth Cells in Intestinal Homeostasis and Tissue Injury." *PLoS ONE* 7 (6): e38965. https://doi.org/10.1371/journal.pone.0038965.

Sano, Hiroko, Akira Nakamura, Michael J. Texada, James W. Truman, Hiroshi Ishimoto, Azusa Kamikouchi, Yutaka Nibu, Kazuhiko Kume, Takanori Ida, and Masayasu Kojima. 2015. "The Nutrient-Responsive Hormone CCHamide-2 Controls Growth by Regulating Insulin-like Peptides in the Brain of Drosophila Melanogaster." *PLoS Genetics* 11 (5): e1005209. https://doi.org/10.1371/journal.pgen.1005209.

Schaum, Nicholas, Jim Karkanias, Norma F. Neff, Andrew P. May, Stephen R. Quake, Tony Wyss-Coray, Spyros Darmanis, et al. 2018. "Single-Cell Transcriptomics of 20 Mouse Organs Creates a Tabula Muris." *Nature* 562 (7727): 367–72. https://doi.org/10.1038/s41586-018-0590-4.

Schuijers, Jurian, and Hans Clevers. 2012. "Adult Mammalian Stem Cells: The Role of Wnt, Lgr5 and R-Spondins." *The EMBO Journal* 31 (12): 2685–96. https://doi.org/10.1038/emboj.2012.149.

Scopelliti, Alessandro, Christin Bauer, Yachuan Yu, Tong Zhang, Björn Kruspig, Daniel J. Murphy, Marcos Vidal, Oliver D. K. Maddocks, and Julia B. Cordero. 2019. "A Neuronal Relay Mediates a Nutrient

Responsive Gut/Fat Body Axis Regulating Energy Homeostasis in Adult Drosophila." *Cell Metabolism* 29 (2): 269-284.e10. https://doi.org/10.1016/j.cmet.2018.09.021.

Shcherbata, Halyna R., Cassandra Althauser, Seth D. Findley, and Hannele Ruohola-Baker. 2004. "The Mitotic-to-Endocycle Switch in Drosophila Follicle Cells Is Executed by Notch-Dependent Regulation of G1/S, G2/M and M/G1 Cell-Cycle Transitions." *Development (Cambridge, England)* 131 (13): 3169–81. https://doi.org/10.1242/dev.01172.

Shroyer, Noah F., Deeann Wallis, Koen J. T. Venken, Hugo J. Bellen, and Huda Y. Zoghbi. 2005. "Gfi1 Functions Downstream of Math1 to Control Intestinal Secretory Cell Subtype Allocation and Differentiation." *Genes & Development* 19 (20): 2412–17. https://doi.org/10.1101/gad.1353905.

Sjöqvist, Marika, and Emma R. Andersson. 2019. "Do as I Say, Not(Ch) as I Do: Lateral Control of Cell Fate." *Developmental Biology*, Signaling pathways in development, 447 (1): 58–70. https://doi.org/10.1016/j.ydbio.2017.09.032.

Song, Wei, Jan A. Veenstra, and Norbert Perrimon. 2020. "Control of Lipid Metabolism by Tachykinin in Drosophila." *Cell Reports* 30 (7): 2461. https://doi.org/10.1016/j.celrep.2020.02.011.

Strand, Marie, and Craig A. Micchelli. 2011. "Quiescent Gastric Stem Cells Maintain the Adult *Drosophila* Stomach." *Proceedings of the National Academy of Sciences* 108 (43): 17696–701. https://doi.org/10.1073/pnas.1109794108.

Sun, Deqiang, Min Luo, Mira Jeong, Benjamin Rodriguez, Zheng Xia, Rebecca Hannah, Hui Wang, et al. 2014. "Epigenomic Profiling of Young and Aged HSCs Reveals Concerted Changes during Aging That Reinforce Self-Renewal." *Cell Stem Cell* 14 (5): 673–88. https://doi.org/10.1016/j.stem.2014.03.002.

Tauc, Helen M., Imilce A. Rodriguez-Fernandez, Jason A. Hackney, Michal Pawlak, Tal Ronnen Oron, Jerome Korzelius, Hagar F. Moussa, et al. 2021. "Age-Related Changes in Polycomb Gene Regulation Disrupt Lineage Fidelity in Intestinal Stem Cells." *ELife* 10 (March): e62250. https://doi.org/10.7554/eLife.62250.

Tayler, Timothy D., Diego A. Pacheco, Anne C. Hergarden, Mala Murthy, and David J. Anderson. 2012. "A Neuropeptide Circuit That Coordinates Sperm Transfer and Copulation Duration in Drosophila." *Proceedings of the National Academy of Sciences* 109 (50): 20697–702. https://doi.org/10.1073/pnas.1218246109.

Terriente-Felix, Ana, Jinghua Li, Stephanie Collins, Amy Mulligan, Ian Reekie, Fred Bernard, Alena Krejci, and Sarah Bray. 2013. "Notch Cooperates with Lozenge/Runx to Lock Haemocytes into a Differentiation Programme." *Development (Cambridge, England)* 140 (4): 926–37. https://doi.org/10.1242/dev.086785.

Thevaranjan, Netusha, Alicja Puchta, Christian Schulz, Avee Naidoo, J.C. Szamosi, Chris P. Verschoor, Dessi Loukov, et al. 2017. "Age-Associated Microbial Dysbiosis Promotes Intestinal Permeability, Systemic Inflammation, and Macrophage Dysfunction." *Cell Host & Microbe* 21 (4): 455-466.e4. https://doi.org/10.1016/j.chom.2017.03.002.

Tian, Ai, Hassina Benchabane, Zhenghan Wang, and Yashi Ahmed. 2016. "Regulation of Stem Cell Proliferation and Cell Fate Specification by Wingless/Wnt Signaling Gradients Enriched at Adult Intestinal Compartment Boundaries." *PLoS Genetics* 12 (2): e1005822. https://doi.org/10.1371/journal.pgen.1005822.

Tian, Aiguo, Virginia Morejon, Sarah Kohoutek, Yi-Chun Huang, Wu-Min Deng, and Jin Jiang. 2022. "Damage-Induced Regeneration of the Intestinal Stem Cell Pool through Enteroblast Mitosis in the Drosophila Midgut." *The EMBO Journal*, August, e110834. https://doi.org/10.15252/embj.2022110834.

Tian, Hua, Brian Biehs, Søren Warming, Kevin G. Leong, Linda Rangell, Ophir D. Klein, and Frederic J. de Sauvage. 2011. "A Reserve Stem Cell Population in Small Intestine Renders Lgr5-Positive Cells Dispensable." *Nature* 478 (7368): 255–59. https://doi.org/10.1038/nature10408.

Tracy Cai, Xiaoyu, Hongjie Li, Abu Safyan, Jennifer Gawlik, George Pyrowolakis, and Heinrich Jasper. 2019. "AWD Regulates Timed Activation of BMP Signaling in Intestinal Stem Cells to Maintain Tissue Homeostasis." *Nature Communications* 10 (1): 2988. https://doi.org/10.1038/s41467-019-10926-2.

VanDussen, Kelli L., Alexis J. Carulli, Theresa M. Keeley, Sanjeevkumar R. Patel, Brent J. Puthoff, Scott T. Magness, Ivy T. Tran, et al. 2012. "Notch Signaling Modulates Proliferation and Differentiation of Intestinal Crypt Base Columnar Stem Cells." *Development (Cambridge, England)* 139 (3): 488–97. https://doi.org/10.1242/dev.070763.

Wachsmuth, Hallie R., Savanna N. Weninger, and Frank A. Duca. 2022. "Role of the Gut–Brain Axis in Energy and Glucose Metabolism." *Experimental & Molecular Medicine* 54 (4): 377–92. https://doi.org/10.1038/s12276-021-00677-w.

Wang, Chenhui, Xingting Guo, Kun Dou, Hongyan Chen, and Rongwen Xi. 2015. "Ttk69 Acts as a Master Repressor of Enteroendocrine Cell Specification in Drosophila Intestinal Stem Cell Lineages." *Development (Cambridge, England)* 142 (19): 3321–31. https://doi.org/10.1242/dev.123208.

Wang, Y, R Perfetti, N H Greig, H W Holloway, K A DeOre, C Montrose-Rafizadeh, D Elahi, and J M Egan. 1997. "Glucagon-like Peptide-1 Can Reverse the Age-Related Decline in Glucose Tolerance in Rats." *Journal of Clinical Investigation* 99 (12): 2883–89.

Wegener, Christian, Henrik Herbert, Jörg Kahnt, Michael Bender, and Jeanne M. Rhea. 2011. "Deficiency of Prohormone Convertase DPC2 (AMONTILLADO) Results in Impaired Production of Bioactive Neuropeptide Hormones in Drosophila." *Journal of Neurochemistry* 118 (4): 581–95. https://doi.org/10.1111/j.1471-4159.2010.07130.x.

Wen, Tieqiao, Clayton A. Parrish, Dan Xu, Qi Wu, and Ping Shen. 2005. "Drosophila Neuropeptide F and Its Receptor, NPFR1, Define a Signaling Pathway That Acutely Modulates Alcohol Sensitivity." *Proceedings of the National Academy of Sciences of the United States of America* 102 (6): 2141–46. https://doi.org/10.1073/pnas.0406814102.

Wetering, Marc van de, Elena Sancho, Cornelis Verweij, Wim de Lau, Irma Oving, Adam Hurlstone, Karin van der Horn, et al. 2002. "The Beta-Catenin/TCF-4 Complex Imposes a Crypt Progenitor Phenotype on Colorectal Cancer Cells." *Cell* 111 (2): 241–50. https://doi.org/10.1016/s0092-8674(02)01014-0.

Winton, D. J., M. A. Blount, and B. A. Ponder. 1988. "A Clonal Marker Induced by Mutation in Mouse Intestinal Epithelium." *Nature* 333 (6172): 463–66. https://doi.org/10.1038/333463a0.

Wu, Angela R., Norma F. Neff, Tomer Kalisky, Piero Dalerba, Barbara Treutlein, Michael E. Rothenberg, Francis M. Mburu, et al. 2014. "Quantitative Assessment of Single-Cell RNA-Sequencing Methods." *Nature Methods* 11 (1): 41–46. https://doi.org/10.1038/nmeth.2694.

Xiang, Jinyi, Jennifer Bandura, Peng Zhang, Yinhua Jin, Hanna Reuter, and Bruce A. Edgar. 2017. "EGFR-Dependent TOR-Independent Endocycles Support Drosophila Gut Epithelial Regeneration." *Nature Communications* 8 (1): 15125. https://doi.org/10.1038/ncomms15125.

Xiao, Qi, Hideyuki Komori, and Cheng-Yu Lee. 2012. "Klumpfuss Distinguishes Stem Cells from Progenitor Cells during Asymmetric Neuroblast Division." *Development (Cambridge, England)* 139 (15): 2670–80. https://doi.org/10.1242/dev.081687.

Yan, Kelley S., Olivier Gevaert, Grace X. Y. Zheng, Benedict Anchang, Christopher S. Probert, Kathryn A. Larkin, Paige S. Davies, et al. 2017. "Intestinal Enteroendocrine Lineage Cells Possess Homeostatic and Injury-Inducible Stem Cell Activity." *Cell Stem Cell* 21 (1): 78-90.e6. https://doi.org/10.1016/j.stem.2017.06.014.

Yang, Q., N. A. Bermingham, M. J. Finegold, and H. Y. Zoghbi. 2001. "Requirement of Math1 for Secretory Cell Lineage Commitment in the Mouse Intestine." *Science (New York, N.Y.)* 294 (5549): 2155–58. https://doi.org/10.1126/science.1065718.

Yang, X., S. Bahri, T. Klein, and W. Chia. 1997. "Klumpfuss, a Putative Drosophila Zinc Finger Transcription Factor, Acts to Differentiate between the Identities of Two Secondary Precursor Cells within One Neuroblast Lineage." *Genes & Development* 11 (11): 1396–1408. https://doi.org/10.1101/gad.11.11.1396.

Yin, Chang, and Rongwen Xi. 2018. "A Phyllopod-Mediated Feedback Loop Promotes Intestinal Stem Cell Enteroendocrine Commitment in Drosophila." *Stem Cell Reports* 10 (1): 43–57. https://doi.org/10.1016/j.stemcr.2017.11.014.

Yoshinari, Yuto, Hina Kosakamoto, Takumi Kamiyama, Ryo Hoshino, Rena Matsuoka, Shu Kondo, Hiromu Tanimoto, Akira Nakamura, Fumiaki Obata, and Ryusuke Niwa. 2021. "The Sugar-Responsive Enteroendocrine Neuropeptide F Regulates Lipid Metabolism through Glucagon-like and Insulin-like Hormones in Drosophila Melanogaster." *Nature Communications* 12 (1): 4818. https://doi.org/10.1038/s41467-021-25146-w.

Zeng, Xiankun, and Steven X. Hou. 2015. "Enteroendocrine Cells Are Generated from Stem Cells through a Distinct Progenitor in the Adult Drosophila Posterior Midgut." *Development (Cambridge, England)* 142 (4): 644–53. https://doi.org/10.1242/dev.113357.

Zhao, Qi, Yan-Yan Chen, Ding-Qiao Xu, Shi-Jun Yue, Rui-Jia Fu, Jie Yang, Li-Ming Xing, and Yu-Ping Tang. 2021. "Action Mode of Gut Motility, Fluid and Electrolyte Transport in Chronic Constipation." *Frontiers in Pharmacology* 12 (July): 630249. https://doi.org/10.3389/fphar.2021.630249.

Zielke, Norman, Kerry J. Kim, Vuong Tran, Shusaku T. Shibutani, Maria-Jose Bravo, Sabarish Nagarajan, Monique van Straaten, et al. 2011. "Control of Drosophila Endocycles by E2F and CRL4Cdt2." *Nature* 480 (7375): 123–27. https://doi.org/10.1038/nature10579.

9. Signed thesis declaration

Erklärung zur Dissertation
gemäß der Promotionsordnung vom 12. März 2020

Diese Erklärung muss in der Dissertation enthalten sein.
(***This version must be included in the doctoral thesis***)

„Hiermit versichere ich an Eides statt, dass ich die vorliegende Dissertation selbstständig und ohne die Benutzung anderer als der angegebenen Hilfsmittel und Literatur angefertigt habe. Alle Stellen, die wörtlich oder sinngemäß aus veröffentlichten und nicht veröffentlichten Werken dem Wortlaut oder dem Sinn nach entnommen wurden, sind als solche kenntlich gemacht. Ich versichere an Eides statt, dass diese Dissertation noch keiner anderen Fakultät oder Universität zur Prüfung vorgelegen hat; dass sie - abgesehen von unten angegebenen Teilpublikationen und eingebundenen Artikeln und Manuskripten - noch nicht veröffentlicht worden ist sowie, dass ich eine Veröffentlichung der Dissertation vor Abschluss der Promotion nicht ohne Genehmigung des Promotionsausschusses vornehmen werde. Die Bestimmungen dieser Ordnung sind mir bekannt. Darüber hinaus erkläre ich hiermit, dass ich die Ordnung zur Sicherung guter wissenschaftlicher Praxis und zum Umgang mit wissenschaftlichem Fehlverhalten der Universität zu Köln gelesen und sie bei der Durchführung der Dissertation zugrundeliegenden Arbeiten und der schriftlich verfassten Dissertation beachtet habe und verpflichte mich hiermit, die dort genannten Vorgaben bei allen wissenschaftlichen Tätigkeiten zu beachten und umzusetzen. Ich versichere, dass die eingereichte elektronische Fassung der eingereichten Druckfassung vollständig entspricht."

Teilpublikationen:

- Norzelius et al, 2019, Natale Communications

Datum, Name und Unterschrift

18.09.2022, Sina Azami, *[Unterschrift]*

10. Publications

Part of the results presented in chapter 3.1 were published in 2019 in Nature communications journal. Sina Azami performed fly crossing, dissection of the guts, staining, imaging and analyzing of the data. Together with Dr Jerome Korzelius and Prof. Dr. Heinrich Jasper, SA was involved in the revision of the manuscript.

The published paper has been added to this thesis.

The WT1-like transcription factor *Klumpfuss* maintains lineage commitment of enterocyte progenitors in the *Drosophila* intestine

Jerome Korzelius[1,4], Sina Azami [1,4], Tal Ronnen-Oron[2], Philipp Koch [1], Maik Baldauf[1], Elke Meier[1], Imilce A. Rodriguez-Fernandez[3], Marco Groth [1], Pedro Sousa-Victor[2] & Heinrich Jasper[1,2,3]

In adult epithelial stem cell lineages, the precise differentiation of daughter cells is critical to maintain tissue homeostasis. Notch signaling controls the choice between absorptive and entero-endocrine cell differentiation in both the mammalian small intestine and the *Drosophila* midgut, yet how Notch promotes lineage restriction remains unclear. Here, we describe a role for the transcription factor Klumpfuss (Klu) in restricting the fate of enteroblasts (EBs) in the *Drosophila* intestine. Klu is induced in Notch-positive EBs and its activity restricts cell fate towards the enterocyte (EC) lineage. Transcriptomics and DamID profiling show that Klu suppresses enteroendocrine (EE) fate by repressing the action of the proneural gene Scute, which is essential for EE differentiation. Loss of Klu results in differentiation of EBs into EE cells. Our findings provide mechanistic insight into how lineage commitment in progenitor cell differentiation can be ensured downstream of initial specification cues.

[1] Leibniz Institute on Aging–Fritz Lipmann Institute (FLI), Jena, Germany. [2] Buck Institute for Research on Aging, 8001 Redwood Boulevard, Novato, CA 94945-1400, USA. [3] Immunology Discovery, Genentech, Inc., 1 DNA Way, South San Francisco, CA 94080, USA. [4] Present address: Max-Planck-Institute for Biology of Aging, Cologne, Germany. Correspondence and requests for materials should be addressed to J.K. (email: jkorzelius@age.mpg.de) or to H.J. (email: jasper.heinrich@gene.com)

In many tissues, somatic stem cells respond to tissue injury by increasing their proliferative potential and producing new differentiating cell progeny. To maintain homeostasis during such periods of regeneration, cell specification and differentiation need to be precisely coordinated within a dynamic environment. Studies in the mammalian intestine have demonstrated a surprising plasticity in such specification events, showing that even differentiated cells can revert into a stem cell state during times in which tissue homeostasis is perturbed[1,2]. These findings highlight the critical role of gene regulatory networks in establishing and maintaining differentiated and committed cell states in homeostatic conditions.

The *Drosophila* midgut is an excellent model to study lineage differentiation of adult stem cells both in homeostasis as well as during regeneration and aging. The *Drosophila* midgut is maintained by intestinal stem cells (ISCs), which can generate differentiated enterocytes (EC) or enteroendocrine (EE) cells[3,4]. Upon injury or infection, ISC proliferation is dramatically increased in response to mitogenic signals from damaged enterocytes[5–7]. Misregulation of cell specification and differentiation in this lineage can lead to substantial dysfunction, as evidenced in aging intestines, where disruption of normal Notch signaling due to elevated Jun-N-terminal Kinase (JNK) signaling leads to an accumulation of mis-differentiated cells that contribute to epithelial dysplasia and barrier dysfunction[8,9].

Notch signaling plays a central role in both ISC proliferation and lineage differentiation. ISCs produce the Notch-ligand Delta and activate Notch in the enteroblast (EB) daughter cell. This Notch-positive EB is the precursor of mature enterocytes (ECs). Levels of Delta vary markedly between ISCs in the homeostatic intestine. These differences have been proposed to underlie the decision between EC and EE differentiation in the ISC lineage:[10] high Dl-N signaling activity between the stem cell and its daughter is associated with EC differentiation, while lower Dl-N signaling activity between the ISC and its daughter promotes EE differentiation[10,11]. Loss of Notch in ISC lineages leads to the formation of tumors that consist of highly Delta-expressing ISCs and of Prospero (Pros)-expressing EEs[10,12,13]. These tumors are likely a consequence of impaired EB differentiation, resulting in an increased frequency of symmetric divisions, as well as excess EE differentiation, suggesting that EE differentiation is the default state when Notch signaling activity is absent or reduced.

Interestingly, recent work has shown that lineage specification in ISC daughter cells is likely more complex than previously thought. It has been shown that ISCs exist that express the EE marker Prospero and generate daughter cells that differentiate into EEs[14,15]. A transient specification step has been identified in EE differentiation, in which cells transiently express Scute, a transcription factor that negatively regulates Notch-responsive genes such as Enhancer of Split-m8 (*E(Spl)m8*), as well as its own expression[16]. Furthermore, EBs have been shown to remain in a transient state for a prolonged period of time before differentiating into an EC fate[17]. The exact cell state in which the decision between EE and EC fates is cemented, however, remains unclear.

Here we describe a role for the transcription factor Klumpfuss (Klu) in lineage commitment during EC differentiation in the adult fly intestine. Klu is related to the mammalian tumor-suppressor gene Wilms' Tumor 1 (WT1), and its overexpression in neuroblast stem cells leads to tumorous overgrowths in the brain of flies[18–20]. In the intestine, we find Klu to be expressed specifically in EBs. Loss of Klu leads to aberrant EE differentiation of EB cells, whereas ectopic activation of Klu results in a failure to differentiate. Transcriptomics and DNA-binding studies reveal that Klu controls EE differentiation by repressing genes involved in Notch signaling, as well as by indirectly controlling the levels of the Achaete-Scute complex members *asense* and *scute*. Klu acts in a negative feedback loop by regulating its own expression and the expression of Notch target genes. We propose that Klu defines a transient state of EBs in which specification into ECs is cemented by precise regulation of Notch signaling: the expression of Klu locks in the EC fate in EBs by preventing ectopic proneural gene activation and thus ensuring lineage commitment into the EC fate.

Results

Klu is expressed in the enteroblast precursor cells. We identified Klumpfuss (Klu) transcripts to be significantly down-regulated upon loss of the stem and progenitor specific transcription factor Escargot (Esg) and to be enriched in transcriptomes of sorted Esg-positive (Esg+) cells[21,22]. To confirm *klu* expression in the *Drosophila* posterior midgut, we used a *klu-Gal4, UAS-GFP* reporter line that reflects Klu expression in wing and eye discs of wandering third instar larvae[23,24]. In the midgut, GFP expression was seen in the larger cells of the stem-progenitor nests (ISC+EB) and resembled EBs based on both nuclear and cellular size (Fig. 1a–c arrowheads). To confirm their identity, we combined the *klu-Gal4, UAS-GFP* line with the Notch activity reporter *Su(H)GBE-lacZ*, which is exclusively activated in EBs[10]. In addition, we used *Delta-lacZ* (*Dl-lacZ*) as a marker for ISCs. The expression of *klu-Gal4, UAS-GFP* overlapped almost exclusively with *Su(H)GBE-lacZ*. In contrast, *Dl-lacZ* staining was mostly found in small, diploid cells neighboring the GFP-positive cells (Fig. 1d–i, quantification in j, k). We confirmed the EB-specific expression of the enhancer-trap line by performing a knock-in replacement of the Klu Coding Sequence (CDS) with the Gal4 CDS (Supplementary Fig. 1, see Methods). To further confirm the expression of Klu in EBs, we used a FISH-probe for *klu* mRNA: this labeled *klu* mRNA in *Su(H)GBE-Gal4>UAS-GFP* marked EBs (Supplementary Fig. 1h, i, arrows).

Lineage-tracing experiments have previously shown that Notch-positive EB precursor cells exclusively give rise to enterocytes, whereas Delta-positive ISCs can give rise to clones with both ECs and EEs[14,15]. To trace the fate of Klu-expressing cells, we crossed the *klu-Gal4* enhancer-trap line to a Actin promoter-driven FlipOut (F/O) lineage-tracing cassette (*UAS-GFP, tub-Gal80ts; UAS-Flp, Act >STOP> Gal4*). As expected, *Dl-Gal4*-expressing ISCs gave rise to both ECs as well as EEs, marked by expression of the transcription factor Prospero (Pros) (Fig. 1l, m, arrows). In contrast, Notch-positive EBs (*Su(H)GBE-Gal4*) only gave rise to ECs, but not EEs (Fig. 1n, o, arrowheads). Similar to Notch-positive EBs, *klu-Gal4*-traced cells gave rise exclusively to ECs, but not EEs (Fig. 1p, q). We conclude that Klu is expressed in the EC-generating EBs in the *Drosophila* midgut.

Klu loss of function leads to excess EE differentiation. To determine the role of Klu in the specification and/or differentiation of cells in the ISC lineage, we first inhibited Klu function using the temperature-inducible TARGET-system to express RNAi constructs in specific lineages[25]. We used *esg-Gal4ts* to express *kluRNAi* in ISCs and EBs, and *Su(H)GBE-Gal4ts* to express *kluRNAi* in EBs only. In both conditions, knockdown of Klu increased EE numbers in the posterior midgut (Fig. 2a–d, quantification in Fig. 2i), suggesting that knockdown of Klu in EBs promoted the adoption of EE over EC fates in these cells. To confirm this, we used EB-specific FlipOut lineage tracing in combination with *kluRNAi* to trace the fate of *kluRNAi*-expressing EBs. We induced clones for 10 days at 29 °C, followed by a short 16-hour infection with the pathogen *Erwinia carotovora* (*Ecc15*) to induce gut turnover. Pros-positive EEs are seldom found in such EB-derived *Su(H)GBE-F/O* clones in control backgrounds, yet we found a significant increase of such
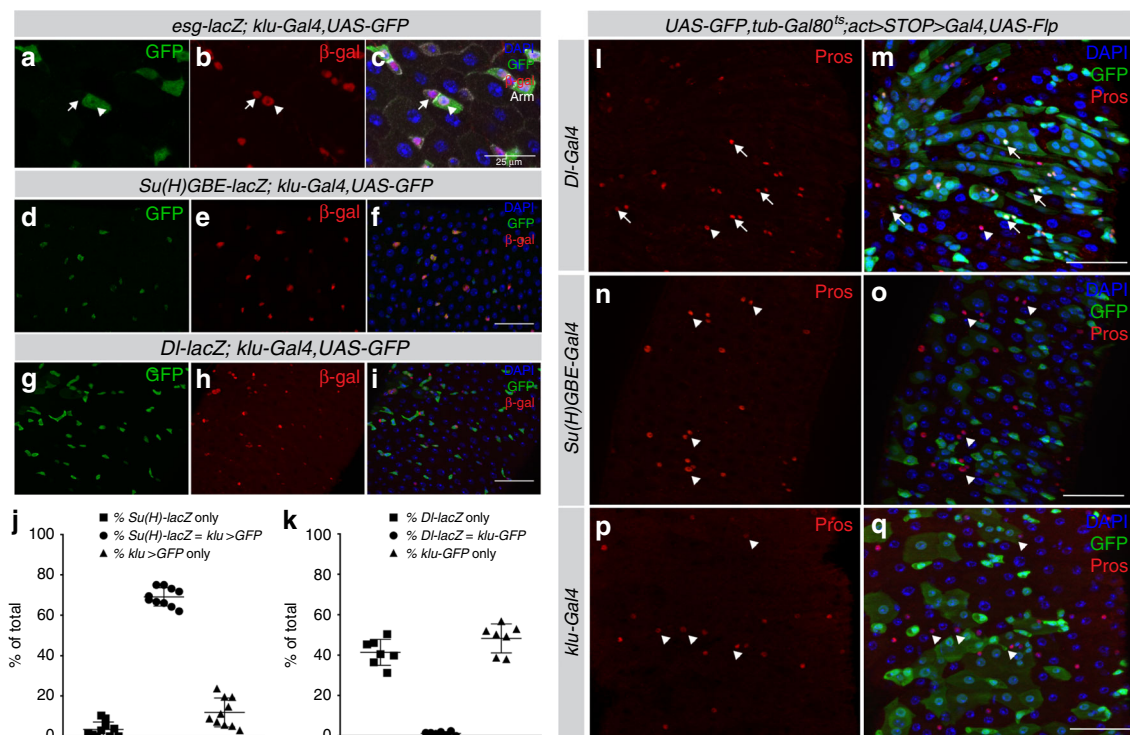
Fig. 1 Klu is specifically expressed in enteroblast cells. **a–c** The *klu-Gal4, UAS-GFP* reporter line shows expression in the midgut epithelium. ISCs (arrows) and EBs (arrowheads) are visualized by *esg-lacZ* (beta-galactosidase, red). Cells are outlined with Armadillo/beta-catenin (Arm, grayscale). Representative area of posterior midgut is shown. *n* = 3 animals. **d–i** The *klu-Gal4, UAS-GFP* was combined with *Su(H)-GBE-lacZ* (enteroblast (EB) marker) or *Dl-lacZ* (intestinal stem cell (ISC) marker). Expression of Klu largely overlaps with the EB marker *Su(H)-GBE-lacZ* (**d–f**), and Klu-positive cells are found adjacent to the Delta-positive ISCs (**g–i**). **j** Quantification of EB-marker gene overlap of the genotypes displayed in **d–f**. *n* = 10 guts/animals (*Su(H)-GBE-lacZ*, *n* = 572 cells counted). **k** Quantification of ISC-marker gene overlap of the genotypes displayed in **g–i**. *n* = 7 guts/animals (*Dl-lacZ*, *n* = 1370 cells counted). **l–q** Lineage-tracing of cells in the intestine using different cell-specific drivers. EEs are marked by antibody staining for the transcription factor Prospero (Pros, red). Arrows indicate GFP-Pros double-positive EEs in the clonal area, whereas arrowheads indicate EEs outside the clonal area. **l, m** The *Dl-Gal4*-positive ISCs give rise to both differentiated cell types of the intestinal lineage (enterocytes (EC) and enteroendocrine (EE) cells). **n, o** *Su(H)-GBE*-positive EB cells exclusively give rise to ECs, but not to EEs. **p, q** Similar to *Su(H)-GBE*-positive EBs, *klu-Gal4*-positive cells give rise exclusively to ECs. Representative areas of posterior midgut are shown. *n* = 7 guts examined for **l, m**, *n* = 7 guts examined for **n, o** and *n* = 10 guts examined for **p, q**. Scale bar = 50 μm, except in **a–c**: scale bar is 25 μm

cells in clones expressing *klu^RNAi* (Fig. 2e, f, quantification in Fig. 2j). To further confirm these results, we generated GFP-marked clones homozygous for a null allele of Klu, *klu^R51* using the MARCM technique[24,26] and quantified EE numbers. Quantification showed that *klu^R51* MARCM clones had more EE cells/clone (Fig. 2g, h, quantification in Fig. 2k). Interestingly, the GFP-negative tissue also contained more EEs in *klu^R51* MARCM animals than in control animals (*FRT2A*, Fig. 2g, compare with Fig. 2h). This is likely due to the fact that in this genotype, the GFP-negative tissue is heterozygous for *klu^R51*. Accordingly, MARCM RNAi (*FRT40A*; *klu^RNAi*) clones (in which the surrounding tissue is wild type for Klu) had an increase in the number of EE cells/clone, but no difference in EE cells in the non-clonal surrounding tissue (Supplementary Fig. 2g, h, quantification in Supplementary Fig. 2i, j). These results strongly suggest that Klu acts cell-autonomously in preventing EE differentiation of EB.

Interestingly, EB-to-EC differentiation could still occur in *klu*-deficient lineages: *esg-F/O* clones expressing *klu^RNAi* (*esg-F/O>klu^RNAi*) still contained cells with large nuclear size and positive for the EC marker Pdm1 (refs. [21,27]) (Supplementary Fig. 2a–f). In summary, our results indicate that loss of *klu* alters the EE-to-EC ratio in ISC lineages, but does not fully impair EC differentiation.

Ectopic Klu blocks proliferation and EB differentiation. Based on these observations, we hypothesized that constitutive Klu

overexpression could reduce EE differentiation in the ISC lineage and might trigger ectopic differentiation of ISCs into ECs. To test this, we used the *esg-F/O* system to express full-length Klu in ISC-derived clones. Wild-type *esg-F/O* clones take up most of the posterior midgut 2 weeks after induction, containing a mixture of ECs and EEs (Fig. 3a). In contrast, clones expressing full-length Klu remained very small, containing only a few cells that did not exhibit any hallmarks of differentiation into either EEs or ECs (Fig. 3b). Klu is thought to act mainly as a repressor of transcription based on studies in other organs[18,23,28]. To ask whether this repressor function of Klu would elicit the phenotypes observed, we expressed the zinc-finger DNA-binding domain of Klu fused to either a VP16 activation domain (Klu-VP16) or fused to the repressor domain from Engrailed (Klu-ERD)[28]. Whereas clones grew normally and differentiation still occurred in clones expressing the activating Klu-VP16, clone size was smaller and differentiated cells were not observed in clones expressing the repressing Klu-ERD, confirming that transcriptional repression of genes regulated by Klu is sufficient to limit growth of ISC-derived clones (Fig. 3c, d, quantification in Fig. 3e). Similarly, *UAS-klu* expression in *esg-F/O* clones inhibited proliferation of ISCs (measured by quantifying mitotic figures in the gut) both in homeostatic and infected conditions (infection with *Ecc15*; Supplementary Fig. 3a). Restriction of Klu expression solely to ISC (using *esg^ts* combined with *Su(H)-Gal80* (ref. [29]) showed that the repression of mitosis upon *Ecc15*
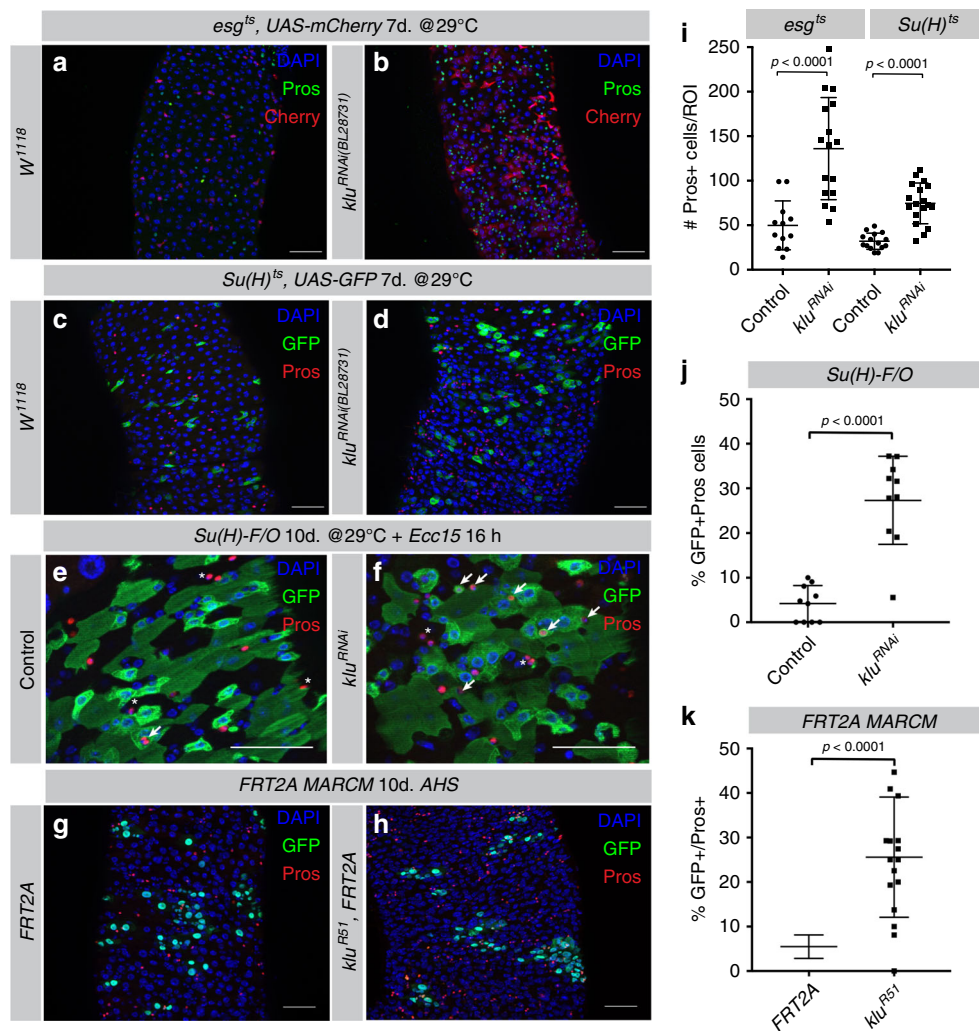
Fig. 2 Loss of Klu leads to excess EE differentiation. **a–d** RNAi-mediated knockdown of Klu results in an excess of Pros-positive EE cells. Expression of klu^{RNAi} using the ISC + EB driver esg-$Gal4^{ts}$ (Pros in green, compare **a** with **b**) or the EB-specific $Su(H)GBE$-$Gal4^{ts}$ driver (Pros in red, compare **c** with **d**). **e**, **f** $Su(H)$-GBE-driven FlipOut ($Su(H)$-F/O) clones expressing klu^{RNAi} show an increased number of Pros-positive EE cells in the clonal area upon $Ecc15$ infection compared to controls (**e** compare with **f** quantification in **j**). **g**, **h** Clonal analysis of control $FRT2A$ (**g**) or $FRT2A$, klu^{R51} (**h**) null mutant MARCM clones. Representative areas of posterior midguts are shown. **i** EE cell quantification of the posterior midgut for the genotypes in **a–d**. Number of midguts $n = 12$ (control w^{1118}) and $n = 16$ (klu^{RNAi}) for **a** and **b** and $n = 15$ (control w^{1118}) and $n = 18$ (klu^{RNAi}) in **c** and **d**. **j** Quantification of GFP-Pros double-positive cells/ROI in control and klu^{RNAi}-expressing $Su(H)$-F/O clones in **e** and **f**. $n = 10$ for control and $n = 10$ for klu^{RNAi} guts. **k** Quantification of the number of Pros-positive EEs/clone and the total number of Pros-positive EEs/ROI for the genotypes in **g** and **h**. $n = 15$ guts ($FRT2A$ control) and $n = 17$ guts (klu^{R51}). For quantifications in **i–k**: error bars represent mean ± SD. Significance was calculated using Student's t-test with Welch's correction. Scale bar = 50 μm

infection is mainly due to the ectopic expression of Klu in ISCs, although we do observe a small but significant decrease if we express Klu using the EB-driver $Su(H)^{ts}$ (Supplementary Fig. 3b). We also combined expression of Klu (UAS-klu) with expression of the oncogenic Ras^{V12} variant (UAS-Ras^{V12}) in esg-F/O clones. Whereas esg-F/O>Ras^{V12} clones occupy the entire posterior midgut 2 days after induction and contribute to a rapid loss of viability of the animal, co-expression of UAS-klu markedly reduced clonal size and rescued viability (Supplementary Fig. 3c–g). This is consistent with an anti-mitotic effect of ectopic Klu expression in ISCs.

To ask whether sustained expression of Klu in EBs would influence their differentiation, we performed lineage-tracing initiated from EBs. Indeed, continuously expressing Klu in EBs using $Su(H)$-F/O >UAS-klu impaired the formation of differentiated Pdm1-positive enterocytes (Fig. 3f–i, compare with Fig. 3j–m, quantification in Fig. 3n). While ectopic expression in ISCs thus impairs proliferation, sustained expression of Klu in

EBs impairs EC differentiation. These results support a model in which Klu acts in early EBs to restrict EE differentiation, but it needs to be suppressed to allow EC differentiation.

To further characterize the gain-of-function phenotype, we combined UAS-klu with the ISC-marker Dl-$lacZ$ and the EB-marker $Su(H)GBE$-$lacZ$. Interestingly, esg-F/O clones expressing UAS-klu did not stain positive for either Dl-$lacZ$ (Fig. 4a–d) or $Su(H)GBE$-$lacZ$ (Fig. 4e–h), suggesting that ectopic Klu expression in ISCs interferes with normal Dl-Notch signaling in ISC-EB pairs. To investigate this interaction between Notch signaling and Klu activity further, we performed epistasis experiments: Klu overexpression prevented the formation of large tumors in Notch loss of function esg-F/O clones (Supplementary Fig. 4a–l) and UAS-klu can repress the excess mitosis seen in the esg^{ts}>N^{RNAi} genotype (Fig. 4i), consistent with the inhibition of ISC proliferation upon Klu expression.

To test whether Notch is required for Klu expression in EBs, we performed qRT-PCR for klu on progenitor cells expressing
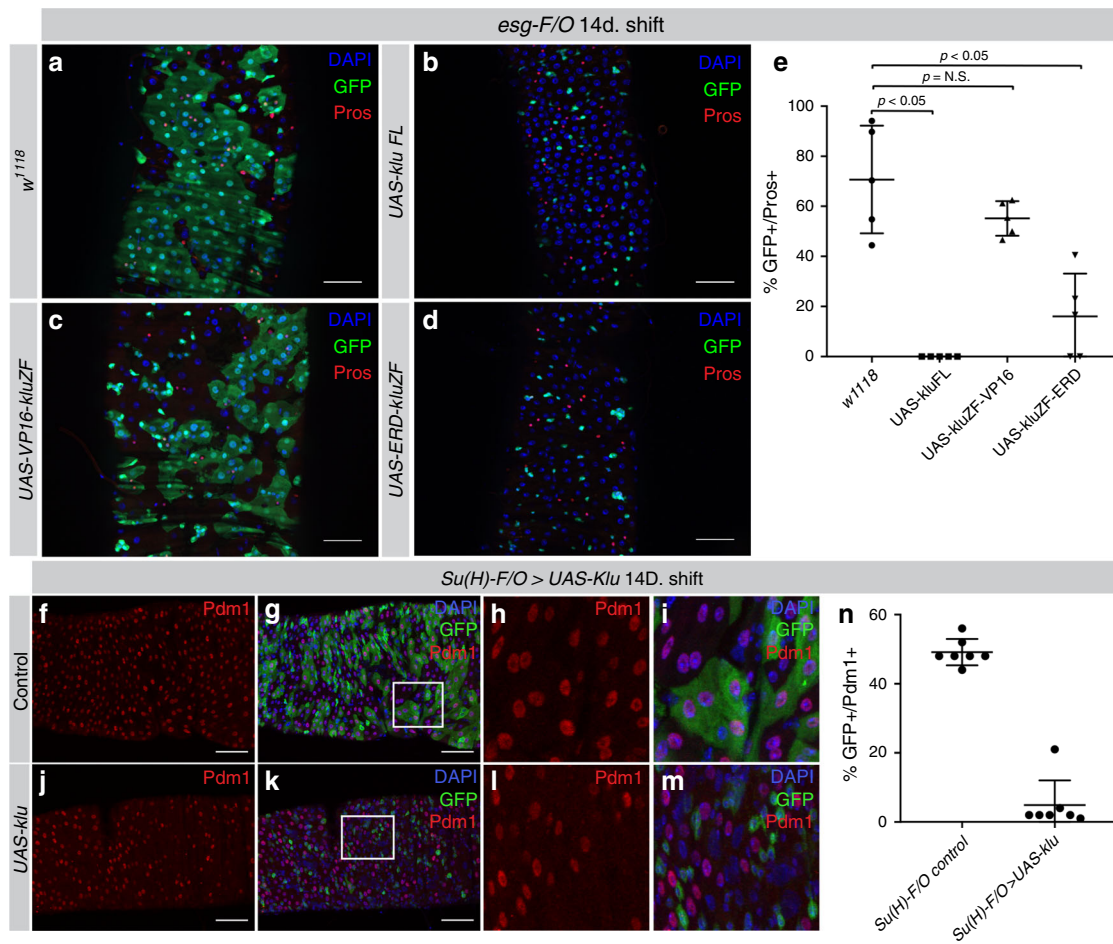
Fig. 3 Klu overactivation results in a loss of Delta-Notch signaling and ISC differentiation. **a–d** Clonal expression of different Klu isoforms using the *esg-Gal4*-driven FlipOut (*esg-F/O*) system to generate ISC clones. **a** Control *esg-FO* clones grow to occupy most of the posterior midgut 2 weeks after clonal induction. **b–d** Clones expressing either full-length Klu (*UAS-kluFL*, **b**) or the Klu zinc-finger DNA-binding domain fused to the Engrailed Repressor Domain (*UAS-ERD-kluZF*, **d**) resulted in a block of differentiation. This was not observed when expressing the Klu zinc-finger DNA-binding domain fused to the VP16 transcriptional activator domain (*UAS-VP16-kluZF*, **c**). Representative areas of posterior midguts are shown. **e** Quantification of genotypes in **a–d**. $n = 5$ midguts for each genotype. **f–i** *Su(H)-F/O* control clones contain GFP-Pdm1 double-positive cells, representative of EB > EC differentiation (**f**, **g** closeup in **h**, **i**). **j–m** *Su(H)-F/O>UAS-klu* clones contained much less GFP-Pdm1 double-positive cells, indicative of impaired EB > EC differentiation upon Klu expression. **n** Quantification of the percentage of GFP-Pdm1 double-positive cells in images of posterior midguts from control (**f–i**) and *UAS-klu Su(H)-F/O* (**j–m**) clones. $n = 7$ midguts for each genotype. For quantifications in **e** and **n**: Error bars represent mean ± SD. Significance was calculated using Student's *t*-test with Welch's correction. Scale bar = 50 μm

N^{RNAi} for 1 week ($esg^{ts} > N^{RNAi}$). Consistent with the formation of Pros$^+$ cell tumors, loss of Notch leads to a 5.5-fold upregulation of *pros* mRNA in Esg$^+$ cells. However, *klu* expression is almost absent from N^{RNAi} cells (Fig. 4j), strongly suggesting that Klu expression depends on Notch activity.

Ectopic activation of Notch in stem-progenitor cells using the Intracellular domain of Notch ($esg^{ts} > UAS-N^{ICD}$) results in a loss of the stem-progenitor compartment due to premature differentiation into EC cells[10]. $UAS-N^{ICD}$ expression resulted in *klu* mRNA expression in large Esg$^+$ cells that seem to be differentiating into ECs based on their nuclear size (Fig. 4m, n, compare with Fig. 4k, l), suggesting that Notch activation is sufficient to induce Klu expression. However, combining $UAS-N^{ICD}$ with *klu^{RNAi}* did not alter the premature differentiation phenotype of $UAS-N^{ICD}$ (Supplementary Fig. 4m–t).

Since Notch activation is thus sufficient to induce differentiation of Esg$^+$ progenitors into ECs even in the absence of Klu, we conclude that induction of Klu by Notch in EBs is important to prevent specification of EBs into EE progenitors, but is not essential for other steps in EC differentiation.

Altogether, our results indicate that the Notch-mediated induction of Klu in EBs is required to restrict lineage commitment of EBs to the EC fate. Reciprocally, ectopic Klu expression interferes with normal Delta-Notch signaling between ISC and EB and inhibits proliferation. We propose that ISC-derived EB daughter cells that express Klu enter a cell cycle arrested, undifferentiated state, and that Klu needs to be downregulated for EC differentiation to proceed. To test this hypothesis, and to understand how Klu expression controls the EB state, we decided to explore the transcriptional program downstream of Klu.

RNA-Seq supports role of Klu in Notch and EE differentiation. To gain a comprehensive overview of the genes controlled by Klu in the intestine, we performed RNA-Sequencing (RNA-Seq) on FACS-sorted Esg$^+$ progenitor cells expressing either *klu^{RNAi}* or *UAS-klu*[30] (see Fig. 5a, and Methods for details). Principal component analysis on the transcriptome of these populations showed that all sample groups form distinct clusters and that group replicates cluster closely together (Supplementary Fig. 5a). We also
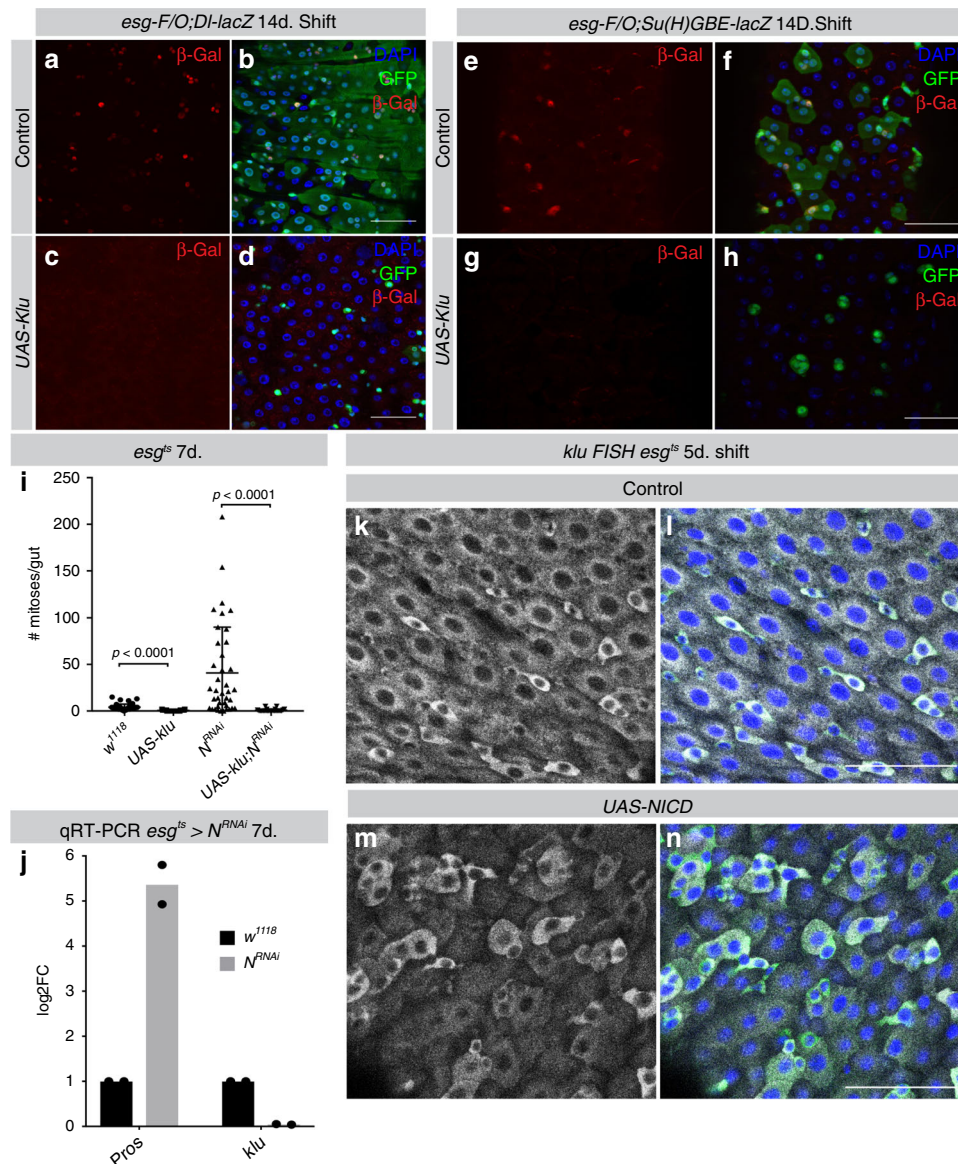
Fig. 4 Klu is regulated by Notch and represses Notch-induced tumor formation. **a, b** Control *esg-F/O* clones always contain 1 or more ISCs expressing *Dl-lacZ*. **c, d** *esg-F/O>UAS-klu* clones have no detectable *Dl-lacZ* expression. **e, f** Similarly, control *esg-F/O* clones contain EBs expressing *Su(H)-GBE-lacZ*, but not *esg-F/O* clones expressing *UAS-klu* (**g, h**). Representative areas of posterior midgut are shown. $n = 3$ midguts examined/genotype in **a–h**. **i** Quantification of the number of mitoses per midgut in *esg^{ts}* guts expressing *N^{RNAi}* alone or in combination with *UAS-klu*. Klu expression also reduced mitosis compared to control midguts (*esg^{ts} × w^{1118}*, control average = 4.2 mitoses/midgut, compare to *UAS-klu*: 0.48 mitoses/midgut, $P < 0.0001$). $n = 42$ for control (crossed with *w^{1118}*) *esg^{ts}* animals and *N^{RNAi}* animals, $n = 33$ for *UAS-klu* and $n = 24$ for *UAS-klu;N^{RNAi}*. **j** Quantitative real-time PCR of sorted *esg^{ts}* GFP+ cells expressing *N^{RNAi}* for the EE-marker Pros and Klu. cDNA was derived from two replicates/genotype, each replicate containing mRNA isolated from *esg^{ts}* GFP+ cells from 100 midguts/genotype. **k–n** Fluorescent in situ hybridization for a *klu* probe showed induced expression in *esg^{ts}* GFP+ cells that overexpress constitutively active Notch intracellular domain (NICD, **m, n**) compared to control *esg^{ts}* cells (**k, l**). Representative areas of posterior midgut are shown. $n = 4$ midguts examined/genotype in **k–n**. Scale bar = 50 μm

noticed that the distance between control and *klu^{RNAi}* sample groups and the *UAS-klu* group in the largest principal component PC1 is much larger (Supplementary Fig. 5a). This indicates more profound transcriptional changes in the *UAS-klu* samples compared to controls than between *klu^{RNAi}* and controls. This is also reflected in the FACS-profile of Esg+ cells expressing *klu^{RNAi}* and *UAS-klu*: whereas ISC and EB population sizes appeared similar between control and *klu^{RNAi}*, the *UAS-klu*-expressing Esg+ cells showed a loss of clearly distinguishable ISC and EB compartments (Supplementary Fig. 5b–d). We first confirmed that the transcriptome of *esg^{ts}>klu^{RNAi}* sorted cells indeed reflects the excess EE differentiation phenotype seen in *klu^{RNAi}* animals by

performing qRT-PCR for *prospero* (*pros*) and *scute* (*sc*). The EE marker *pros* was upregulated 5-fold upon *klu^{RNAi}* (Fig. 5b). The proneural transcription factor Scute (*sc*) is necessary and sufficient for EE generation in the *Drosophila* midgut[14,31,32] and many upstream factors impinge on the expression of *sc* to regulate EE differentiation[33]. mRNA levels of *sc* increased ~2.5-fold upon *klu^{RNAi}* expression, and *UAS-klu* expression completely abolished *sc* mRNA expression in stem-progenitor cells (Fig. 5b).

In addition, we checked *klu* mRNA levels to verify knockdown and overexpression efficiency. As expected, we saw a 70% reduction in *klu* mRNA upon *klu^{RNAi}*. Surprisingly, however, expression of *klu* mRNA in *UAS-klu*-expressing progenitor cells
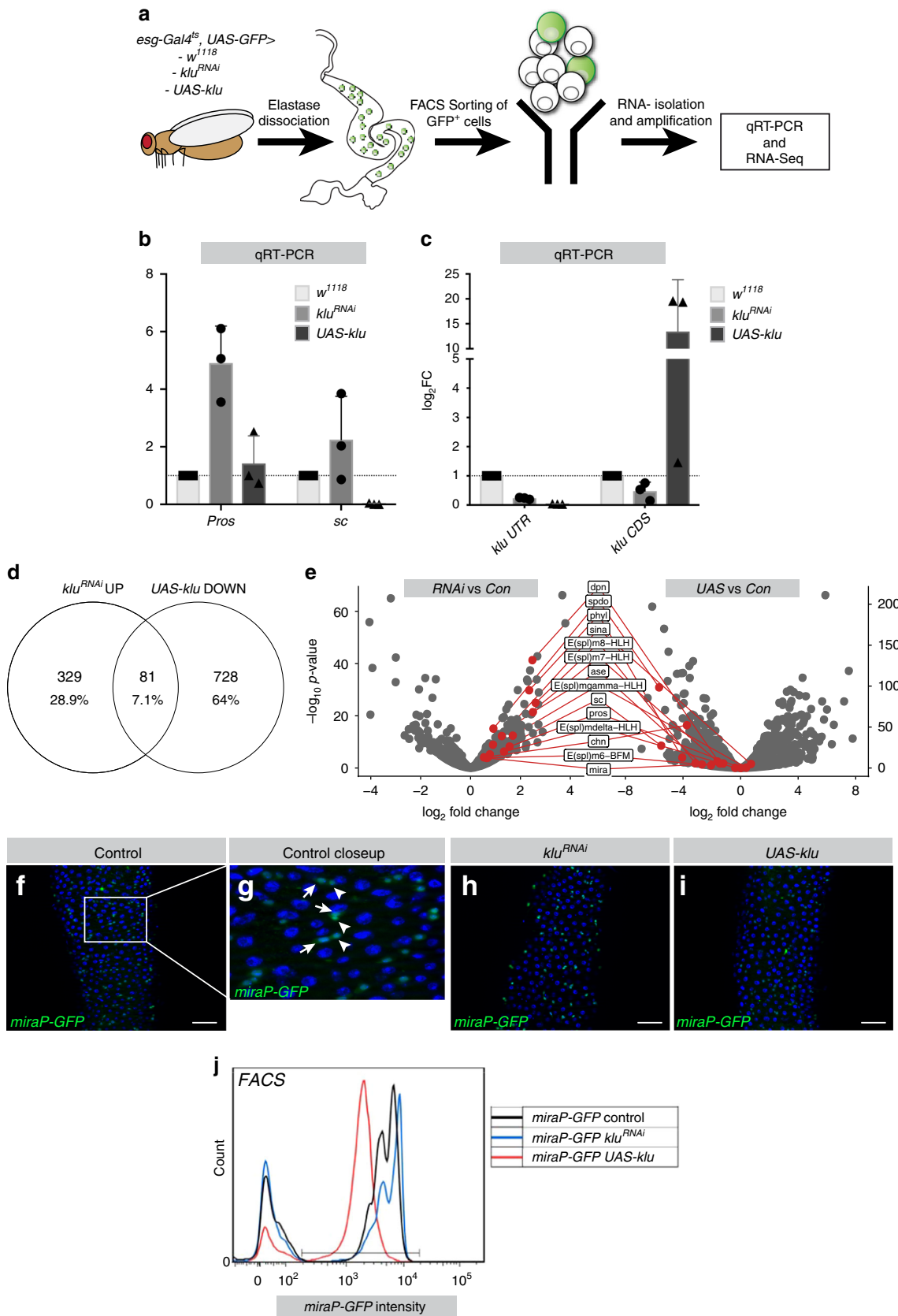
Fig. 5 RNA-Seq indicates Klu represses Notch targets and EE differentiation genes. **a** Overview of the experiment: esg^{ts} GFP+ cells either expressing klu^{RNAi} or UAS-kluFL were sorted in triplicate and their transcriptome was compared to control esg^{ts} GFP cells (see Methods for more details). **b** qRT-PCR analysis of sorted cells for Klu and the critical EE fate regulators Scute (sc) and Prospero (pros). **c** qRT-PCR analysis of klu mRNA expression with a primer pair that targets the endogenous 3′ UTR coding sequence (klu UTR) and a primer pair that targets the coding region only (klu CDS). For **b** and **c**, cDNA was derived from three replicates/genotype, each replicate containing mRNA isolated from esg^{ts} GFP+ cells from 100 midguts/genotype. Data are plotted as mean ± SEM. **d** Overlap of upregulated genes in klu^{RNAi} and downregulated genes in UAS-kluFL. **e** Volcano plots comparing expression of a selection of genes from the overlap of 81 genes shown in **d**. Most genes upregulated in the klu^{RNAi} vs control set (left) are downregulated in the UAS-klu vs control set (right). **f–j** Klu represses Da-dependent miraP-GFP expression in ISC and EB. **f, g** Control miraP-GFP expression is high in ISCs (arrowheads) and EBs (arrows). **h** miraP-GFP was slightly increased in klu^{RNAi} midguts. **i** UAS-kluFL expression resulted in reduced levels of miraP-GFP. Representative areas of posterior midgut are shown. n = 3 animals examined/genotype in **f–i**. **j** GFP intensity of miraP-GFP-positive cells for the genotypes in **f–i** by FACS in a separate experiment. n = 50 midguts per genotype. Scale bar = 50 μm

was almost completely abolished (Fig. 5c). This was contrary to the expected klu overexpression, but was explained by the fact that the UAS-klu construct does not carry the endogenous klu 3′ UTR, which our primers targeted. Primers that solely target the coding region of klu (klu CDS), in turn, readily detected a ~12-fold upregulation of klu transcript. Hence, while transgenic Klu was induced as expected, endogenous Klu expression was repressed, indicating that Klu may repress its own expression. This notion of a negative autoregulatory loop was confirmed in our RNA-seq data, as we detected a high number of reads in the coding region of the gene in UAS-klu samples, and no reads in the 3′UTR (Supplementary Fig. 6).

Comparing the transcriptomes of wild-type progenitors with the experimental samples, we found 410 genes upregulated in klu^{RNAi} and 809 genes downregulated in UAS-klu-expressing Esg+ cells ($P_{adj} < 0.05$, $\log_2 FC > 0.5$ or <-0.5). We also found 283 genes downregulated in klu^{RNAi} and 1025 genes upregulated in UAS-klu with the same criteria ($P_{adj} < 0.05$ and $\log_2 FC < -0.5$ or >0.5, Wald significance test with Benjamini and Hochberg correction, see Methods and Supplementary Data 1). Given that only the repressor form (kluZF-ERD) of Klu could recapitulate the phenotype of the expression of full-length Klu in esg-F/O clones (Fig. 3), we focused our analysis on genes that would be upregulated in the absence of Klu, but downregulated upon UAS-klu expression (Fig. 5d). In this category of 81 genes, many genes involved in the regulation of Notch signaling (the Hairy/Enhancer of Split (E(Spl)) complex genes m6, m7, m8, and the HES-like transcription factor Deadpan), as well as several previously described regulators of EE differentiation (encoding the proneural proteins Asense (ase), Scute (sc), and the adaptor protein Phyllopod, phyl)) could be identified (Fig. 5e). Additional E(Spl) genes (E(Spl)-mδ and E(Spl)-mγ) were significantly upregulated in klu^{RNAi} samples, but did not change significantly in UAS-klu samples (Fig. 5e). E(Spl)-genes are a group of genes activated by Notch that mediate its downstream transcriptional response[34]. Phyl, in turn, acts to destabilize Tramtrack (ttk), a strong repressor of the achaete–scute complex genes scute and asense, loss of which leads to a dramatic increase in EE numbers[33,35]. Reciprocally, loss of phyl stabilizes Ttk and results in a complete loss of EEs[36]. The induction of phyl in klu loss of function conditions thus explains the increase in EEs. We also found that expression of Charlatan (chn) was downregulated by UAS-klu. Chn is a transcription factor that positively regulates Achaete and Scute, and loss of Chn causes proliferation and differentiation defects in the midgut stem-progenitor compartment[37–39]. Hence, Klu represses the expression of several genes that have reported roles in EE differentiation.

Our transcriptome data also revealed changes downstream of Klu that may explain the Klu-induced exit from the stem cell state: ISC maintenance depends on the Class I bHLH-family member daughterless (Da)/E47-like, since loss of Da results in loss of ISC fate and EC differentiation[32]. The gene miranda (mira) is a Da/

proneural target gene that is also highly expressed in ISCs and to a lesser extent in EBs (Fig. 5f, g)[32,39]. Proneural factors such as Ase and Sc require Da to dimerize and regulate transcription[40]. klu^{RNAi} resulted in a slight but significant upregulation of mira in ISC/EB clusters, whereas Klu overexpression resulted in a 2.3-fold downregulation (Fig. 5e). To confirm this, we used a mira-Promoter-GFP (mira-GFP) line[32] and combined this with klu^{RNAi} and UAS-klu. Confocal microscopy and FACS sorting of cells expressing either klu^{RNAi} and UAS-klu confirmed that UAS-klu expression could reduce mira-GFP levels in Esg+ cells, whereas a slight induction is seen in klu^{RNAi} cells (Fig. 5h, i). FACS sorting indicated an increase in GFP intensity of the EB cells (Fig. 5j, rightmost peak) in klu^{RNAi} Esg+ cells. This suggests that physiologically, Klu acts to inhibit mira expression in EBs and that ectopic expression of Klu in ISCs is sufficient to repress the expression of stem cell markers like miranda.

Klu acts upstream of Scute in EE differentiation. Scute plays a critical role in a transcriptional loop that regulates both ISC proliferation and the initiation of EE differentiation[16]. Our genetic and transcriptional profiling experiments suggest that Klu likely acts downstream of Notch, but upstream of the proneural genes Ase and Sc in repressing EE differentiation (Figs. 3–5, Supplementary Fig. 4). We performed epistasis experiments with Klu and Sc to test this hypothesis. We generated esg-F/O clones that express klu^{RNAi} in the presence or absence of sc^{RNAi}. Clones expressing klu^{RNAi} contained more EE cells compared to control clones (Fig. 6c, d compare with Fig. 6a, b), whereas clones expressing sc^{RNAi} are almost completely devoid of EE cells (Fig. 6e, f). The combination of klu^{RNAi} and sc^{RNAi} also resulted in clones with little or no EE differentiation (Fig. 6g, h, quantification in Fig. 6i). This suggests that excess EE differentiation in klu^{RNAi}-expressing clones depends on Scute. To confirm that Scute would act downstream of Klu in determining EE fate, we combined overexpression of Scute and Klu. Clonal expression of Scute using the esg-F/O system resulted in clones consisting almost entirely of Pros-positive EE cells whereas clones expressing UAS-klu are completely devoid of EE cells (quantification in Fig. 6j, images in Supplementary Fig. 7a–l). Co-expression of Klu and Scute leads to a marked reduction in clone size (Supplementary Fig. 7m) but EE differentiation was observed in a large fraction of the clones, although the percentage of differentiated cells is reduced compared to UAS-Sc alone (Fig. 6j). We conclude that Scute can still induce EE differentiation, even in Klu gain-of-function conditions.

We observed an increase in the number of Pros-pH3 double-positive cells in UAS-Sc compared to control, likely representing the EE-progenitor cells (EEp) undergoing a final round of division[16]. Strikingly, this percentage increased in esg-F/O > UAS-klu + UAS-sc clones (Supplementary Fig. 7n). However, the clonal size in this genotype is no larger than in esg-F/O > UAS-klu
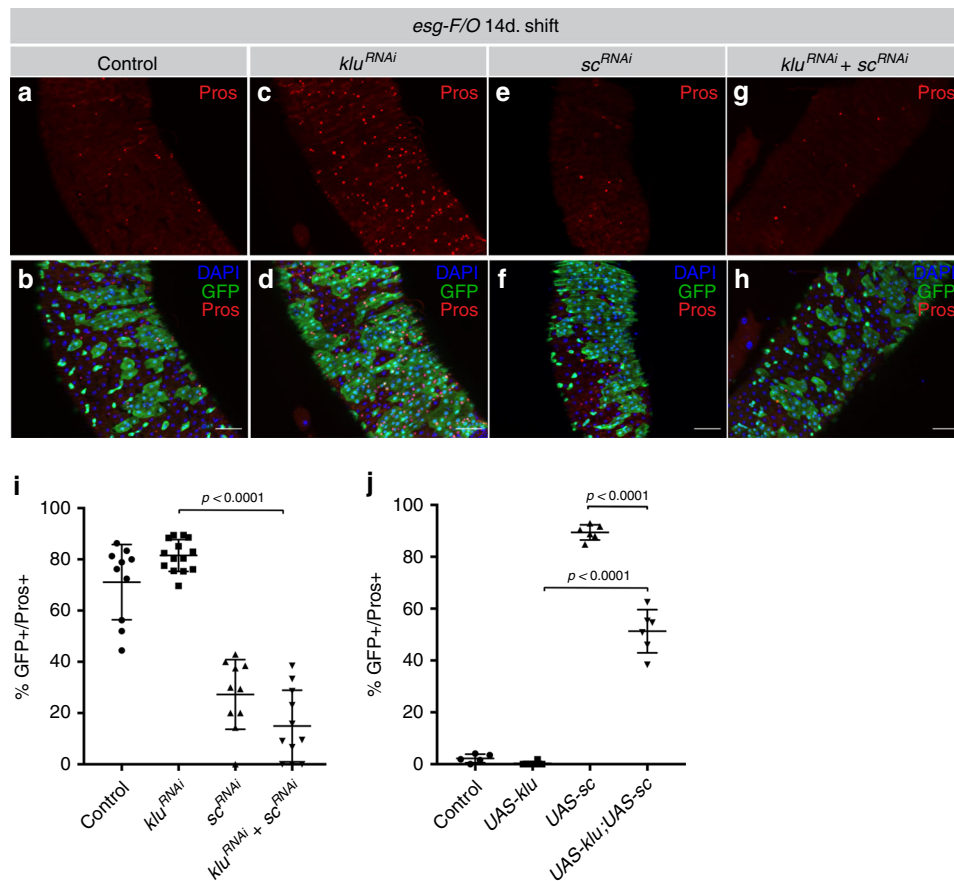
Fig. 6 Scute acts downstream of Klu in enteroendocrine differentiation. **a**, **b** Control *esg-F/O* clones 14 days after clonal induction. **c**, **d** Expression of *klu^RNAi* lead to increased EE differentiation in clones, marked by increased numbers of Pros⁺-cells (red) (**c**, **d**, quantification in **i**, **j**). **e**, **f** *sc^RNAi* clones showed almost no EE differentiation. **g**, **h** Similarly, the combination of *klu^RNAi* with *sc^RNAi* resulted in clones lacking EE differentiation. Representative areas of posterior midgut are shown. **i** Quantification of GFP⁺/Pros⁺ double-positive cells/clone of the genotypes in **a**–**h**. *n* = 10 for control, *n* = 14 for *klu^RNAi*, *n* = 10 for *sc^RNAi* and *n* = 12 for *sc^RNAi;klu^RNAi*. **j** Quantification of GFP⁺/Pros⁺ double-positive cells/clone of *esg-F/O* clones expressing either *UAS-sc*, *UAS-klu*, or the combination. See Supplementary Fig. 7 for images. *n* = 5 for control, *n* = 6 for *UAS-klu*, *UAS-sc*, and *UAS-klu;UAS-sc*. Error bars represent mean ± SD. Significance was calculated using Student's *t*-test with Welch's correction. Scale bar = 50 μm

over-expressing clones (Supplementary Fig. 7n), indicating that these cells might be arrested in mitosis. This suggests that although Klu expression cannot completely repress *UAS-Sc*-induced EE differentiation, the effect of Klu on cell cycle progression interferes with the proliferation-inducing capacity of Scute.

Klu binds to genes regulating EE fate, cell cycle and Notch. The differentially expressed genes (DEGs) from our RNA-Seq analysis might reflect genes that are direct target genes of Klu. Alternatively, the transcriptional changes might be the consequence of a change in cell populations due to the loss or overexpression of Klu. To distinguish between these possibilities and to identify genes directly regulated by Klu, we performed targeted DamID of Klu in Esg⁺ stem-progenitor cells[41]. We used the DamID-seq pipeline (ref. [42], see Methods) to identify 1667 genes that had one or more Klu binding peak(s) within 2 kb of their gene body in all three replicates. Using two published position weight matrices for Klu binding[43], we could establish that 692 of the 1667 genes (41.5%) had one or more Klu-binding motif(s) present in their binding peaks. We considered these peaks as high-confidence Klu-bound sites. Our transcriptomics data on Klu indicated that Klu controls many genes involved in Notch signaling, EE differentiation, and cell cycle regulation. We identified a cluster of binding sites at the centrosomal end of the *E(Spl)*-locus around

the *E(Spl)-mδ* and *E(Spl)-mγ* genes (Fig. 7a). Since our RNA-Seq data showed that many of the *E(Spl)*-genes change expression in both *klu^RNAi* and *UAS-klu* conditions (Fig. 5e), this suggests that Klu could possibly regulate the expression of multiple members of the *E(Spl)*-complex through this binding peak at the centrosomal end of the *E(Spl)*-locus. Furthermore, we identified a Klu-Dam binding peak at the *klu* locus, supporting our hypothesis that Klu acts in an autoregulatory loop by negatively regulating its own expression (Fig. 7b). Previous work has shown that Scute and the *E(Spl)*-complex member *E(Spl)m8-HLH* act in a regulatory loop to generate an EE precursor directly from the ISC[16]. Since our results indicate that Scute is upregulated upon loss of Klu and acts epistatically to Klu in EE formation, we first looked for Klu binding in and around the *scute* locus. We did not observe binding of Klu-Dam around any of the genes in the Achaete/ Scute complex. However, we did identify a DamID peak around the *sina* and *sinah* loci (Fig. 7c). Together with the adaptor protein Phyllopod, the Sina and Sinah E3-ubiquitin ligases are able to degrade the transcriptional repressor Tramtrack (*ttk*), which represses EE fate[33,36]. *sina* transcript levels are upregulated 2.2-fold upon *klu* RNAi and *phyl* levels are upregulated 8-fold as well as downregulated 15-fold upon *UAS-klu* expression (Fig. 5e, Supplementary Data File 1). Hence, we propose that Klu represses EE fate determination in EBs upstream of Scute by stabilizing Tramtrack, since Klu directly represses the members of the
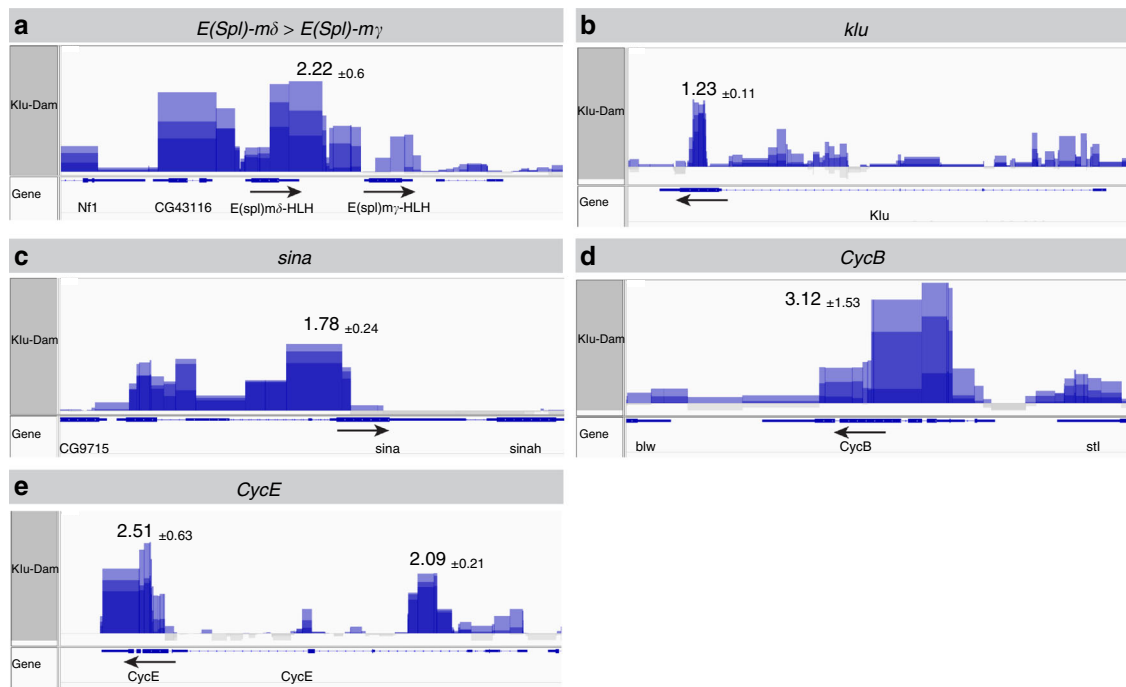
Fig. 7 Klu binds genes involved in Notch, cell cycle, and EE fate. **a–e** Klu-Dam binding tracks (in triplicate) for the *E(Spl)*-complex locus (**a**), *klu* (**b**), *sina* (**c**), and the Cyclins *CycB* (**d**) and *CycE* (**e**). Tracks are displayed in Integrated Genome Viewer (IGV) as overlayed tracks of the triplicate Klu-Dam vs Dam-only control comparisons. Arrows indicate direction of transcription. Numbers indicate average maximum peak height (log$_2$FC of Klu-Dam over Dam-only control ± SD) for each of the three replicates

E3-ligase complex Sina, Sinah, and (indirectly) Phyl that can normally target Ttk for destruction.

In addition to genes involved in Notch signaling and EE specification, we find evidence for direct repression of critical cell cycle regulators by Klu. We find Klu-binding peaks at both the Cyclin B (*CycB*) and Cyclin E (*CycE*) loci (Fig. 7d, e), two Cyclins that are essential for G1–S and G2–M progression, respectively. CycE is also upregulated upon *klu* RNAi expression. Notch activation is essential for the mitotic-to-endocycle switch in follicle cells of the *Drosophila* ovary, and polyploidization is a critical step in the normal process of EB-to-EC differentiation[44,45]. We propose that Klu plays a role in remodeling the cell cycle in response to Notch activation by directly repressing two critical cell cycle regulators. Furthermore, this explains how Klu acts as a potent suppressor of cell proliferation (Fig. 3, Supplementary Fig. 3).

Altogether, our data suggest a model (Fig. 8) in which Klu acts as a Notch effector in the EB that acts to restrict the duration of the Notch transcriptional response (through negative regulation of the E(Spl)-complex members and Klu itself). Second, Klu prevents activation of the Scute-E(Spl)-m8 transcriptional circuit that triggers EE differentiation. Finally, we find evidence that Klu can bind and repress critical cell cycle regulators such as Cyclin B and Cyclin E, likely promoting the switch from a mitotic to an endoreplicating cell cycle in differentiating ECs.

Discussion

Our work identified a mechanism by which lineage decisions are cemented through the coordinated repression of alternative fates and of cell proliferation in somatic stem cell daughter cells. Notch-induced expression of Klu in EBs is necessary to repress EE fates in EBs, but also to restrict Notch target gene expression. Hence, its own expression has to be self-regulated to allow differentiation to ECs to proceed. We find that Klu represses several genes that are critical for EE differentiation; most notably genes that influence the

level of Scute. Transient expression of Scute is necessary and sufficient for EE differentiation and this is accomplished by a double-negative feedback loop between Scute and E(Spl)m8 (ref. [16]). Klu expression results in the repression of both transcription factors in EBs, inactivating the transcriptional circuit that governs EE differentiation (Fig. 8). Previous work has shown that Klu is directly regulated by Su(H) and acts as a Notch effector in hemocyte differentiation[46]. We find that overexpression of Klu results in the loss of Notch signaling activity in stem-progenitor cells, and that Klu is able to repress several Notch effector genes (such as the HES/E(Spl) family and HES/E(Spl)-like genes such as Deadpan). We thus propose that Klu acts in a negative feedback loop downstream of Notch signaling to ensure that Notch effector gene activity is transient in EBs, mirroring the transient nature of EE specification by Scute and E(Spl)m8.

Klu is a zinc-finger transcription factor with some similarity to WT1 (refs. [24,47]). While the sequence similarity between these factors is limited, our data suggest that functional parallels can be drawn: Loss of WT1 in the mouse kidney results in glomerulo-sclerosis and is accompanied by ectopic expression of HES/E(Spl) family genes[48] and in zebrafish kidney podocytes Notch expression induces *Wt1* transcription, while the Notch intracellular domain (NICD) and WT1 synergistically promote transcription at the promoter of the HES/E(Spl) family gene Hey1 (ref. [49]). This suggests that the negative feedback between Notch and its effectors Klu or WT1 might be conserved between species, even though conservation at the sequence level between these transcription factors is low.

Our data also support a role for Klu for regulating cell cycle progression. Overexpression of Klu results in a strong block in cell proliferation in N^{RNAi} or oncogenic Ras^{V12}-induced tumors and our DamID data suggest that Klu can directly regulate Cyclins B and E. The phenotype of Klu in EBs is in stark contrast to its role in the neuroblast stem cell lineage, where over-expression of Klu leads to a strong overproliferation of immature
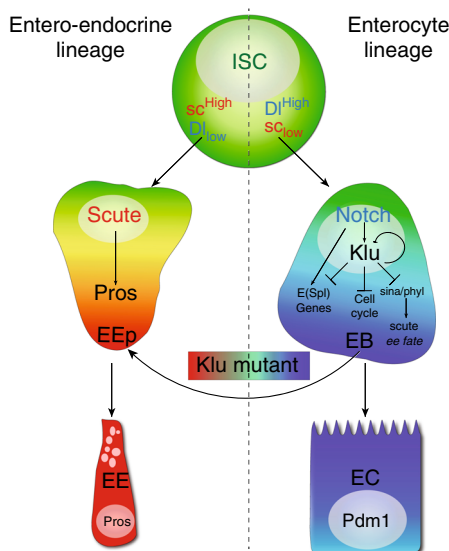
Fig. 8 Model for Klu function in ISC lineage differentiation. Our data suggest that Klu expression is activated by Delta-Notch signaling in the EB, together with other members of the Hairy/Enhancer of Split family of Notch target genes. Klu accumulation in EBs results in a subsequent repression of these target genes, including the repression of its own expression. Additionally, Klu acts as a safeguard to repress erroneous EE differentiation in the enteroblast–enterocyte lineage by indirectly repressing the accumulation of proneural genes such as Asense and Scute through inhibition of the E3-complex members Phyllopod (*phyl*) and Seven-in Absentia (*sina*) that repress the accumulation of Scute and thereby inhibit EE fate. Finally, Klu acts in the regulation of the cell cycle in EB cells, as the cell remodels its cell cycle from a mitotic to an endocycle

neural progenitor cells and the formation of brain tumors[18,19]. However, this likely reflects the different role for Notch in the NB lineage, where continuous activation of Notch similarly leads to INP overproliferation and tumor formation. Thus, the role of Klu in promoting either lineage differentiation or stem-progenitor cell proliferation seems to be context-dependent. Similarly, *Wt1* was initially identified as a tumor-suppressor gene mutated in the rare pediatric kidney cancer Wilms' Tumor[50]. However, expression of WT1 was found to be elevated in many solid tumors and in acute myeloid leukemia[51,52]. During development, WT1 plays a role in the formation of many different tissues of mesodermal and neurectodermal origin[47]. Although WT1 expression seems restricted in adult animals at first glance, whole-body knock-out of WT1 in adult mice results in rapid demise of the animals with kidney, spleen, bone, and fat tissue defects as well as defective erythropoiesis[53]. Furthermore, recent results in zebrafish have shown that *Wt1b* can be re-activated in specific mesenchymal cells upon damage[54], suggesting that *Wt1b* re-expression is involved in regeneration upon damage. In addition, WT1 is often transiently expressed in both nephric and hematopoietic lineages in committed progenitor cell types, similar to the expression of Klu in the EB, raising the possibility that to fully understand the role of WT1-like proteins in tumorigenesis, cell lineage relationships, as well as cell proliferation and differentiation events in tumors need to be taken into account.

Critically, our work highlights the role for transient transcriptional rewiring events during cell specification in stem cell lineages. This rewiring seems to be required to ensure lineage commitment downstream of initial symmetry breaking signals like Notch, and ensure commitment to cell differentiation into a defined lineage. As such, it can be expected that similar

transcriptional rewiring needs to happen for cells to undergo de-differentiation into stem cells in regenerating tissues. Understanding this transcriptional rewiring process will substantially advance efforts to control tissue repair and regeneration in mammals, including humans.

Methods
Fly strains and husbandry. The following strains were obtained from the Bloomington Stock Center: BL28731 (*klu* RNAi on 3rd) BL60469 (*klu* RNAi on 2nd), BL56535 (*UAS-klu[Htol]*), BL11651 (*Dl[05151]-lacZ*) BL26206 (*sc* RNAi), BL51672 (*UAS-sc*), BL1997 (*w[*]; P{w[+ mW.hs] = FRT(w[hs])}2A*), BL4540 (*w[*]; P{w[+ mC] = UAS-FLP.D}JD2*). BL65433 (*y[1] w[*];M{w[+ mC] = hs.min(FRT.STOP1) dam}ZH-51C*) BL1672 (*w[1118]; sna[Sco]/CyO, P{ry[+ t7.2] = en1}wg[en11]*).

VDRC: v27228 (*N* RNAi). Other stocks: *klu-Gal4 UAS-GFP, FRT2A kluR51/Tm6B, hs-Flp, Tub-Gal4, UAS-GFP/Fm7;FRT2A, TubGal80ts/Tm2,Ubx* (T. Klein, Düsseldorf) *UAS-kluFL, UAS-ERD-kluZF, UAS-VP16-kluZF* (all constructs inserted into *ZH51C* on 2nd, C.Y. Lee, U. Michigan) *esg-F/O (w; esg-Gal4, tub-Gal80ts, UAS-GFP; UAS-flp, Act > CD2 > Gal4(UAS-GFP)/TM6B), esg[ts] (y,w;esg-Gal4, UAS-GFP/CyO;tub-Gal80ts/Tm3), Su(H)[ts] (w;Su(H)GBE-Gal4,UAS-CD8-GFP/CyO;tub-Gal80[ts]/TM3), Su(H)GBE-Gal4,UAS-CD8-GFP/CyO;tub-Gal80[ts]/TM3)*, Su(H)-F/O genotype (control) *w;Su(H)GBE-Gal4, UAS-CD8-GFP/CyO;tub-Gal80[ts]/UAS-Flp, Act > CD2 > Gal4*, Su(H)-F/O genotype (*klu[RNAi]*) *w;Su(H)GBE-Gal4,UAS-CD8-GFP/klu[RNAi BL60469];tub-Gal80ts/UAS-Flp, Act > CD2 > Gal4*, ISC-specific *esg[ts][29] w;esg-GAL4,UAS-2XEYFP/CyO;Su(H)GBE-GAL80,tub-Gal80ts/TM3,Sb, w;esg-gal4, tub-Gal80ts, UAS-GFP/CyO,wg-lacZ;P{w [+ mC] = UAS-FLP.D}JD2/Tm6B*. Stocks generated in this study: *w;If/CyO, P{ry[+ t7.2] = en1}wg[en11];klu[KI]-Gal4/Tm6B* and *w;Klu-Dam(ZH-51C) M4M1/CyO, P{ry [+ t7.2] = en1}wg[en11]*.

Immunostaining and microscopy. Midguts were dissected into ice-cold phosphate-buffered saline (PBS), fixed in 4% formaldehyde, and incubated for 1 h at room temperature. Samples were then washed 3×10 min, first in 1× PBS with 0.5% Triton X-100, then in 1× PBS with Na-deoxycholate (0.3%), and last in PBT (PBS with 0.3% Triton X-100), and incubated in blocking solution (PBT with 0.5% bovine serum albumin) for 30 min at 4 °C. Samples were incubated with primary antibodies overnight at 4 °C, washed 3×20 min at room temperature in PBT, incubated with secondary antibodies diluted in blocking solution at room temperature for 2 h, washed 4×20 min with PBT, and mounted in Vecta-Shield (Vector Laboratories)[55]. Antibodies used include Chicken anti-GFP (1:1000; ThermoFisher A10262), mouse anti-Prospero (MR1A, 1:50, DSHB), mouse anti-beta-galactosidase (40-1a, 1:200; DSHB), rabbit anti-beta-galactosidase (1:200; ThermoFisher A11132), mouse anti-Armadillo (N2 7A1, 1:20; DSHB), rabbit anti-phosphorylated Histone H3-Ser10 (pH3S10, 1:500, sc8656-R; Santa Cruz Biotechnology). Images were taken from the R5 and R4 regions of the posterior midgut on a Zeiss Apotome microscope or Zeiss LSM710 confocal at either ×20 or ×40 magnification. Images were captured as Z-stacks with 8–10 slices of 0.22–1.0 μm thickness. Images were converted to maximum-intensity projections in Fiji (https://fiji.sc) and quantifications were performed using the CellCounter FiJi plugin. ROIs in quantifications are defined as images taken from the posterior midgut R4-R5 region at ×20 magnification in which all cells/clones were quantified. Scale bar = 50 μm in all images, except in Fig. 1a: scale bar = 25 μm. Graphing, statistical analysis, and survival curves were produced in GraphPad Prism. Significance was calculated using Student's *t*-test. In case of unequal variances, Student's *t*-test with Welch's correction was used.

Cloning and transgene generation. We used the Inducible DamID system from the Van Steensel lab to generate klu-Dam[41]. To this end, we amplified the Klu Full-length cDNA (derived from BDGP Gold clone FI01015) using *AscI* and *NotI*-containing primers and cloned the fragment into the vector *p-attB-min.hsp70P-FRT-STOP#1-FRT-DamMyc[open]* (Addgene plasmid #71809). Transgenic lines were generated by Genetivision Inc. using the phiC31 integrase-mediated site-specific transgenesis system[56]. The finished construct was injected into Bloomington stock BL24482 (*ZH-51C* attP-site on 2nd) and the resulting transgenic lines were tested by genotyping PCR. Both control (Dam-only, BL65433) and klu-Dam transgenic lines were crossed to BL1672 (*w[1118]; sna[Sco]/CyO, P{ry[+ t7.2] = en1}wg[en11]*) before use. The *klu-Gal4KI CRISPR* line was generated by Rainbow Transgenics (Camarillo, CA, USA). A targeting construct was designed to replace the *klu* CDS with the Gal4 CDS at the *klu* ATG. Two independent transformants were obtained that both showed identical EB-specific expression.

DamID. Control Dam-only (BL65433) and klu-Dam male flies were crossed to *w; esg-gal4, tub-Gal80ts, UAS-GFP/CyO,wg-lacZ;P{w [+ mC] = UAS-FLP.D}JD2/Tm6B* virgins. Crosses were maintained at 18 °C and progeny was shifted to 29 °C for 24 h to induce the Flp-mediated recombination of the STOP-Cassette. Thirty to 50 midguts of Dam-only and klu-Dam were dissected in 1× PBS in three different batches and used for isolation of total genomic DNA. Isolation of methylated GATC-sequences and subsequent amplification was done according to the protocol published by Marshall et al.[57] until Step 34, from which we continued NGS library

preparation using the Illumina TruSeq nano DNA kit LT. After library quality control, samples were sequenced as 50 bp single-end on an Illumina HiSeq2500.

Midgut FACS RNA isolation and sequencing. For RNA-Seq, UAS-expression of UAS-klu or klu^{RNAi} was induced using esg-Gal4^{ts}, UAS-GFP for 2 days, followed by 16 h of Ecc15 infection to stimulate midgut turnover. We dissected 100 midguts/genotype in triplicate and for each sample 20,000–40,000 cells were sorted into RNAse-free 1× PBS with 5 mM EDTA. RNA was isolated using the Arcturus PicoPure™ RNA Isolation Kit. Subsequently, the entire amount of isolated RNA was used as input for RNA-amplification using the Arcturus™ RiboAmp™ HS PLUS Kit. Two hundred nanograms of amplified aRNA was used as input for RNA-Seq library preparation using the TruSeq Stranded mRNA Library Prep Kit (Illumina) and samples were subsequently sequenced as 50 bp single-end on an Illumina HiSeq2500. For the FACS analysis experiment with DNA staining, we dissected 60–70 midguts/genotype under the same conditions and used NuclearID Red DNA Stain (ENZ-52406, Enzo Life Sciences) for DNA content analysis. FACS-plots were generated with FlowJo v10.

Quantitative real-time PCR. Quantitative real-time PCR (qRT-PCR) was performed using amplified RNA from FACS-sorted Esg$^+$ cell populations (see above) as template. cDNA was generated using the QuantiTect Reverse Transcription Kit. qRT-PCR was performed using the TaqMan FAM-MGB system in a 10 μl reaction on a BioRad CFX384 C1000 Touch Cycler using the following probes: klu (dm02361358 s1), pros (dm02135674 g1), sc (dm01841751 s1). Act5C (dm02361909 s1) was used for normalization. The klu CDS primer assay was ordered as a Custom TaqMan Assay. Reactions were performed in triplicate on three independent biological replicates. Relative expression was quantified using the $^{\Delta\Delta}$Ct method. Data were calculated using Microsoft Excel and plotted as relative fold-changes ± SEM in Graphpad Prism.

klu FISH. A 425 bp region in the klu gene, starting at the middle of the 5′UTR and including the first 279 bases of the CDS, was designed to have an Sp6 promoter and a SpeI site at the 5′ end and a downstream T7 promoter and NotI site at the 3′ end. This DNA fragment was synthesized and cloned into a pUCIDT plasmid (IDT). After linearization of the plasmid, transcription and fluorescent labeling of anti-sense and sense klu probes was done following the manufacturer's instruction of the FISH Tag RNA Multicolor kit (Invitrogen Cat. No. MP 32956) using the Sp6 promoter to generate the sense probe and the T7 promoter to generate the anti-sense probe. In situ hybridization was performed using a protocol adapted from the one suggested in FISH Tag RNA Multicolor kit (Invitrogen Cat. No. MP 32956).

RNA-Seq and DamID data analysis. The 15–21 million quality-passed reads per sample were mapped to the D. melanogaster reference genome (BDGP6) with TopHat2 (version 2.1.0)[58]. Of each sample, approximately 80% of the reads was mapped to the genome. From this, 90% could be assigned to genes using FeatureCounts resulting in 11–15 million analysis-ready reads per sample[59].

The table of raw counts per gene/sample was analyzed with the R package DESeq2 (version 1.16.1) for differential expression[60]. Both sample groups of interest (UAS & RNAi) were pair-wise contrasted with the control sample group (control). For each gene of each comparison, the p-value was calculated using the Wald significance test. Resulting p-values were adjusted for multiple testing with Benjamini & Hochberg correction. Genes with an adjusted p-value <0.05 are considered differentially expressed (DEGs).

For DamID, we used the damid_seq pipeline[42] to generate binding profiles for Klu-Dam. Triplicate samples for Klu-Dam (34.9, 33.5, and 34.1 millions reads) and Dam-only control (34.7, 34.5, and 35.6 million reads) were aligned to the Drosophila genome (UCSC dm6). Overall aligning rate was between 86% and 91% across all samples. First, gat.track.maker.pl script was used to build a GATC fragment file. Then the main utility damidseq_pipeline was used to align the reads to the genome using bowtie2, bin and count reads, normalize counts, and compute log2 ratio between corresponding DamID and control Dam-only samples[42]. The pipeline identified 1707, 1663, 1681 peaks with FDR < 0.01 per each replicate. To test for reproducibly we first used the damid_pipeline[42] to identify peaks with weaker confidence (FDR < 0.1) and the idr python package (https://github.com/nboley/idr) to identify 1169 peaks with IDR < 0.05 between replicate1 and replicate2. We used an in-house developed script to annotate peaks in proximity to genes. In total, 1667 genes found to be in proximity to at least one reproducible peak. To find Klu binding motifs in our reproducible peak set, we scanned for two different Klu PWM (described in ref.[43]) around reproducible peaks using the FIMO tool[61]. Reads were visualized using IGV as overlayed triplicate Klu-Dam (log2FC over Dam-only) tracks.

Data availability
The authors declare that all data supporting the findings of this study are available within the article and its Supplementary Information files or from the corresponding authors upon reasonable request. DamID data have been deposited in the GEO database under the accession code: GSE131878. RNA-Seq data have been deposited in the GEO database under the accession code: GSE132243.

Code availability
The in-house developed script to annotate peaks in proximity to genes from damid_pipeline data is available in the file Supplementary Data 2.

References

1. Tetteh, P. W. et al. Replacement of lost Lgr5-positive stem cells through plasticity of their enterocyte-lineage daughters. *Cell Stem Cell* **18**, 203–213 (2016).
2. Yan, K. S. et al. Intestinal enteroendocrine lineage cells possess homeostatic and injury-inducible stem cell activity. *Cell Stem Cell* **21**, 78–90 (2017).
3. Micchelli, C. A. & Perrimon, N. Evidence that stem cells reside in the adult *Drosophila* midgut epithelium. *Nature* **439**, 475–479 (2006).
4. Ohlstein, B. & Spradling, A. The adult *Drosophila* posterior midgut is maintained by pluripotent stem cells. *Nature* **439**, 470–474 (2006).
5. Buchon, N., Broderick, N. A., Poidevin, M., Pradervand, S. & Lemaitre, B. *Drosophila* intestinal response to bacterial infection: activation of host defense and stem cell proliferation. *Cell Host Microbe* **5**, 200–211 (2009).
6. Jiang, H. et al. Cytokine/Jak/Stat signaling mediates regeneration and homeostasis in the *Drosophila* midgut. *Cell* **137**, 1343–1355 (2009).
7. Biteau, B., Hochmuth, C. E. & Jasper, H. JNK activity in somatic stem cells causes loss of tissue homeostasis in the aging *Drosophila* gut. *Cell Stem Cell* **3**, 442–455 (2008).
8. Li, H. & Jasper, H. Gastrointestinal stem cells in health and disease: from flies to humans. *Dis. Model. Mech.* **9**, 487–499 (2016).
9. Choi, N.-H., Kim, J.-G., Yang, D.-J., Kim, Y.-S. & Yoo, M.-A. Age-related changes in *Drosophila* midgut are associated with PVF2, a PDGF/VEGF-like growth factor. *Aging Cell* **7**, 318–334 (2008).
10. Ohlstein, B. & Spradling, A. Multipotent *Drosophila* intestinal stem cells specify daughter cell fates by differential notch signaling. *Science* **315**, 988–992 (2007).
11. Perdigoto, C. N., Schweisguth, F. & Bardin, A. J. Distinct levels of Notch activity for commitment and terminal differentiation of stem cells in the adult fly intestine. *Development* **138**, 4585–4595 (2011).
12. Patel, P. H., Dutta, D. & Edgar, B. A. Niche appropriation by *Drosophila* intestinal stem cell tumours. *Nat. Cell Biol.* **17**, 1182–1192 (2015).
13. Siudeja, K. et al. Frequent somatic mutation in adult intestinal stem cells drives neoplasia and genetic mosaicism during aging. *Cell Stem Cell* **17**, 663–674 (2015).
14. Zeng, X. & Hou, S. X. Enteroendocrine cells are generated from stem cells through a distinct progenitor in the adult *Drosophila* posterior midgut. *Development* **142**, 644–653 (2015).
15. Biteau, B. & Jasper, H. Slit/Robo signaling regulates cell fate decisions in the intestinal stem cell lineage of *Drosophila*. *Cell Rep.* **7**, 1867–1875 (2014).
16. Chen, J. et al. Transient Scute activation via a self-stimulatory loop directs enteroendocrine cell pair specification from self-renewing intestinal stem cells. *Nat. Cell Biol.* **20**, 152–161 (2018).
17. Antonello, Z. A., Reiff, T., Ballesta-Illan, E. & Dominguez, M. Robust intestinal homeostasis relies on cellular plasticity in enteroblasts mediated by miR-8-Escargot switch. *EMBO J.* **34**, 2025–2041 (2015).
18. Xiao, Q., Komori, H. & Lee, C.-Y. Klumpfuss distinguishes stem cells from progenitor cells during asymmetric neuroblast division. *Development* **139**, 2670–2680 (2012).
19. Berger, C. et al. FACS purification and transcriptome analysis of *Drosophila* neural stem cells reveals a role for Klumpfuss in self-renewal. *Cell Rep.* **2**, 407–418 (2012).
20. Yang, X., Bahri, S., Klein, T. & Chia, W. Klumpfuss, a putative *Drosophila* zinc finger transcription factor, acts to differentiate between the identities of two secondary precursor cells within one neuroblast lineage. *Genes Dev.* **11**, 1396–1408 (1997).
21. Korzelius, J. et al. Escargot maintains stemness and suppresses differentiation in *Drosophila* intestinal stem cells. *EMBO J.* **33**, 2967–2982 (2014).
22. Sousa-Victor, P. et al. Piwi is required to limit exhaustion of aging somatic stem cells. *Cell Rep.* **20**, 2527–2537 (2017).
23. Kaspar, M., Schneider, M., Chia, W. & Klein, T. Klumpfuss is involved in the determination of sensory organ precursors in *Drosophila*. *Dev. Biol.* **324**, 177–191 (2008).
24. Klein, T. & Campos-Ortega, J. A. klumpfuss, a *Drosophila* gene encoding a member of the EGR family of transcription factors, is involved in bristle and leg development. *Development* **124**, 3123–3134 (1997).
25. McGuire, S. E., Mao, Z. & Davis, R. L. Spatiotemporal gene expression targeting with the TARGET and gene-switch systems in *Drosophila*. *Sci. STKE* **2004**, pl6 (2004).

26. Lee, T. & Luo, L. Mosaic analysis with a repressible cell marker (MARCM) for *Drosophila* neural development. *Trends Neurosci.* **24**, 251–254 (2001).

27. Lee, W.-C., Beebe, K., Sudmeier, L. & Micchelli, C. A. Adenomatous polyposis coli regulates *Drosophila* intestinal stem cell proliferation. *Development* **136**, 2255–2264 (2009).

28. Janssens, D. H. et al. An Hdac1/Rpd3-poised circuit balances continual self-renewal and rapid restriction of developmental potential during asymmetric stem cell division. *Dev. Cell* **40**, 367–380 (2017).

29. Wang, L., Ryoo, H. D., Qi, Y. & Jasper, H. PERK limits *Drosophila* lifespan by promoting intestinal stem cell proliferation in response to ER stress. *PLoS Genet.* **11**, e1005220 (2015).

30. Dutta, D., Xiang, J. & Edgar, B. A. RNA expression profiling from FACS-isolated cells of the *Drosophila* intestine. *Curr. Protoc. Stem Cell Biol.* **27**, Unit 2F.2 (2013).

31. Amcheslavsky, A. et al. Enteroendocrine cells support intestinal stem-cell-mediated homeostasis in *Drosophila*. *Cell Rep.* **9**, 32–39 (2014).

32. Bardin, A. J., Perdigoto, C. N., Southall, T. D., Brand, A. H. & Schweisguth, F. Transcriptional control of stem cell maintenance in the *Drosophila* intestine. *Development* **137**, 705–714 (2010).

33. Wang, C., Guo, X., Dou, K., Chen, H. & Xi, R. Ttk69 acts as a master repressor of enteroendocrine cell specification in *Drosophila* intestinal stem cell lineages. *Development* **142**, 3321–3331 (2015).

34. Delidakis, C., Monastirioti, M. & Magadi, S. S. E(spl): genetic, developmental, and evolutionary aspects of a group of invertebrate Hes proteins with close ties to Notch signaling. *Curr. Top. Dev. Biol.* **110**, 217–262 (2014).

35. Pi, H., Huang, S.-K., Tang, C.-Y., Sun, Y. H. & Chien, C.-T. phyllopod is a target gene of proneural proteins in *Drosophila* external sensory organ development. *Proc. Natl Acad. Sci. USA* **101**, 8378–8383 (2004).

36. Yin, C. & Xi, R. A phyllopod-mediated feedback loop promotes intestinal stem cell enteroendocrine commitment in *Drosophila*. *Stem Cell Rep.* **10**, 43–57 (2018).

37. Escudero, L. M., Caminero, E., Schulze, K. L., Bellen, H. J. & Modolell, J. Charlatan, a Zn-finger transcription factor, establishes a novel level of regulation of the proneural achaete/scute genes of *Drosophila*. *Development* **132**, 1211–1222 (2005).

38. Amcheslavsky, A. et al. Gene expression profiling identifies the zinc-finger protein Charlatan as a regulator of intestinal stem cells in *Drosophila*. *Development* **141**, 2621–2632 (2014).

39. Reeves, N. & Posakony, J. W. Genetic programs activated by proneural proteins in the developing *Drosophila* PNS. *Dev. Cell* **8**, 413–425 (2005).

40. Cabrera, C. V. & Alonso, M. C. Transcriptional activation by heterodimers of the achaete-scute and daughterless gene products of *Drosophila*. *EMBO J.* **10**, 2965–2973 (1991).

41. Pindyurin, A. V., Pagie, L., Kozhevnikova, E. N., van Arensbergen, J. & van Steensel, B. Inducible DamID systems for genomic mapping of chromatin proteins in *Drosophila*. *Nucleic Acids Res.* **44**, 5646–5657 (2016).

42. Marshall, O. J. & Brand, A. H. damidseq_pipeline: an automated pipeline for processing DamID sequencing datasets. *Bioinformatics* **31**, 3371–3373 (2015).

43. Nitta, K. R. et al. Conservation of transcription factor binding specificities across 600 million years of bilateria evolution. *eLife* **4**, e04837 (2015).

44. Shcherbata, H. R., Althauser, C., Findley, S. D. & Ruohola-Baker, H. The mitotic-to-endocycle switch in *Drosophila* follicle cells is executed by Notch-dependent regulation of G1/S, G2/M and M/G1 cell-cycle transitions. *Development* **131**, 3169–3181 (2004).

45. Xiang, J. et al. EGFR-dependent TOR-independent endocycles support *Drosophila* gut epithelial regeneration. *Nat. Commun.* **8**, 15125 (2017).

46. Terriente-Felix, A. et al. Notch cooperates with Lozenge/Runx to lock haemocytes into a differentiation programme. *Development* **140**, 926–937 (2013).

47. Hastie, N. D. Wilms' tumour 1 (WT1) in development, homeostasis and disease. *Development* **144**, 2862–2872 (2017).

48. Asfahani, R. I. et al. Activation of podocyte Notch mediates early Wt1 glomerulopathy. *Kidney Int.* **93**, 903–920 (2018).

49. O'Brien, L. L. et al. Wt1a, Foxc1a, and the Notch mediator Rbpj physically interact and regulate the formation of podocytes in zebrafish. *Dev. Biol.* **358**, 318–330 (2011).

50. Call, K. M. et al. Isolation and characterization of a zinc finger polypeptide gene at the human chromosome 11 Wilms' tumor locus. *Cell* **60**, 509–520 (1990).

51. Qi, X. et al. Wilms' tumor 1 (WT1) expression and prognosis in solid cancer patients: a systematic review and meta-analysis. *Sci. Rep.* **5**, 8924 (2015).

52. Huff, V. Wilms' tumours: about tumour suppressor genes, an oncogene and a chameleon gene. *Nat. Rev. Cancer* **11**, 111–121 (2011).

53. Chau, Y.-Y. et al. Acute multiple organ failure in adult mice deleted for the developmental regulator Wt1. *PLoS Genet.* **7**, e1002404 (2011).

54. Lopez-Baez, J. C. et al. Wilms Tumor 1b defines a wound-specific sheath cell subpopulation associated with notochord repair. *eLife* **7**, e30657 (2018).

55. Resnik-Docampo, M. et al. Tricellular junctions regulate intestinal stem cell behaviour to maintain homeostasis. *Nat. Cell Biol.* **19**, 52–59 (2017).

56. Bischof, J., Maeda, R. K., Hediger, M., Karch, F. & Basler, K. An optimized transgenesis system for *Drosophila* using germ-line-specific phiC31 integrases. *Proc. Natl Acad. Sci. USA* **104**, 3312–3317 (2007).

57. Marshall, O. J., Southall, T. D., Cheetham, S. W. & Brand, A. H. Cell-type-specific profiling of protein-DNA interactions without cell isolation using targeted DamID with next-generation sequencing. *Nat. Protoc.* **11**, 1586–1598 (2016).

58. Kim, D. et al. TopHat2: accurate alignment of transcriptomes in the presence of insertions, deletions and gene fusions. *Genome Biol.* **14**, R36 (2013).

59. Liao, Y., Smyth, G. K. & Shi, W. featureCounts: an efficient general purpose program for assigning sequence reads to genomic features. *Bioinformatics* **30**, 923–930 (2014).

60. Love, M. I., Huber, W. & Anders, S. Moderated estimation of fold change and dispersion for RNA-seq data with DESeq2. *Genome Biol.* **15**, 550 (2014).

61. Grant, C. E., Bailey, T. L. & Noble, W. S. FIMO: scanning for occurrences of a given motif. *Bioinformatics* **27**, 1017–1018 (2011).

Author contributions

J.K. and H.J. conceived the project and designed experiments. J.K., S.A., I.A.R.-F., M.B., and E.M. performed experiments and collected data. M.G. helped with optimizing the RNA-Seq library amplification protocol and Dam-ID protocol. T.R.-O. and P.K. performed data analysis on the RNA-Seq and DamID samples. P.S-V. provided preliminary data for the study. J.K. and H.J. wrote the manuscript.

Additional information

Supplementary Information accompanies this paper at https://doi.org/10.1038/s41467-019-12003-0.

Competing interests: The authors declare no competing interests.

Reprints and permission information is available online at http://npg.nature.com/reprintsandpermissions/

Peer review information *Nature Communications* thanks the anonymous reviewer(s) for their contribution to the peer review of this work. Peer reviewer reports are available.

Publisher's note Springer Nature remains neutral with regard to jurisdictional claims in published maps and institutional affiliations.